UNIVERSAL SIGNAL CONDITIONING SYSTEM FOR ELECTROCHEMICAL AND BIOLUMINESCENT SENSOR ARRAYS

Teză destinată obţinerii
titlului ştiinţific de doctor inginer
la
Universitatea "Politehnica" din Timişoara
în domeniul INGINERIE ELECTRONICĂ
ŞI TELECOMUNICAŢII
de către

Ing. David George Cristea

Conducător ştiinţific: prof.univ.dr.ing. Virgil Tiponuţ
Referenţi ştiinţifici: prof.univ.dr.ing. Yosi Shacham-Diamand
prof.univ.dr.ing. Adrian Graur
prof.univ.dr.ing. Dorina Isar

Ziua susţinerii tezei: 11.11.2011

Seriile Teze de doctorat ale UPT sunt:

1. Automatică
2. Chimie
3. Energetică
4. Ingineria Chimică
5. Inginerie Civilă
6. Inginerie Electrică
7. Inginerie Electronică şi Telecomunicaţii
8. Inginerie Industrială
9. Inginerie Mecanică
10. Ştiinţa Calculatoarelor
11. Ştiinţa şi Ingineria Materialelor
12. Ingineria sistemelor
13. Inginerie energetică
14. Calculatoare şi tehnologia informaţiei

Universitatea „Politehnica” din Timişoara a iniţiat seriile de mai sus în scopul diseminării expertizei, cunoştinţelor şi rezultatelor cercetărilor întreprinse în cadrul şcolii doctorale a universităţii. Seriile conţin, potrivit H.B.Ex.S Nr. 14 / 14.07.2006, tezele de doctorat susţinute în universitate începând cu 1 octombrie 2006.

România, 300159 Timişoara, Bd. Republicii 9,
tel. 0256 403823, fax. 0256 403221
e-mail: editura@edipol.upt.ro

ACKNOWLEDGEMENTS

This doctoral thesis was supported in part by POSDRU/6/1.5/S/13 strategic grant, ID6998, financed from European Social Fund "Investing in people" in the Human Resources Development Operational Programme 2007-2013.

This thesis would not have been completed without the perfect team of researchers and friends that God blessed me with. The encouragements and advice from my PhD. advisor, Prof. Dr. Eng. Virgil Tiponut were priceless, he was available everywhere and anywhere, during the day or at night, always having a good piece of advice, encouragements, being first of all a friend, an advisor, a colleague. We stayed together and learned, trying to understand the electrochemistry and biotechnology fields and for these are only a few reasons for my owing gratitude to him. I express special thanks for my unofficial co-advisor, Prof. Dr. Eng. Yosi Shacham who has shown me what a real researcher means, being a model of honesty and availability. He helped me with the biochemistry, biology and electrochemistry part, with all the experiments performed in this work. His multi - disciplinary abilities never stopped to amaze us. This research would not have been possible without his help.

I also want to express my gratitude to my colleagues, real team players with whom I have elaborated papers and articles based on my research. Special thanks to Eng. Mihai Basch (UPT), Eng. Hadar Ben Yoav (USA) and Amit Ron (USA) for their patience, explanations and advice, they have become my friends! Thank you, Guys!

I also owe my gratitude to the Applied Electronics Department Director, Prof. Dr. Eng Ivan Bogdanov and to Electronics and Telecommunications Faculty Dean, Prof. Dr. Eng. Marius Otesteanu.

Special thanks to the PhD committee, Prof. Dr. Eng Yosi Shacham Diamand, Tel Aviv University, Prof. Dr. Eng. Adrian Graur, Stefan Cel Mare University, Suceava and Prof. Dr. Eng Dorina Isar, Politehnica University, Timisoara. I am honored to present my results in front of you.

Again, I want to mention for their support Yosi's team from Tel Aviv University for showing me that everything is possible when you are ready to make sacrifices.

There are not enough words to express my gratitude for my parents. They taught me that a researcher is a person that sees what everybody else sees but understands in a totally different way. They have served me as models and friends, guides and they have been there for me, supporting me with everything in their powers.

Timişoara, November 2011 David George Cristea

This doctoral thesis was supported in part by POSDRU/6/1.5/S/13 strategic grant, ID6998, financed from European Social Fund "Investing in people" in the Human Resources Development Operational Programme 2007-2013.

Cristea, David George

UNIVERSAL SIGNAL CONDITIONING SYSTEM FOR ELECTROCHEMICAL AND BIOLUMINESCENT SENSOR ARRAYS

Teze de doctorat ale UPT, Seria 7, Nr. 37, Editura Politehnica, 2011, 128 pagini, 60 figuri, 1 tabel.

ISSN: 1842-7014

ISBN: 978-606-554-356-0

Cuvinte cheie: amperometric sensors, electrochemical sensors, bioluminescent sensors, simulation, sensor array, 3 electrode cells, universal signal conditioning system, sensory system.

Rezumat,
Sensors are devices widely used in all areas of activity, from the cars on the roads to the implanted sensors in animal bodies and more recent in human bodies. Life cannot be imagined without sensors. In the last decade, new principles of sensors emerged, sensors that use more than one principle to detect and quantify a phenomenon. Sensors that use living cells, biotic elements such as mammalian cells, bacteria, and living tissues are relatively new. Moreover, applying biotic materials, whole cell biosensors started to be discovered and implemented. These types of sensors have the capacity to perform more than one task at a time, from detection, measurements (usually based on more than one type of reaction) and quantification of the reactions. The author focussed his research on developing a new signal conditioning system able to work with both electrochemical and bioluminescent sensors array.

This work presents a new signal conditioning system for electrochemical and bioluminescent sensors array. The system is able to work with both kinds of amperometric sensors, amperometric sensors which inject and subtract current from and into circuits. This property makes the system a universal signal conditioning system for amperometric sensors. The bases of the research are the electrochemical sensors designed at Tel Aviv University by Prof. Yosi Shacham and his team. The signal conditioning system is able to work with a quite large field of currents, from several hundreds of micro amps to several hundreds of nano amps.

CONTENT

FIGURES LIST

1. INTRODUCTION

In this chapter the author presents a short history of biosensors, the first concepts of biosensing devices and the firs biosensors documented in literature. The author is also trying to present a list with qualities and requirements that a biosensor should accomplish. Due to the fact that E coli bacteria is used in both types of biosensors that the author has used, a few data about bacteria is given. The last paragraph of this chapter is dedicated to the presentation of the motivations that drove him to investigate this topic.

Definitions

Sensor: Any kind of device that can detect something (light, substance, phenomenon, change or variation of the medium) and transform that into a measurable signal (current, voltage, light). Came from Latin *sēnsus* perceived, from *sentīre* to observe.

Biosensor: A device that uses specific biochemical reactions mediated by isolated enzymes, immunosystems, tissues or whole cells to detect chemical compounds usually by electrical, thermal or optical signals. (IUPAC 1997). From Latin Bios Life.

Disclaimers

Some of the figures and theories used in this paper, mainly in electrochemistry and biotechnology fields are borrowed from other sources and used here only for academics purpose and the author doesn't claim any originality for the same.

1.1. History of biosensors

The first types of biosensors used in recorded history were real humans. Kings used to have a special person that tasted their food to see if any kind of poison was present in the food. Of course, this kind of „biosensor" was disposable. Later, in the mines, miners used to carry birds with them to check if any dangerous gas is present in the air. Because of their sensibility to gases, usually metan gas, birds, usually canaries because of their size, low cost and availability, die from methan gas sooner than a human would be affected. Also in mines, miners look after rats because of one special sense that they have to detect an earthquake or some other real danger so when rats run away from mines, miners become aware of a possible danger.

A more recent example of „biosensor" are rats, trained rats to detect mines in the fields. These rats were trained to smell mines and due to their light weight, they usually do not trigger them, of course, in case of a too high sensitivity to pressure mine, the mine tester becomes disposable.

The first articles on biosensors:

1956 - Clark published an article on oxygen electrode called „enzyme electrode". This was the early beginning of biosensors.

1969 - Guilbault and Montalvo used urease to detect urea in the first described potentiometric enzime electrode
1975 - The Yellow Springs Instrument Co. , based on an amperometric detection algorithm for hydrogen peroxide launched a glucose biosensor
1976 - Electrochemical glucose biosensor in artificial pancreas was patented.
1982 - Needle type enzyme electrode for subcutaneous implantation of glucose biosensors was invented.
1987 - MediSense introduced on the market a miniaturized pen-sized meter for glucose in blood monitoring.

1.2. Biosensors qualities

To be able to enter on the public market, a biosensor must satisfy next demands:

1. Easy to manufacture in massive numbers
2. Easy to use without extended training of personnel
3. Cheap if disposable or reusable if expensive
4. To have a fast response
5. To perform multiple tests at the same time-microarrays

Usually biosensors are based on three components:

- A support
- A biological recognition element
- A signal conversion unit.

The support can be any material as silicon wafer, gold foil, glass, mica, graphite, nitrocellulose, nylon etc. that can be used with biotic elements. Biomlolecule immobilization can be made on the support in two main ways: Passive adsorption and covalent immobilization, the methods will be detailed in next chapters.

The most important characteristic of biological recognition unit is affinity or specificity. Biological recognition unit can consist in molecules, macromolecules, tissues and microorganisms (E coli-our case), whole cells.

Signal conversion unit or transducer converts electrochemical, electrooptical, acoustical, thermal or mechanical variation into measurable electronic signal. Signal conversion units can work directly or indirectly.

There are many cutting edge technologies in microelectronic industry that can be used for micro and nano scaled biosensors fabrication:

- Screen printing
- Photolithography
- Nanopatterning
- Liquid handling techniques

Biological sensors need high sensitive system to detect very small signals, to amplify or to quantify them in order to be useful. Almost all biosensor produce signals in nano-micro scale range so they need dedicated signal processing systems to detect and measure the useful signals.

1.3. E coli Bacteria

In this paragraph the author is presenting a few data about E Coli bacteria because this bacteria is the living component of both electrochemical and bioluminescent sensors that have been used in this research.

Escherichia coli- discovered in 1919 by the german-austrian bacteriologist Theodor Escherich.

A few data about E coli bacteria.

Toxic agents

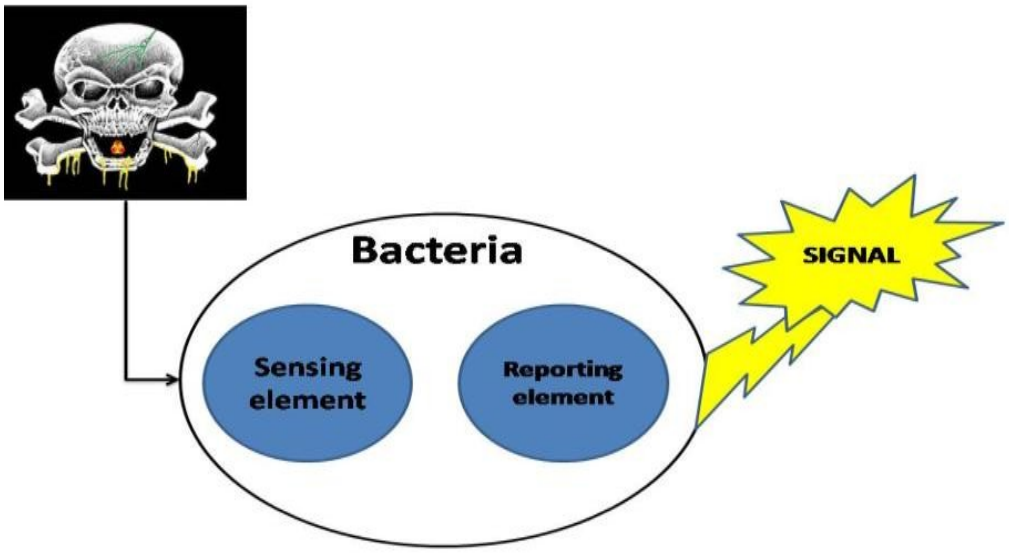

Fig.1.1 Biosensors concept.

Escherichia coli (*E. coli*) are members of a large group of bacterial germs that inhabit the intestinal tract of humans and other warm-blooded animals. *Escherichia coli* is a model organism for studying many of life's essential processes partly because of rapid growth rate and simple nutritional requirements. Researches have well established information about *E. coli*'s genetics and completed many of its genome sequences - presently, we know more about *E. coli* than any other living organism (Microbes in Norwich).

Several strains of *E. coli* have been sequenced and studied in detail. *E. coli* K-12 was the earliest organism to be "suggested as a candidate for whole genome sequencing" (Blattner et al. 1997 [1]). It has a single circular chromosome with 4, 639, 221 base pairs and 4288 protein-coding genes. Of these protein-coding genes, 38% have no attributed function. *E. coli* K-12's genome, like other *E. coli* genomes, has a 50.8% G+C content. Genes which coded for proteins account for 87.8% of the genome, stable RNA-encoding genes make up 0.8%, 0.7% is made of noncoding repeats, and about 11% is for regulatory and other functions, as seen in [2].

Escherichia coli has become a model organism for studying many of life's essential processes partly due to its rapid growth rate and simple nutritional requirements. Researches have well established information about *E. coli*'s genetics and completed many of its genome sequences - presently, we know more about *E. coli* than any other living organism. (Microbes in Norwich) [3].

- **Domain:** *Bacteria* - (Haeckel, 1894) C.r. Woese Et Al., 1990
- **Kingdom:** *Bacteria* - (Cohn, 1870) Cavalier-Smith, 1983 Ex Cavalier-Smith, 2002

- **Phylum:** *Proteobacteria* - Garrity Et Al., 2005
- **Class:** *Schizomycetes* - Garrity Et Al., 2005
- **Order:** *Eubacteriales*
- **Family:** *Enterobacteriaceae* - Rahn, 1937, Nom. Cons.
- **Genus:** *Escherichia* - Castellani & Chalmers, 1919, nom. cons.
- **Specific descriptor:** *coli* - (Migula 1895) Castellani and Chalmers 1919 (Approved Lists 1980)
- **Scientific name:** - *Escherichia coli* (Migula 1895) Castellani and Chalmers 1919 (Approved Lists 1980)

1.4. Motivation

In the last decade, terrorism has become more and more present all over the globe. From classical bombes, anthrax infested letters (September 2001, USA, 11 letters) to water reserve infestation is only a small step. Governments all over the globe invests huge amounts of money for preventing and dealing with all kinds of terrorism, from state terrorism, bioterrorism, ecoterrorism, nuclear terrorism, all the way to cyberterrorism. The truth is that is better to prevent than to cure but when secret services fail, a second line of defence is to detect the infestation as soon as possible and to block all the processes so to limit the number of people affected. Cutting edge science made huge progress over the last years, from E Nose to artificial vision for blind people [4]- [8] new application are emerging and also old technologies are improved [9]- [10] so is a continuous battle of cat and mouse between terrorists and governments based on cutting edge technologies and imagination. The thesis is multidisciplinary and involves fields like electronics, biology, chemistry and electrochemistry. There are many fields of activity that involve all kind of sensors. All those sensors or reading heads need a system to read and quantify the information carrier signal. Because of the wide range of principles which the sensors operation are based on, the signal conditioning systems available today are sensor-orientated and are not able to work with more than one type of sensors.

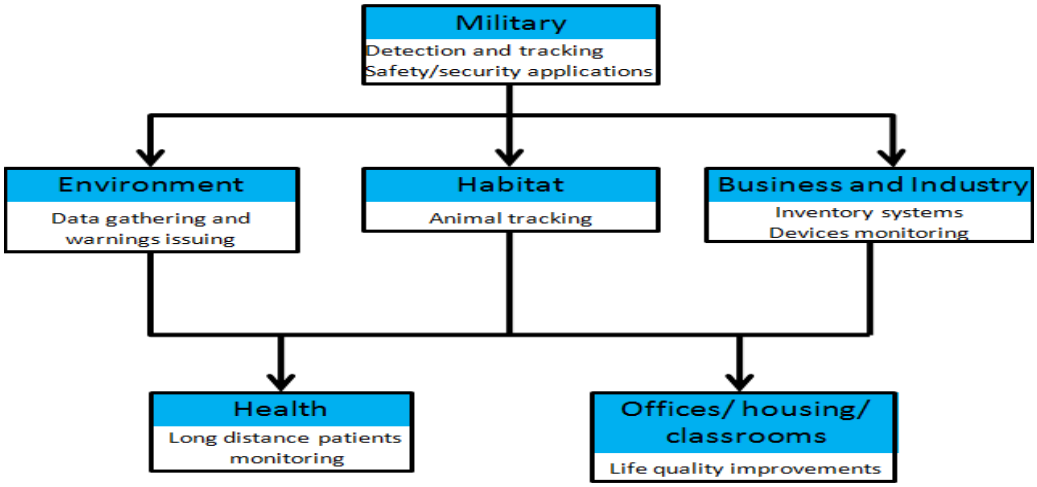

Fig. 1.2 Application oriented sensor application areas classification.

The author claims contributions in chapters 3, 5, 6 and 7, chapters 2 and 4 which have the role to introduce the reader into biotechnology, sensors and state of the art in electronics in general and system conditioning systems specially. The system presented in this work is made to be used in water analysis and toxin detection. It consists of an 8X8 array of electrochemical and bioluminescent sensors, selection system and signal conditioning system. The system is created to detect toxins in water and works with both electrochemical and bioluminescent sensors. Another reason why I chose this research is because it combines electronics with biology, chemistry and electrochemistry thus it is an opportunity to study new fields.

2. BIOSENSORS TECHNOLOGY, A LITERATURE SURVEY

In this chapter the author makes an introduction into the amazing world of biotechnology, with accentuation on electrochemical sensors types, fabrication and deposition based on literature survey. The author is presenting the main types of sensors, classification and functionality based on their sensing element, transducer and the variation that it measures.

The role of this paragraph is to show the complexity of the sensor world and the multitude of applications in which the sensors can be used. The author makes the bio sensors a priority of this paragraph. In the first section of this chapter, the author is presenting the basic concepts of biosensors based on their principles and functionality. In the second section of this chapter, a short review of bioluminescent principles and mechanisms is reported. After, special attention is given in section 3 to the electrochemical sensors in general and amperometric sensors in special. The amperometric sensors are detailed with reviews of mediators, mechanisms involved and significance of mediated sensors, cell deposition and integration. In this paragraph, the author does not claim any originality or contributions other than gathering the materials.

2.1. A brief overview of biosensors

A device that transforms chemical information ranging from concentration of a given chemical compound to total analysis into an useful and quantifiable signal, usually light, current or voltage is called chemical sensor. The information obtained, mentioned above, may originate from a physical property of the integrated system or from a chemical reaction.

A device that provide information about physical property of a system is called physical sensor. Biosensors concept was borne in 1962 when enzyme electrode was designed by scientist Leland C. Clark. After this moment, communities of researchers from various fields as VLSI, biology, physics, chemistry, material science, biotechnology and so on showed increased interest in developing more tough, dependable, reliable and more sophisticated biosensing devices for fields such as medicine, agriculture, environmental monitoring etc.

An essential component of an analyzer is the reading head, chemical sensor**.** Other than the reading head, the analyzer contains devices that perform functions as : sampling, sample transport or signal processing. An analyzer is an important part of an automated system. The analyzer working according to a sampling plan as a function of time acts as a monitor.

At least three functional units are contained in biochemical sensors, a receptor part, a transducer part and a membrane that works as a separator. Not all biochemical sensors contain the third element, the membrane.

Biosensors are also known as *immunosensors*, *optrodes*, *chemical canaries*, *resonant mirrors*, *biochips*, *biocomputers* etc. A commonly accepted definition is [11]: "a lab on a chip is a chemical sensing device in which a biologically derived recognition entity (cells, bacteria, tissue) is coupled to a transducer, to allow the quantitative development of some complex biochemical parameter", or "a biosensor

is an analytical device incorporating a deliberate and intimate combination of a specific biological element (that creates a recognition event) and a physical element (that transduces the recognition event)".

A very specific analyte activate a specific "living" element (enzyme or cell) and the "transducer" element translate the change from the biomolecule into an useful, measurable signal. The living element is very specific to the analyte to which it is sensitive. It does not recognize other analytes so one can know for sure which element was present when the sensor was activated. On the other hand, the problem is that for a wide range of elements to be detected one need a wide range of bio elements.

The major application so far is in blood glucose sensing because of its abundant market potential.

The chemical information is transformed into a form of energy by the receptor part of a sensor, usually electrical or electrochemical, which is detected and measured by the transducer.

The transducer is the component that transforms the energy carrying the chemical information from the actual reading head into a useful analytical signal, usually electric signal. The transducer, being usually an electronic circuit, does not show selectivity. The receptor part of chemical sensors may be based upon several principles:

- physical, where no chemical reaction takes place.
- chemical, in which a chemical reaction gives rise to the analytical signal.
- biochemical.

Electrochemical devices, devices that are used in this research, transform the effect of the electrochemical interaction analyte – electrode into a useful signal. Such effects may be stimulated electrically. The electrochemical biosensors are divided in 2 main categories:

a) voltmetric sensors, including amperometric and conductimetric devices, in which current is measured in the d.c. or a.c. mode.

b) potentiometric sensors, in which the potential of the indicator electrode is measured against a reference electrode.

A special class of electrochemical sensors started to emerge, chemically sensitized field effect transistor (CHEMFET) in which change of the source-drain current is obtained in the effect of the interaction between the analyte and the active coating.

The interactions between the analyte and the coating are, from the chemical point of view, similar to those found in potentiometric ion-selective sensors.

The signal arises from the change of electrical properties caused by the interaction of the analyte is typical for another classification of sensors based on measurements, where no electrochemical processes take place.

a) organic semiconductor sensors, based on the formation of charge transfer complexes, which modify the charge carrier density.

b) electrolytic conductivity sensors.

c) metal oxide semiconductor sensors used principally as gas phase detectors, based on reversible redox processes of analyte gas components.

d) electric permittivity sensors [11].

Biosensors have tremendous potential for commercialization in many fields of application. In spite of this potential, however, commercial adoption has been slow because of several technological difficulties. For example, due to the presence of biomolecules along with semiconductor materials, biosensor contamination is a major issue.

2.1.1. Basic concepts for biosensors

A biosensor consists of a bio-element and a sensor-element. An enzyme, antibody, living cells, mammalian tissue, etc can be the living element, while sensing element may be electric current, electric potential, light, heat and so on. A detailed list of different possible bio-elements and sensor-elements is shown in [12]. Different combinations of bio-elements and sensor-elements constitute several types of biosensors to suit a vast pool of applications.

The "living" and the "sensor" elements can be coupled together in one of the four possible ways:

- Membrane Entrapment
- Physical Adsorption
- Matrix Entrapment, and
- Covalent Bonding.

A semi permeable membrane separates the analyte and the bioelement in the membrane entrapment scheme, the sensor being attached to the bioelement.

The physical adsorption scheme is dependent on a combination of van der Waals forces, hydrogen bonds, hydrophobic forces, and ionic forces to attach the biomaterial to the surface of the sensor. The porous entrapment scheme is based on forming a porous encapsulation matrix around the biological material that helps in binding it to the sensor. The sensor surface is treated as a reactive group to which the biological materials can bind in the case of the covalent bonding.

The typically used bio-element is a large protein molecule that acts as a catalyst in
chemical reactions, but remains unchanged at the end of reaction. This enzyme forms a complex molecule which under appropriate conditions forms the desirable product molecule releasing the enzyme at the end, in a reaction with a substrate.

2.1.2. Types of biosensors

In this section we will discuss some common types of biosensors available on the market or for laboratory use. The classification is made so the reader may be able to understand the comprehensive world of biosensing devices.

Optical-detection Biosensors

The output transduced signal that is measured is light for this type of biosensor. The biosensor can be made based on optical diffraction or electrochemical luminescence. A silicon wafer is coated with a protein for optical diffraction based devices,. The wafer is exposed to UV light through a photo-mask and the antibodies start to be inactive in the exposed regions. When the diced wafer chips are incubated in an analyte, antigen-antibody bindings are formed in the active regions, a diffraction grating is created. This grating produces a diffraction signal when illuminated with a light source such as laser. The resulting signal can be measured.

Resonant Biosensors

An acoustic wave transducer is coupled with a bio-element in this type of biosensor. The mass of the membrane changes when the analyte molecule (or

antigen) gets attached to the membrane. The resulting change in the mass subsequently changes the resonant frequency of the transducer. This frequency change is the carrier of information.

Thermal-detection Biosensors

Based on one of the fundamental properties of biological reactions, namely absorption or production of heat, which in turn changes the temperature of the analyte in which the reaction takes place. They are constructed by combining immobilized enzyme molecules with temperature sensors. The heat reaction of the enzyme is measured when the substance to be analyzed comes in contact with the enzyme, and is calibrated against the analyte concentration. The measurement of the temperature is typically accomplished via a thermistor, known as enzyme thermistors. Usually applications of this biosensor include the detection of pesticides and pathogenic bacteria.

Ion-Sensitive Biosensors

Use semiconductor FETs that have an ion-sensitive surface. When the ions and the semiconductor interact, the electrical potential change. The change in the potential can be measured. This type of biosensor are used for pH detection.

Electrochemical Biosensors

Electrochemical biosensors are mainly used for the detection of hybridized DNA, DNA-binding drugs, glucose concentration, toxicagents etc. The underlying principle for this class of biosensors is that many chemical reactions produce or consume ions or electrons which in turn cause some change in the electrical properties of the solution which can be sensed out and used as measuring parameter. Electrochemical biosensors can be classified based on the measuring electrical parameters as:

(1) Conductimetric

The carrier of the information is the electrical conductance / resistance of the solution. The overall conductivity or resistivity of the solution changes when electrochemical reactions produce ions or electrons. This change is measured and calibrated to a proper scale. Conductance measurements have relatively low sensitivity. The electric field is generated using a sinusoidal voltage (AC) which helps in minimizing undesirable effects such as Faradaic processes, double layer charging concentration polarization etc.

(2)Amperometric

This high sensitivity biosensor can detect electroactive species present in biological test samples. The measured parameter is current. Since this type of sensors are the main sensors for what the system is designed for, a greater attention will be given in next chapters.

(3)Potentiometric

In this type of sensor the measured parameter is oxidation or reduction potential of an electrochemical reaction. The working principle relies on the fact that when a ramp voltage is applied to an electrode in solution, a current flow occurs because of electrochemical reactions. The voltage at which these reactions occur indicates a particular reaction and particular species [13].

A more detailed history of sensors and companies that used to produce and still producing sensors is presented in [14].

2.1.3. Mechanism of bioluminescence

First, the author will present the mechanism of bioluminescence. The SOS response is a common used biological mechanisms in whole cell biosensors. The SOS response in the bacteria E coli activate many proteins involved in detecting and repairing DNA damaged by a variety of agents, UV radiation, chemicals etc. The synthesis of DNA in *E* Coli is inhibited by Nalidixic acid (NA) analyte by the process of binding the Nalidixic acid to gyrase enzymes. During DNA replication, the ability of gyrase to relax positive supercoils comes into play. This relaxation starts when gyrase analyte complex attached to chromosomal DNA it damage the DNA and create lesions. The LexA (Lex) repressor undergoes a self cleavage reaction when the cell senses the presence of an increased level of DNA damage, and the SOS genes are depressed. Two proteins, the LexA repressor and the RecA filament (Rec) play key roles in the regulation of the SOS response, RecA filament (Rec) induces the LexA cleavage reaction, which can be described as:

$$\frac{dLex}{dt} = \frac{\alpha_x}{1+\beta_x Lex} - \gamma_x Lex - \theta_x Rec\ Lex \tag{2.1}$$

where Lex are the concentration of the LexA. The first term models the self repression of LexA production, in steady state with Hill coefficient 1. The second term describes the degradation of the LexA in non damaged cell and the third term describes the reaction of the cleavage of LexA by RecA filament. Microorganisms survive in a wide variety of harsh environments by processing information and arriving at 'decisions' (what to metabolize, what to transport into the cell, where to locate or attach, etc.) that are imperative to cell survival. Even in simple cells, this is a complex operation that involves memory, sensing, feedback, and communication. Even a casual glance at the information processing density of prokaryotic cells will produce a major appreciation for the advanced state of the cell's capabilities. A bacterial cell, such as E coli (~2 μm2 cross-sectional area) with a 4.6 million basepair chromosome, has the equivalent of a 9.19 megabit memory. The cell uses to code, a portion of its memory as many as 4300 different polypeptides under the inducible control of several hundred promoters [15].

If we assume just 4 transistors/ logic function, then 2 μm^2 of silica (Si) could contain approximately three simple logic gates or a 0.5 kbit memory. Even this level of functionality depends on an unsure path of technology development that will require breakthroughs in lithography, materials, processing, defect detection, as well as many other areas of technology in the future. For scientists, today, is impossible to approach bacterial-scale integration today or within the closest future. Furthermore, microorganisms have some qualities that are desirable for sensing, information processing and actuating devices and systems that are not yet replicated by human devices. They are relatively tough 'devices' that exist in such diverse environments as deep-sea, without light or oxygen, sub-zero arctic seawaters, water saturated with organic solvents, contaminated soils and industrial wastes [16]. The ability to survive in such harsh environments of organisms is a consequence of their capacity to sensing and adjusting to changing environmental conditions and ability to process information. Prokaryotic cells are suitable to

genetically manipulation due to the diverse set of gene systems possessed. These cells can easily be incorporated into a 3D instead of the 2D structures of integrated circuits. Cells are very easy to manufacture and require no lithography, mask alignment or other technologically challenging processing steps to produce highly functional systems because of their self-replicating and self-assembling into groups capacity (biofilms). The usage of biological material in devices and systems is not new. In the last decade, using nucleic acids, enzymes and whole cells as sensing elements significant progress has been made.

Many whole-cell biosensors used electrochemical transducers to detect the activity of growing cells. Cells or bioreporter strains that have much greater sensitivity and selectivity ware produce more recently with the help of the developments registered in molecular biological techniques. The bioluminescent bioreporter integrated circuit is one such device that combines the information processing capabilities of genetically engineered whole cells and the functionality, ruggedness and inexpensive fabrication of integrated circuits. This biosensor accesses a small portion of the capabilities of the cells by accepting a chemical or physical input, addressing a small part of the cell's DNA memory by interacting with a particular promoter, generating outputs in the form of a few polypeptides and communicating through bioluminescent means [16]. Since cell-based biosensors provide detection capability for previously unknown agents due to the usage of direct measurements of physiologic function (toxins that induce changes). Cell-based biosensors are distinguished by these properties from molecular biosensors that rely on the detection of molecular events such as antibody binding, DNA hybridization, or enzymatic reactions. Even if these sensors are limited to the detection of specific known agents, they can provide high sensitivity. Additionally, detection of a binding event does not provide any information on the physiological effects of the analyte. In the fields of environmental monitoring and detection of chemical and biological warfare agents there are numerous applications for the functional screening of unknown agents. Two transduction stages can describe cell-based biosensor. Converting detected analyte into a biochemistry response (product), the cells serve as the primary transducer. A secondary transducer is required to convert the biochemistry response signal into an electronic signal that can be processed and analyzed. Optical (luminescence or fluorescence) and electrochemical methods are the most common in transducing cellular responses. A variety of different primary transducers have been used to create Cell Based Biosensors, such us mammalian cells, animal tissue and bacteria. Microbes or bacteria have been employed as the most useful and common detectors in numerous Cell Based Biosensors. When compared with cells from higher organisms, microbes are readily amenable to genetic manipulation, stable in various environmental settings, easily to prepare and multiply and require minimal maintenance. Different works have presented and described whole cell based biosensors, based on Bioluminescence signal which is integrated with CMOS silicon chip. Usually, the cell-cartridge contains a CMOS silicon chip that incorporates a digital interface, temperature control system, microelectrode electrophysiology sensors, and analog signal buffering [15].The choice of the gene promoter determine the specificity of the different strains of bacteria or microbes. Very little attention has been devoted to biochips long-term storage and use in an immobilized form, in field utilization while the high sensitivity and applicability of these and similarly constructed bacterial sensor cells under controlled laboratory conditions has been repeatedly demonstrated. Integration of such microorganisms in solid-state matrices is an important step on the way to the conversion of these bioassays

into user-friendly sensing devices capable of continuous monitoring or multiple use detection.

A few attempts to integrate genetically engineered bacteria in solid matrices based on encapsulation in soft gels were reported. In [17]- [19] was reported that, due to the thick films, alginate-based matrices suffer from diffusion limitations but viable biosensors have been created. Alginates are unstable in calcium-poor solutions and deteriorate in the presence of phosphate. The low deformation resistance and the biodegradability of most soft gels are additional impossible to be overcome problems for a search for an alternative encapsulating procedure. A first step in the construction of complex sensing elements is provided by the technology for bonding antibodies on different flat or porous substrates which is very versatile and well developed. The successful combination of this generic approach with reporting microorganisms opens the way for their incorporation on or in virtually any substrate [19].

2.1.4. Bioluminescent sensors

Light emission concepts from luminescent and fluorescent bacteria and more recently, yeast, ware created to act as reporters for various environmental conditions is finding application in several areas of biology, including toxicity assays for environmental pollutants, chemical detection and gene expression profiling [20]-[22]. The importance of bioluminescence as a marker for gene expression was first described in 1985, when a DNA fragment from the marine bacteria Vibrio fischeri was used to construct recombinant E coli strains that produced light as a response to activation of a specific gene. In the same time the understanding of bioluminescence biochemistry [23]- [25] has become. The use of green fluorescent protein (GFP) as a gene expression marker was first described, the properties of GFP having been described in [26] and later [27]. There are three major areas in which luminescent and fluorescent reporters are being used.

The first is for nonspecific environmental reporting. For these applications, the lux operon [28], [29] or gfp gene [30], [31] was fused to a stress response promoter that responds to more than one chemical stresses. For instance, the heat shock response is activated when environmental conditions cause changes in protein structure, and the SOS regulatory circuit is activated in response to DNA damage. A second area is that of monitoring for specific substances in the environment. Examples include reporters for metals (Interactions between metals, microbes and plants – Bioremediation of arsenic and lead contaminated soils [32] and organic compounds [33], [34]. Chains of strains ware created in which lux and gfp fusions representing large portions of the bacterial genome can be used as an alternative to microarray technology and for clarifying metabolic pathways [35]- [37]. Similar examples of these applications exist with yeast as the model organism [38], [39].

The choice between the use of luminescence and fluorescence must be taken having in mind the application for what the sensor was designed for. Faster response time [35] and a lower detection limit are the advantages of the lux system. Because of the absence of the interference that cellular autofluorescence causes when gfp is used determine the lower detection limit [40]. The fact that gfp is not a self-regulator like lux represents an advantages of gfp [41] and that the response of autofluorescent gfp is independent, regardless substrate concentrations in the medium. High-throughput experiments are generally made with fluorescent and luminescent bacteria on agar plates, in microtiter plates, or shake flasks.

Limited data is imposed by these approaches because in such systems a lot of growth parameters cannot be measured online. On the other hand, when growth data is needed bioreactors are used [42], [43]. One must keep in its mind that this approach is both time-consuming and costly. Furthermore, the very concept of the experimental design dictates that a large number of experiments are needed because an indicator for gene expression are the fluorescent and luminescent response. A researcher can run multiple small-scale experiments in parallel due to the ability to measure fluorescence and luminescence in integrated, multiplexed micro bioreactors, with the cost of decreasing the resources needed per experiment as well as increasing the number of experiments needed to be run. The collection of additional data such as growth kinetics, dissolved oxygen over time, and pH are possible because of the use of a microbioreactor with integrated sensors.

When shake flasks and microtiter plates are used [44], [45], this information is generally not available. Genetically engineered cells, bacteria or mammalian cells designed to detect environmental pollutants using promoters and reporter genes are called generically microbial biosensors.

Typically, also for this type of sensors, *E coli* bacteria in which plasmids containing the promoter-reporter gene conjugation are introduced are used as bio element. Expression genes that encode for proteins or enzymes that function as light sources or electron sources for monitoring metabolic cell activity (SOS response in presence of different chemicals) are the roles of reporters.

Bio-reporter expression activators are promoter genes. As activators, environmental pollutants, , activates promoter genes (SOS), starts a genetic signal transduction and regulates the intensity of the bio-reporter emission. Whole cells metabolize the pollutants, the genetic control mechanism turns on the synthesis of the reporter. Microbial cell sensors have been constructed by genetically binding the *Lux* gene with an inducible gene promoter for toxicity testing. Genetic promoters are utilized to act as precise detectors of environmental toxins. Providing a readable signal response correlated to the magnitude of the bio-chemical input is the main function of the bio-reporters , the promoter exposed to an analyte, transcribing messenger RNA (mRNA), which is in turn translated into a light emitting reporter [46].

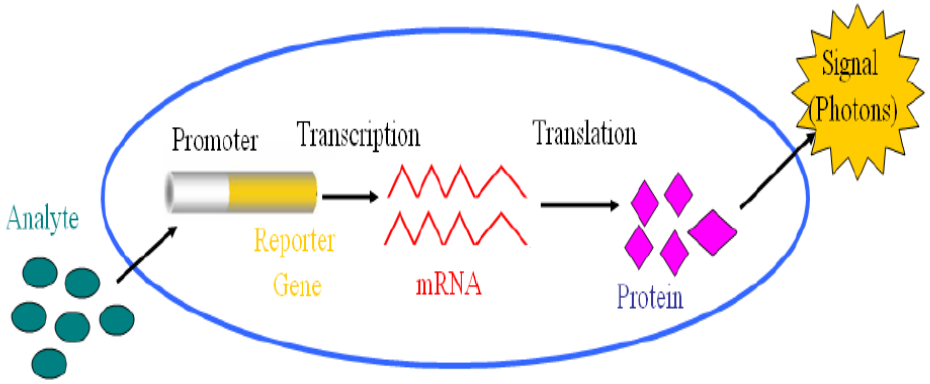

Fig. 2.1. The anatomy of bio-reporter organism.

2.1.5. Bioluminescent concepts

In the last years, the main goal of electrochemical and biological scientist working with micro fluidic systems was to integrate complete analytical process into one micro device, labonchip that can perform sequential sampling, sample pretreatment, analytical separation, chemical reaction, analyte detection, and data analysis operations. As a result, the development of miniaturized detection modules with high sensitivities and signal-to-noise ratios, fast response times and multiplex functions for microfluidic systems is an important issue that needs to be addressed. There are numerous reports of integrating various detection schemes with microfluidic systems, which can be categorized into optical detectors, electrochemical detectors, mass spectrometric (MS) detectors and nuclear magnetic resonance (NMR) detectors according to the different detection principles. Among these detection methods, optical and electrochemical detection techniques are the most frequently employed.

The biological and biochemical fields have wide applicability in the areas of bio-warfare, clinical medicine, biological experimentation and environmental monitoring. Medical diagnostics still works with time consuming, expensive to use and expensive to train personnel techniques. Unfortunately, modern days medicine deals with methods that take days or even weeks to have the results of test for infection disease.

Small , complex, integrated on chip micro-total analysis systems (μTAS) engaged to provide immediate point of care services that would facilitate detection of disease and bio-warfare agents. A wide are of sensing designs have been developed for molecular detection, such as electrochemical, optical absorption etc. Anyhow, fluorescence sensing remains the most widely used methodology in biotechnology, followed closely by electrochemical and amperometric sensors methodologies, thus electrochemistry recorded fast advance in recent years. Separation technologies, such as capillary array electrophoresis and micro-array technology use fluorescent labeling for the detection of proteins and DNA. Fluorescence detection offers tremendous sensitivity, specificity, complexity and compatibility compared standard biochemical reactions, such as polymerase chain reaction (PCR). Bio-fluorescence traditional and universal accepted readers use bulky and discrete elements, which are expensive and require large footprint and extremely precise alignment and they are highly susceptible to errors. The advantages of biological analysis systems are dramatically reduced when these systems is based on fragile and expensive, hard and time consuming to fabricate optical sensing equipment. Integrated on-chip sensing architectures make portable and robust medical care equipment practical. As a result of the recent explosion in optoelectronics for telecommunications, a variety of interesting and useful integrated optical sensing architectures can now be realized [47].

In Fig. 2.2 it has been illustrated some possible general sensor architectures with vertical oriented optical devices, such as VCSELs, PIN photodiodes and emission filters. For focusing the laser beam and collecting the fluorescence the imaging concepts use refractive or diffractive micro-optics [48]. The proximity sensor permits the laser beam to propagate freely to the biological sample, and a large detector area that surrounds the VCSEL, collecting fluorescence. Gratings are used in this architecture of waveguide to couple the laser beam into the waveguide. After, the fluorescence is collected by the waveguide and coupled out onto the detector.

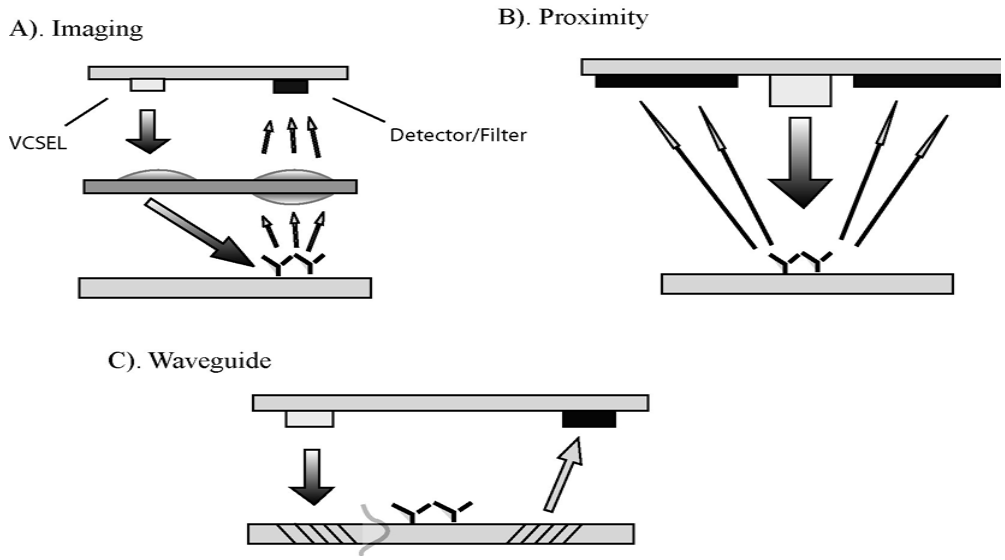

Fig. 2.2 Possible general luminescent sensor architectures [48].

In the last years, the main goal of electrochemical and biological scientist working with micro fluidic systems was to integrate complete analytical process into one micro device, labonchip that can perform sequential sampling, sample pretreatment, analytical separation, chemical reaction, analyte detection, and data analysis operations. As a result, the development of miniaturized detection modules with high sensitivities and signal-to-noise ratios, fast response times and multiplex functions for microfluidic systems is an important issue that needs to be addressed. There are numerous reports of integrating various detection schemes with microfluidic systems, which can be categorized into optical detectors, electrochemical detectors, mass spectrometric (MS) detectors and nuclear magnetic resonance (NMR) detectors according to the different detection principles. Among these detection methods, optical and electrochemical detection techniques are the most frequently employed.

Due to their accessibility in laboratories and the simplicity of the microfluidics–detector interface optical detectors are commonly used. Electrochemical detection offers good detection limits for various analytes of biological interest and so it is preffered to integrate such a detector with other microfluidic components within a microchip. Due to recent growing of interest in molecular biology has also determined the development of micro-scale architectures that interface microfluidics with mass spectrometers (MS). The ability to fabricate microfluidic systems with very complex structures and with compatible dimensions between the microfluidics and biological cells has generated significant attention among those developing microchips that can analyze the biophysical and biochemical functions of cells. In the same way as cell-based microfluidics have become versatile tools for biosensing, diagnostics, drug screening and biological research, detector modules for microfluidic based cells have also undergone major development over the past years [49]. Usually for cells involving bacteria, E coli is most commonly used for both electrochemical and bioluminescent sensors.

Another reason for combining the 2 types of sensors is because, using the same type of bacteria to detect toxins in the water, soil etc. one can use the same cell both as electrochemical and bioluminescent sensor, in this way reducing area on chip, maximizing in the same time the number of sensors used so improving the sensitivity of the system.

Electrochemical sensors also require very little power to operate reason for what the sensors are widely used in portable instruments that contain multiple sensors. They are the most popular sensors in confined space applications.

A life sensor's expectancy is usually predicted by its manufacturer under conditions that are considered normal. Thus the life expectancy of the sensor is highly dependent on the environmental contaminants, temperature, humidity and other chemical and mechanical factors to which it may be subjected to in lab or in field applications.

The life expectancy of an electrochemical sensor depends on a large number of factors, including the toxins to be detected , the environmental conditions in which the sensor is used, type of bacteria and genetically modifications. Generally, a one- to three-year life expectancy is specified. The oldest electrochemical sensors date back to the 1950s and were used for oxygen monitoring. More details about sensors can be found in [50].

2.2. Electrochemical biosensors

In the last few years, electrochemical biosensors had become the most commonly used class of biosensors. In electrochemical sensors or 3 electrode cells, electrons are consumed or generated during a biointeraction processes, resulting an electrochemical signal which can in turn be measured by an electrochemical detector, potentiostat and analyzed. Electrochemical biosensors are suitable to miniaturization, widely accepted in biosensing fields and have comparable instrumental sensitivity. Electrochemical biosensors are most often based on potentiometry and amperometry. Ion selective electrodes (ISE), ion selective field effect transistors (ISFET) and pH electrodes are based on the oxidation of the substrate/ product e.g. oxygen electrode, detection of H2O2. Depending upon the electrochemical principle used, electrochemical biosensors are further divided into :

- conductometric,
- potentiometric and
- amperometric biosensors.

Conductometric biosensors measure the changes in the conductance between a pair of metal electrodes as a consequence of the biological component [51]. The electrochemical biosensors, recently attracted much attention. They can be classified into several types depending on the mode of detection.

Potentiometric biosensors [52]- [55] consist of measurement of potentials between the working electrode and the reference electrode. They monitor the accumulation of charge, at zero current, created by selective binding at the electrode surface and function under equilibrium conditions.

Amperometric biosensors measure, due to direct oxidation of the products of a biochemical reaction, the changes in the current on the working electrode. Amperometric techniques give a normal dynamic range and a response to errors in the measurement of current and are linearly dependent on analyte concentration. Oxygen and H_2O_2 being the co-substrate and the product of several enzyme reactions, are detected for amperometric estimation [56], [57].

Electrochemical biosensors are based on electron transfer, mediated or unmediated.

Different conducting polymers have also been used for fabricating electrochemical biosensors,. Amperometric biosensors may be used as direct or indirect systems. Indirect sensors are based on conventional detectors utilization for measure the metabolic substrate or product of biological material. Direct amperometry concept is based on biological redox reaction, with an intimate relationship between biology and electrochemistry. Modified electrodes are involved, with, usually an electron acceptor in place of the natural electron donors. The fact that are cheaper and highly sensitive are the two main, well known qualities of amperometric biosensors, qualities that make them suitable for the clinical, environmental and industrial purposes. Being capable of directly transduce the rate of reaction in currents, the amperometric enzyme electrodes have been used widely. Amperometric biosensors function when a potential is applied between two electrodes, starting the production of a current. The simplest amperometric biosensors are based on the Clark. This oxygen electrode consists of a platinum cathode (where oxygen is reduced) and a Ag/AgCl reference electrode when a potential of −0.6 V versus Ag/AgCl electrode is applied to the Pt electrode, a current proportional to the oxygen concentration is produced.

$$\text{Ag anode: } 4Ag + 4Cl \rightarrow 4AgCl + 4e^- \tag{2.2}$$

$$\text{Pt cathode: } O_2 + 4H^+ + 4e- \rightarrow 2H_2O \tag{2.3}$$

The rate of electrochemical reduction of O_2, in this case, depends on the rate of diffusion of the oxygen from the bulk solution. The rate of diffusion, in turn depends on the concentration gradient and hence the bulk oxygen concentration, alternatively, the rate of production of H_2O_2 directly by applying a potential of 0.68 V versus Ag/AgCl to the Pt electrode.

$$\text{Pt anode: } H_2O_2 \rightarrow O_2 + 2H^+ + 2e^- \tag{2.4}$$

$$\text{Ag cathode: } 2AgCl + 2e \rightarrow 2Ag + 2Cl^- \tag{2.5}$$

The most important factor is the concentration of dissolved oxygen in the bulk solution [58], [59] for these 'first generation biosensors'. For overcoming these problems, the 'second generation biosensors' concept was borne, using artificial electron acceptors concepts which can avoid the reduction of oxygen. In these biosensors, all the substances with conversion potential lower than the electrode potentials contribute to the overall signal. Applying a potential as low as possible is essential. In this context, a few artificial electron acceptors having low oxidation potentials were discovered. These artificial electron acceptors are actually the mediators. This approach leads to the development of mediated biosensors and considerable reduction of electrochemical interferences. Mediated biosensors are constructed with several types of enzymes that can donate electrons to electrochemically active artificial electron acceptors. Mediated electron transfer from an enzyme to an electrode may be studied in rapid systems using direct current (dc) cyclic voltammery and established reaction kinetics [60].

The second generation biosensor concept involves a two step procedure in which the enzyme takes part in first redox reaction with the substrate and is reoxidized by a mediator and after, the mediator is oxidized by the electrode.

$$\text{Gluconolactone+GOD/FADH}_2 \quad (2.6)$$

$$\text{GOD/FADH}_2\text{+2MGOD/FAD+2 M*+2H}^+ \quad (2.7)$$

$$\text{2M*2M+2e}^- \quad (2.8)$$

where FAD represents a flavin redox center in GOD and the mediator, M/M* are the oxidized and reduced mediator in forms.

The immobilization of the redox species are carried out by adsorption, covalent attachment and polymer coating. The operational stability of the sensor can be increased only if the fixed concentration of an acceptor of electrons is retained within the layer of enzymes. Some electrodes have been developed, electrodes which can directly oxidize the reduced enzyme and so, do not require any exogenous mediator. These electrodes have been called 'third generation biosensors'. Such enzyme electrodes can be prepared by the coating of the electronic conductors (conducting salts) and are stable for several months.

The current produced in the amperometric biosensors can be related to the rate of reaction (VA) by the equation (2.9)

$$i=nFAVA \quad (2.9)$$

where n is the number of electrons transferred, F is Faraday constant and A is the electrode area. Usually the rate of reaction is a diffusion controlled phenomenon where the current produced is proportional to the analyte concentration and independent of both the enzyme and electrochemical kinetics because of external membranes ussage [61].

Biochips can be used for a large area of application fields, ranging from laboratory- based assays to in situ environmental monitoring. For "in lab" purposes, microfluidic devices are designed for performing continuous-flow biochemical and cell-based assays, having the potential for implementing high throughput screening in formats that integrate up-front compound handling with unique assay functionality. For environmental purposes, examples include biochips incorporating genetically engineered microorganisms, cells, tissue for the detection of either toxic effects or of specific classes of chemicals.

2.2.1. Physical mechanism of electrochemical cells functionality and fabrication

As it has been previously stated, cells can be integrated onto a functional biochip either by direct attachment to its surface or by embedding in a suitable polymer. Direct surface attachment can be improved by chemical modification of the solid substrate and/or biological modification of the cellular surface properties. Deposition of live cells or any other biological material, needs to obey to the restricting constraints of the biological environment such as temperature, pH, or ionic strength, as well as to the vulnerability of the cells to mechanical stress. Once deposited, the coupling to the solid substrate can be based on covalent bonding, ionic or affinity interactions [62].

The mechanisms involved in bacterial cell adhesion to solid surfaces or the development of the biomaterial onto a mature biofilm are relevant to many biomedical, industrial, environmental and military applications. Suspended bacteria

tend to colonize on solid state surfaces forming biofilms [63] which are heterogeneous and complex structures of cells grouped in a hydrated extracellular matrix comprised of polysaccharides, proteins, lipids and so on. A few distinctive steps characterize biofilm formation, begining with an initial pre-attachment of soluble molecules e.g. proteins to the surface, than reversible attachment of cells, which becomes irreversible following the secretion of specific polysaccharides and the expression of adhesins, leading to the formation of a mature and stable biofilm. In the biomedical applications case, many pathogenic bacteria attach and colonize both on medical devices and on tissues, forming highly resistant antibiotic biofilms. Monitoring of the process of biofilm formation using several electrochemical and optical techniques ware reported [64]- [66]. The electrochemical monitoring techniques usually include impedance measurements [67], voltammetry and amperometry on various substrates [68] and on rotating disk electrode (RDE) , corrosion potential, polarization resistance measurements and self-referencing technique, a sensing technique which is used in non-invasively measuring real time analyte flux.

All the electrochemical measurements on biofilm were focused on the detection of enzymatic activity monitored by the oxidation of small molecules as hydrogen peroxide. These measurements are based on amperometric, potentiometric and impedance detection methods. Electrochemical impedance spectroscopy (EIS) has been previously applied to bacterial cells attachment monitor [69]– [72] and formation of biofilm [73]– [75] when various bio electrical modeling approaches were used to characterize the electrode/ electrolyte and the electrode/electrolyte/bacteria interfaces, the electrode polarization resistance, and the corrosion rate of metallic substrates to interpret the measured impedance data. The anomalous diffusion theory is used to model the effect where some particles in the electrolyte remain stuck due to interactions with the surrounding bio- material environment, for a long time and diffusion is slower (subdiffusion) [76].

Amperometric biosensors measure the changes in the current on the working electrode based on direct oxidation of the products of a biochemical reaction. Amperometric techniques are linearly dependent on analyte concentration giveing a normal dynamic range and a response to the current errors. For electron transfer electrochemical biosensors are based on mediated or unmediated electrochemistry. Ferrocene and its derivatives, ferricyanide, methylene blue, benzoquinone and N-methyl phenazine etc. are most commonly used mediators in mediated biosensors but also various conducting polymers such as polyaniline, polypyrrole etc. have been used on common bases for fabricating electrochemical biosensors. Direct/indirect systems are the bases for amperometric biosensors. For measuring the metabolic substrate or product of biological material, indirect sensors exploit conventional detectors. Direct amperometry involves a biological redox reaction, with an intimate relationship between electrochemistry and biology. The amperometric biosensors are known to be reliable, cheaper and highly sensitive for the clinical, environmental, experimental and industrial purposes.

2.2.2. Functionality of amperometric biosensors

As they are capable of directly transducing the rate of reaction into a current amperometric enzyme electrodes have been commonly accepted. Amperometric biosensors functionality is based on the production of a current when a potential is applied between two electrodes. The simplest amperometric biosensors are based

on the Clark oxygen electrode. This consists of a platinum cathode (where oxygen is reduced) and a Ag/AgCl reference electrode when a potential of −0.6 V versus Ag/AgCl electrode is applied to the Pt electrode, a current proportional to the oxygen concentration is produced.

Ag anode: $$4Ag + 4Cl^- \rightarrow 4AgCl + 4e^- \quad (2.10)$$

Pt cathode: $$O_2 + 4H^+ + 4e^- \rightarrow 2H_2O \quad (2.11)$$

The rate of electrochemical reduction of O_2 closely depends on the rate of diffusion of the oxygen from the bulk solution. Bulk Solution is dependent the bulk oxygen concentration and on the concentration gradient.

These 'first generation biosensors' are dependent on the concentration of dissolved oxygen in the bulk solution. In order to overcome these problems, the concept of using artificial electron acceptors evolved in the 'second generation biosensors' which can avoid the reduction of oxygen. In these biosensors, all the substances having conversion potential lower than the electrode potentials contribute to the overall electrochemical signal. The most common example is the oxidation potential of +600 mV of H_2O_2 along with other metabolites such as uric acid, ascorbic acid, glutathione etc. that also get oxidized and interfere with the electrochemical signal. It is mandatory to apply an electrode potential as low as possible. In this context, artificial electron acceptors having low oxidation potentials have been discovered. These artificial electron acceptors are commonly called mediators. This approach leads to an important reduction of electrochemical interferences and the development of mediated biosensors. Mediated biosensors can be constructed with the enzymes that can donate electrons to electrochemically active artificial electron acceptors.

Mediated electron transfer from an enzyme to an electrode are usually studied in rapid systems using direct current (dc) cyclic voltammery and established reaction kinetics concepts. The development of second generation biosensor [60], [77] is based on a two step procedure in which the enzyme takes part in first redox reaction with the substrate and than, in turn is reoxidized by a mediator and finally the mediator is oxidized by the electrode.

$$\text{Glucose} + \text{GOD/FAD} \rightarrow \text{Gluconolactone} + \text{GOD/FADH2} \quad (2.12)$$

$$\text{GOD/FADH}_2 + 2M \rightarrow \text{GOD/FAD} + 2\,M^* + 2H^+ \quad (2.13)$$

$$2M^* \rightarrow 2M + 2e^- \quad (2.14)$$

where FAD represents a flavin redox center in GOD and the mediator, M/M* are the oxidized and reduced forms of mediator. e.g. Ferrocene, ferricyanide, NMP etc. are the commonly used mediators. The immobilization of the redox species can be carried out by adsorption, polymer coating and covalent attachment.

Usually the rate of reaction is a diffusion controlled phenomenon in which external membranes are used, the current produced is proportional to the analyte concentration and independent of both the enzyme and electrochemical kinetics.

2.2.2.1. Significance of mediated systems

Due to lower electrode potentials, mediated enzyme electrodes are known to be less susceptible to interfering substances. In [56] authors have investigated a system in which the oxidation of glucose by glucose oxidase can be detected with help of hydrogen peroxide generated during the reaction at the peroxidase modified electrode. During the process, with the subsequent reduction of the mediator at the working electrode, a polymer bound mediator is oxidized by the peroxidase. Highly flexible ferrocene containing siloxane polymers has been designed. These facilitate electron transfer from the reduced flavin co-factor of several oxidases. Based on these polymeric systems, highly stable amperometric biosensors have been reported [78]- [80]. During the past few years, amperometric biosensors have been reported with the help of water insoluble exchange polymers. This approach has as seen in [61], several advantages:

(1) During casting procedure of the polymer enzyme solution at the electrode, the enzymes can be immobilized;

(2) Negative charges of the polymer enzyme film usually acts as a barrier for the negatively charged biological interferents present in biological fluids;

(3) The polymer enzyme film offers the possibility of incorporation by ion exchange, positively charged electron mediators which can be used for shuttling for electron transport from the redox site of the enzyme to the electrode surface.

In all cases, when hydrophobic and cationic mediators are incorporated in the polymer GOD films, an increase in the permeability interferents is observed. During this process of permeability, reorganization of the polymer structure takes place and in turn leads to an increase in the porosity of polymer films. This increase can be related to the neutralization of the polymer charge by the mediator.

The enzymatic film was covered by Nafion polymer obtaining a repulsive barrier in order to avoid the leaching of the mediator from the enzymatic film and to block the entry of anionic biological crossings. The electrons pass from an enzyme based biological component to the amplifier or a microprocessor component during the electrochemical reaction. The biological component immobilized onto the surface of the transducer provides reliability, adaptability and even if immobilization is expected to have effects such as specificity, good stability to temperature, pH and ionic strength etc. The sensor and the biological component combination has been report by the use of mediator sandwich molecules between the sensor and the biological component i.e. with ferrocene. It has been suggested that avoidance overloading of the surface support with the biological componentis highly recommended. This recommendation is due the fact that the activity increases with loading initially but may change direction of variation with high loading due to restricted access. By a porous surface on the support, this may be overcome as seen in [81]. A large number of dehydrogenases utilize NADH as a cofactor. Therefore, a particular attention must be given to its electrochemical oxidation at low potentials. It has been reported that the direct oxidation of NADH at the above electrode requires large over-potentials [82].

2.2.2.2. Mediators

Mediators are artificial electron transferring agents that can participate as they are in the redox reaction with the biological component and so help in the rapid

electron transfer. It is the low molecular weight redox couple that shuttles electrons from the redox center of the enzyme to the surface of the indicator electrode. During the catalytic reaction, two reaction take place, first the mediator reacts with the reduced enzyme and then diffuses to the electrode surface to undergo rapid electron transfer.

Oxidation at one electrode produce current. With the help of an potentiostat, this current is measured. The current represents the rate of production of the reduced mediator (Mred).

During electron transfer, mediator must be stable under required working conditions and should not participate in the side reactions. The mediator should be chosen in such a way that it has the lowest redox from all the other electrochemically active interferents in the sample. Between enzyme's active site and electrode the redox potential of a suitable mediator should provide an appropriate potential gradient for electron transfer. The redox potential of the mediator (compared to the redox potential of enzyme active site) should be more negative for reductive biocatalysis or more positive for oxidative biocatalysis. Direct current voltammetry is an important assay in studying the properties of mediators and for an amperometric biosensor it helps in selecting a suitable mediator.

Characteristics mediators and advantages of using them as seen in [61]:

(a) It should be able to react rapidly with the reduced enzyme
(b) It should exhibit reversible heterogeneous kinetics
(c) The reduced form should not react with oxygen.
(d) It should have stable oxidized and reduced forms.
(e) The overpotential for the regeneration of the oxidized mediator should be low and pH Independent

Advantages of using mediators

(a) measurements are less dependent on oxygen concentration
(b) the working potential of the enzyme electrode is determined by the oxidation potential of the mediator
(c) with the use of mediators at low oxidation potentials, the interference of unwanted species can be avoided.
(d) if the oxidation of reduced mediator does not involve protons, it can make the enzyme electrode relatively pH insensitive.

Some commonly used mediators:

- Ferrocene and derivatives
- Tetrathiaful_alene (TTF)
- Conducting salts
- Quinones
- Ferri/ferrocyanide

2.2.2.3. Mechanism of electron transfer

It has been demonstrated that electrogenerated small molecular reactants are the most recommendable to be used to couple biological redox couples to an electrode [83], [84]. For facilitating a biological electron transfer the mediators are used. This biological electron transfer is favorable thermodynamically but not kinetically.

$$MO + e- \rightarrow MR \text{ electrochemical} \quad (2.15)$$

$$BO + e- \rightarrow BR \text{ electrochemical (very slow reaction)} \quad (2.16)$$

$$MR + BO \rightarrow MO + BR \text{ chemical} \quad (2.17)$$

where MO and BO are the oxidized forms and MR and BR are the reduced forms of the mediator and respectively the biological molecule. The reaction happens at the characteristic potential of the mediator. As a consequence of reaction, MO is close regenerated to the electrode surface and it does not have to diffuse very far to again undergo electron transfer. If the chemical reaction is rapid, for only a small amount of BO present, a significant enhancement of the current can be observed. The current observed can be related to the concentration of BO present, and for this reason, this approach has been widely applied for the biosensors' fabrication. Since electrogenerated MR reaction is not very specific, to exclude other potential oxidants must represent a priority, oxidants that can compete with BO [61].

Mediators, as already presented, have a wide range of structures, properties and a range of redox potentials that make them one of the first options in applications in all fields of activity, from in lab applications to military and commercial use. During the electron shuttling process between the active site of the enzyme and the electrode, the mediator is cycled between its reduced and oxidized forms. The mediator competes with the enzyme's natural substrate (molecular oxygen), effectively and efficiently diverting the flow of electrons to the electrode. Anyway, there are redox mediators that can work only in a deoxygenated environment. The criteria, which must be met for an ideal redox mediator for sensor applications has been shortly presented and is presented in more detailed way in [85] and [86]. Both homogeneous mediation and eterogeneous mediation are included in mediated bioelectrochemistry.

2.2.2.4. Enzyme electrodes

The simplest enzyme electrode consists of a thin layer of enzyme held in close proximity to the active surface of a transducer, a suitable reference electrode and a circuit, usually a potentiostat for measuring the signal, the current or the voltage, either by amperometry or potentiometry. The enzyme electrode is immersed into the analyte to be detected while carrying out the measurements and the steady state potential or current is read. Usually, a linear behavior for the amperometric electrodes and a logarithmic relationship is observed for the potentiometric electrodes. In general, the electrocatalysts are immobilized onto an electrode surface by adsorption [87], polymerization [88] or electrodeposition [89].

The peak potentials for NADH electrocatalysis for different electrocatalysts was presented in [90]. As compared to the NADH oxidation the authors found dramatic potential shifts at the bare glassy carbon electrode (0.7 V). The steady state current is proportional to the initial rate of enzymatic process for a kinetically controlled biochemical reaction catalyzed by the immobilized enzyme. A plot of I versus substrate concentration S yields a typical Michaelis–Menten type response. A linear Lineweaver–Burke plot, 1/I versus 1/S is the diagnostic technique for kinetic control of the electrochemical response. The response of a biosensor is typically dependent on the amount of active enzyme immobilized. A low molecular weight soluble mediator is disadvantageous as it can leach out of the electrode and be lost to the bulk solution. This may lead to a significant signal loss and is considered as a serious problem for in vitro applications. To overcome this, several groups have investigated the use of immobilized mediators either with enzyme in solution or with co-immobilized enzyme [61].

2.2.2.5. Whole-cell deposition and integration

Cells can be integrated into biochips by direct attachment to its surface or by embedding in a suitable polymer. By modifying biological properties of the cellular surface and/or by solid substrate chemical modification, the direct surface attachment can be improved [91] [92]. Matrix-aided immobilization offers additional benefits including enhanced viability maintenance [93] and [94].

Deposition, like for any other biological material, deposition for living cells needs to obey to the restricting constraints of the biological environment such as pH, temperature, or ionic strength, as well as to the vulnerability of the cells to mechanical stresses. After deposition, the coupling to the solid substrate can be based on covalent bonding, ionic or affinity interactions [95], [96]. In recent years, several biocompatible deposition techniques has been developed. For adsorption of biological cells onto hardware platforms an optimally templated surface for a specific biological function must take both physical and chemical aspects into account, e.g. superimposed chemical architecture, fundamental interactions, dynamic properties, and the3D topography. While chemical aspects occur at the molecular scale and the physical aspects occur at the micrometer scale, there is a unique synergy between them [97], [98] in the presence of live cells, as in medical implants, tissue engineering, and cell-based bioelectronics.

Its first interaction at the nano-second time scale, after the exposure of an inanimate surface to an aqueous cell suspension, will be with water molecules, in a dependent manner upon the surface characteristics. The properties of the surface boundary layer similar to a water shell, are an important factor affecting cells, proteins, and water-soluble molecules that are in contact with the surface. A critical role that affect its kinetics and thermo-dynamics in cell adsorption is played by the interaction between the water shell-like boundary layer of the surface with that of soluble biomolecules. So, the cells see a surface-bound organic layer and do not "see" a bare surface. This propertie of surface-bound organic layer which have been determined by the associated water boundary layer previously adsorbed macromolecules. Both biotic and abiotic surface layers can be used by the living cells to adhere to. The microbial initial adhesion of a cell to a solid surface is mediated by hydrophobic interactions and non-specific electrostatic, hydrogen bonds, and van der Waals forces, either repulsive or attractive. One must keep in mind that negatively charged bacterial cells adhere preferentially to positively charged surfaces [99]. Negatively charged bacterial cells may also attach to either hydrophilic or hydrophobic to surfaces, depending upon their outer surface characteristics [100]. Following their initial adhesion, outer cell structures may interact with the surface, making the adhesion stronger and establish it as irreversible. Generation of bonds between individual cells as well as by excreted exopolysaccharides (EPS) that make the attachment of bacteria to each other and to the surface stronger stabilizes bacterial adhesion. Adhesion of eukaryotic cells and tissues is mainly mediated by extracellular proteins. Mammalian cell adhesion to these proteins is primarily mediated by integrins, members of a widely expressed family of heterodimeric transmembrane receptors that bind to adhesive motifs present in various extracellular matrix proteins, including fibronectin, vitronectin, laminin, and collagen.

Integrins are used in both signaling and mechanical capacities [101]. Fallowing the same concept as ligand binding, the integrins bind and associate with

cytoskeletal elements forming focal adhesions, supramolecular assemblies of structural. These processes are signaling proteins that provide anchorage forces, activate signaling cascades regulating cell cycle progression and some times differentiation [102]. The adhesion of prokaryotic and eukaryotic cells to a surface as well as degree of adsorption of proteins is influenced by a variety of parameters including surface roughness and texture, hydrophobicity or hydrophilicity that is dictated by the functional chemical groups, and also by electrostatic, van der Waals, and hydrophobic forces [103]. Protein conformation can be changed upon adsorption leading to non-uniform surface properties [104].

While direct immobilization using adsorption of living cells on solid supports is possible, this process may be greatly aided by several modifications of the surface properties of either the deposited cells and/or the platform on which the cells are deposited to. The platform modification can be achieved by physical or chemical means, including specific pre-deposition of polymeric and biological molecules. The biocompatibility of the surface is one of the most important parameters that affect adhesion of cells. This is a property often related to surface microtopography, microchemistry and microtexture. The nature and the strength of the interactions between live cells and inanimate surfaces are affected by these characteristics. A comprehensive review of surface functionalization for protein and cell patterning (both prokaryotic and eukaryotic) has recently been published in [105]. Self-assembled monolayers (SAM technique) of alkanethiols on gold and of silanes on glass is one of the common methods to promote cell attachment to a surface. This is made by generating an organized molecule-deep structure with a distinct terminal functional group, enabling protein and cell adsorption. Patterned SAM surfaces by the serial adsorption of two or more ω-substituted alkanethiols (HS (CH2)nR) on gold had been reported.The reported papers are based on the immobilization of two mammalian cell lines. Adhesion of cells is prevented by SAMs terminating in an oligo (ethylene glycol) group uniformly, as they resisted adsorption of proteins.

Depending upon the stamp's design, a SAM pattern is designed in micrometer dimensions. Patterning by μCP in laboratory experiments is quite simple, allowing enhanced flexibility and high resolution. Alignment of two nonoverlapping patterns can be facilitated by the use of a single multilevel stamp. Thus, μCP is suitable for parallel patterning of only a limited number of cell types. Robotic printing is desirable in forming a pattern with a larger number of eukaryotic cell types as seen in [106]. Extracellular matrix proteins such as fibronectin (FN) promote the adhesion of bacterial and mammalian cells to substrates. A a gold surface was coated with SAMs of alkanethiolates (terminated with either CH3, OH, COOH or NH2) and with FN, and it has been demonstrated that surface chemistry modulates myogenic proliferation and differentiation via alterations in integrin binding.

Eukaryotic cells adhered well to all the SAMs because of their integrin proteins, although there were differences in the identity of the FN-bound integrin due to surface chemistry-dependent variability in protein structure. Myogenic differentiation was correlated with differences in the integrin binding [107]. It was suggested in the past that cellular functions are regulated by adherence of the cells to a certain surface and by cell spreading on the substrate. The surface topography and physico-chemical properties can affect intracellular functions [109]. In [108] this approach is presented, developing a dynamic substrate that controlled cell adhesion by modulating the ligand-receptor interactions. Three different alkanethiol SAMs were generated on gold-coated glass, incorporating either an electroactive O-

silyl hydroquinone (SHQ), an electroactive quinone ester (QE) or a nonelectroactive alkanethiol.

All three alkanethiols ware bounded by a peptide containing the Arg-Gly-Asp (RGD) sequence and served as a ligand for the receptor-mediated cell adhesion. When a specific electrical potential is applied the cells will be released. In another study, were printed alkanethiolates SAMs on gold by μCP, forming extracellular matrix (ECM) "islands", separated by nonadhesive regions of alkanethiol SAM terminated with ethylene glycol. Eukaryotic cells specifically adhered to the ECM islands. Later, this concept was used for the construction of a microarray platform for probing cellular differentiation. Glass slides were coated with a thin polyacrylamide gel, and ECM arrays were generated by a contact array providing deposited spots of collagen I, collagen III, collagen IV, FN and laminin in 32 different combinations.

Mouse embryonic stem cells and hepatocytes have been attached to the ECM islands. Combinations of ECM synergistically affected both embryonic stem cell differentiation and hepatocyte function. The micropatterned cell co-cultures formation was recently described using layered deposition of ECM components. Hyaluronic acid (HA) was micro-patterned on a glass substrate and the regions of exposed glass were coated with FN to generate cell adhesive islands, onto which a first cell type (AML12 or cells ES cells) was immobilized. It was turned into an adherent surface by the subsequent electrostatic adsorption of collagen to the HA patterns and so facilitating the adhesion of a second cell type (NIH-3T3 fibroblasts) [110]. It is worth mentioning that following immobilization, adhesive properties of the surface can be affected by the compounds secreted by the cells and the perfectness of the patterns can be impaired. A different technique for micro-patterning of two different cell types, hepatocytes, and 3T3 fibroblasts, consisted of patterning a positive photoresist onto glass, followed by deposition of aminosilane, glutaraldehyde and collagen. Seeded on the glass in a serum-free medium, hepatocytes attache only to the collagen I regions, followed which 3T3 fibroblasts attached to the bare glass.

This methodology being use, it is possible to control and manipulate cell-cell contact and so controlling cell-cell interactions. More than one technique are combined for surface modification, which is also a possibility, for example "cold" exciter laser beam technology combine with microlithography to create surfaces with defined 3D microgrooves. This surface modification, by adding biological media, such as fetal bovine serum can be further improved. Moreover, it was shown that cell behavior is affected by micro-topographical features.

In [92], researchers have tested and compared the adhesion of both prokaryotic and eukaryotic cells to modified silicon wafers. Thin layers of alkylsilanes exhibiting different functional groups (hydrocarbon, fluorocarbon, and PEG) were deposited on the silicon wafers, where oxidized surfaces provided differently wettable sites, with or without the addition of FN or serum proteins. Highlighting the differences in adhesion parameters between prokaryotic and eukaryotic cells, the adhesion of human, mouse and Staphylococcus aureus cells to the modified surfaces exhibited different patterns [92].

One of the parameters that affects adhesion of both cell types to a surface is electrostatic interaction. Scientists has referred to this parameter [111] when they tested the attachment of Escherichia coli cells to microsized holes (3 × 0.5 μm) patterned on gold-coated silicon.

SAMs were generated on gold surface functionalized with poly-l-lysine (PLL). Motile E. coli cells attached through electrostatic interaction between negatively

charged groups at the bacterial cell surface and positively charged PLL assemblies to the surface; PLL pH variation controlled the degree of attachment [111]. The effect of different glass or silicon coatings on the adhesion and the morphology of Chinese hamster ovary (CHO) cells were examined in a comprehensive study reported. Glass surfaces were coated with either PLL, FN, 3- aminopropyltriethoxysilane (APTES) or UV/O3-modified PDMS. PLL or SiO2 coated silicon wafers, or were activated with O_2. Adhesion was as high on APTES- as on PLL-coated glass.

On the other direction, a reduction in adhesion was observed on FN- and UV/O3-modified PDMS-coated glass. On PLL or with O_2 plasma treated silicon chips, cell adhesion was as high as on PLL- or APTES-coated glass. If SiO_2 coatings are uniformly, a reduced adhesion is obtained. A disconnection between cell morphology and cell adhesion was systematically observed for all substrates and is quite possible, in the specific adsorption of ECM molecule active domains on the surfaces, to reside. These discoveries bring into attention the importance of the appropriate materials selection for surface modification.

Microfluidic channels are an alternative soft lithography technique for patterning and immobilizing cells. The fluid flow is restricted in this technique. The flow is restricted to desired regions in the substrate, enabling the formation of a pattern of SAMs, in the same time leading to selective cell immobilization. When multiple ligands need to be patterned, microfluidic channels are useful, even if the range of possible patterns is quite limited. Spatial control over the surface, in last papers in the literature, was maintained with the PDMS microchip, which limited electrolyte flow within the channels. The regions on the surface under the channels were oxidation activated by the hydroquinone to quinine of the SAMs. Once the surface was activated, a RGD oxyamine-containing peptide attached selectively to the activated portions of the surface leading to Swiss 3T3 fibroblasts adhesion [112]. Several additional surface modifications based upon the use of biological molecules were reported over the last decade. [113] used a microstamp for the formation of patterns of proteins on glass for the localization of neurons, axons, and dendrites. In another work, a self assembled synthetic oligopeptide, C $(RGD)_4$, immobilized directly on the surface, was used for the immobilization of HeLa cells [114].

Depending upon their structure and affinity, specific peptides can be used for specific cell types immobilization. A lamininderived synthetic peptide, PA22-2, known to bind the integrin α6β1 of hippocampal neurons, has been presented to sustain cell adhesion and to promote neurite outgrowth [115]. PA22-2 have been immobilized on different SAM-modified surfaces and it promoted neuronal attachment. The different SAMs affected cell morphology, the effect on the adsorption of proteins present in the culture medium being a possible reason. This peptide anchors the cells to the surface much more firmly than in PLL-mediated attachment or other cases based on electrostatic interactions [116].

3. ELECTROCHEMICAL CELL

To have a functional system, first, one need to be able to simulate all the component parts, individual simulation and as a whole system. For this purpose, the author designed an equivalent electronic model for electrochemical sensors. In this chapter author is presenting his design, the mathematic algorithm used for this model and the experimental validation for the results on the background of a literature survey of electrochemical cells designs reported.

Bacteria are our invisible friends, or our invisible enemies. Some aid our digestion, others destroy our poisons. Still other bugs make us affect us in bad ways, from common disease like diarrhea to disease with major effect in our life like trichinelosis, West Nile etc. Living inside and outside our bodies, natural bacteria are a fact of life. We have learned to live with them and they have learned to live with us. A recent U.S. Arms Control and Disarmament Agency report on worldwide arms control compliance states on the existence of offensive biological and chemical warfare programs. The key to protecting a military unit or community from dangerous bacteria or toxicants is to detect them before they reach their intended victims. Bacteria and toxicants can be detected using "whole cell biosensors". A biosensor is an analytical device which converts a biological response into an electrical signal. The term "biosensor" is often used to cover devices used to detect, record, and transmit information regarding a physiological change or the presence of various chemical or biological materials in the environment in real time results [1].

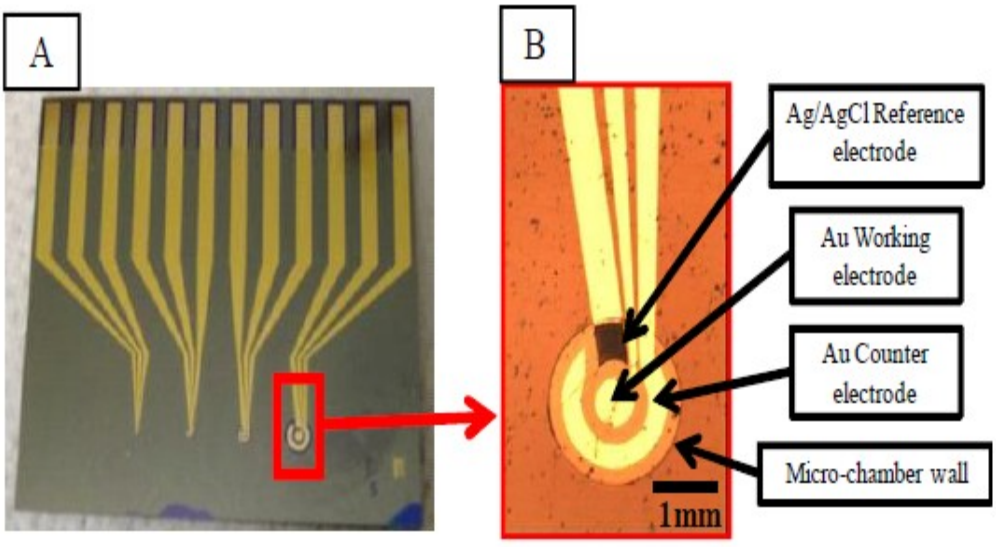

Fig. 3.1 Experimental electrochemical cell.

Nowadays, due to the fact that more and more bioterrorism represent a treat to our communities, more and more attention is given to methods to detect bacteria and

chemical agents. Usually, chemical agents are detected using chemical procedures. These procedures take time to instruct people, are expensive and can be contaminated very easy. Why not to use bacteria in our advantage? In the last decade, scientists managed to genetically modify bacteria, so they will react with chemical agents, these reactions can be quantified and used.
The main advantage of using live organisms to detect chemical agents is, that is relatively cheap to produce and easy to use in the field with minimum of training for the users. Disadvantages are that using living organisms, someone can never predict the exact behavior of the bacteria in any given situation and that the life on the shelf of this kind of sensor is relatively short, approximately 2 years, but research is made to extend this period. Another important disadvantage in using living organisms in detection fields is temperature. Bacteria and living cells usually die at boiling point or sooner and living cells loose their integrity at freezing point so operating area is somewhere between 10 and 70C.

3.1. Electrochemical cells theory

The electrochemical sensor, also known as cell or three electrode cells, consists of a micro-chamber and three electrodes connected as seen in Fig.1. Initially, electrochemists used only two electrodes, as it has been previously presented, but the following problem occurred: while injecting a voltage into the cell using only the two electrodes, it was impossible to measure the current with sufficient accuracy. Scientists managed to resolve this issue by implementing a third electrode called auxiliary (AE) or counter electrode (CE), as shown in Fig. 3.2.

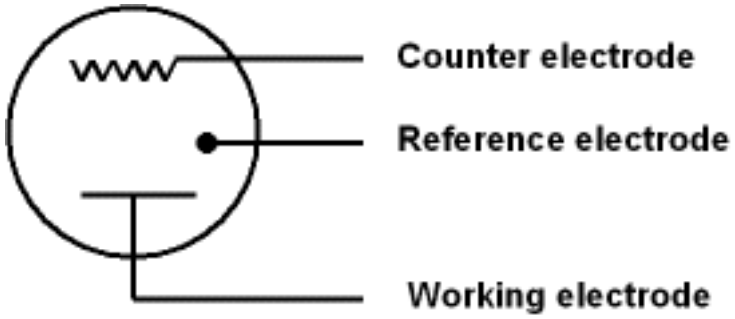

Fig. 3.2 Electrochemical cell symbol.

The presence of toxicants induces a cascade of biological reactions in the genetically engineered bacteria, producing an increased concentration of the enzymatic bio-reporter alkaline phosphatase. This enzyme catalyzes the reaction converting the substrate para-aminophenyl phosphate (pAPP) to the electro-active species para-aminophenol (pAP). Therefore, by using an appropriate electrochemical transducing system, the generated electrochemical bio-signal can be detected. Fig. 2 presents chrono-amperometric results of the response of E. coli bacteria in the presence and the absence of the model toxicant NA. The response of the bacteria in the presence of NA showed an increasing electrochemical current after pAPP was added.

3.2. Equivalent models for simulation for electrochemical sensors

In the literature there are a lot of proposed designs for equivalent electronic model for electrochemical cells. Why do we need equivalent circuits? They can not emulate exactly the behavior of the real sensors, why not to use the real thing? Well, in order to be able to use the real sensors, one need to have the electronic circuit, the chip or the PCB (printed circuit board). If the PCB is quite cheap and easy to produce and reproduce, the chips are quite expensive and can not be fabricated alone, you either fabricate multiple copies of one circuit or you gather many designs and put all of them on the same wafer. Beside the high cost of fabrication another important aspect of chip fabrication is time. Chip fabrication take months so one can not afford to design chips that do not work, this is why we need equivalent models for simulation, models that emulate as closely as possible the behavior of the real sensors. Models and simulation designs for electrochemical sensors are from simplest, that involve only resistors to more complex that have resistors, capacitors and impedances. The model one must chose is accordingly to it's needs and demands of the application that he create. In this part some designs will be presented from the literature. This chapter is a literature survey and author do not demand any rights over designs or principles.

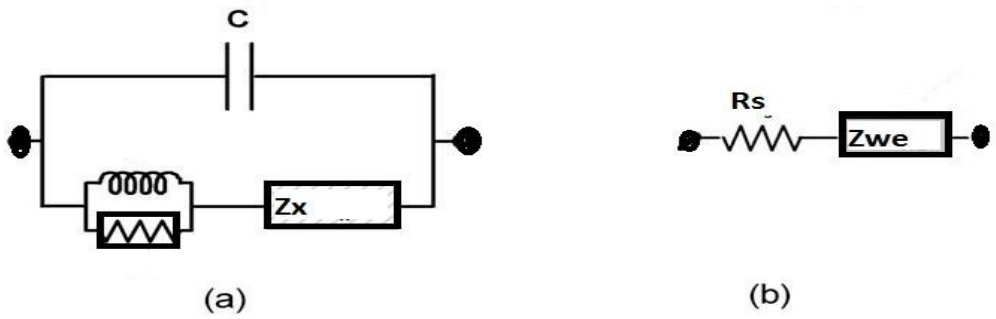

Fig. 3.3. EEC representing: (a) three-electrode cell involving WE branch and stray impedance generated by couplings between three-electrodes, (b) WE branch [140].

It is well known that some WE impedance spectrum, impedance branch, Zx, comprising impedance of WE, Zwe, and the electrolyte solution resistance, Rs, measured in a three-electrode cell, are susceptible to errors caused by experimental distortions. Presence of distortions of various parts of impedance spectra that cannot be counted for by a transfer function or electrical equivalent circuit, postulated in a modelling procedure of Zx. Thus most usually, the problem has been neglected or tried to be solved by simple "cutting" of the distortions frequency region, some efforts exists to define the origins of distortions and to determine a transfer function or electrical equivalent circuit that describes correctly the total measured impedance spectrun. In [119] V. Horvat-Radoševic´ and K. Kvastek reported an equivalent electrochemical schematic that quite closely emulate the very behavior of the real cell, however, this degree of precision is not always necessary, this also depending on what kind of application the sensor is for. Usually, each electrode from the electrochemical cell is seen as an RC circuit and each one of them is treated separately, as seen in [120].

In Sekushin opinion, the process of equivalent circuit construction on the basis of the results of impedance spectroscopy determination must include the following stages. First, one must experimentally determine the number of relaxation processes and their parameters. This will permit the constructon of an universal equivalent circuit that reflects in a concentrated form the empirical material. Further, one can consider a physically meaningful theoretical equivalent circuit modeling a specific electrochemical process. This theoretical equivalent circuit must be transformed using the methods of the linear circuit theory into another universal circuit, which grant the determination of functions that relate to the elements of both circuits. When comparing theoretical universal circuit with the empirical circuits, a system of nonlinear algebraic equations appears [120].

Another possible approach of 3 electrode cell equivalent model for simulation was presented by Amirudin and Thierry in [121]. From their point of view, a simpler design is sufficient to aproximate and emulate the behaviour of the cells, as seen in next figure:

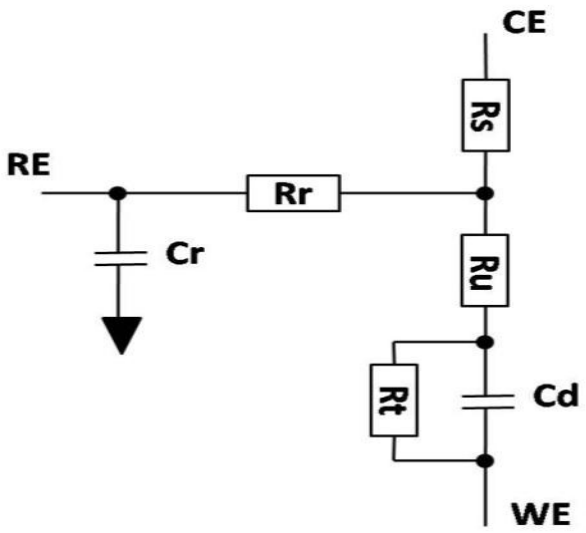

Fig. 3.4 A 3 electrode cell equivalent model [121].

The equivalent circuit of a three-electrode electrochemical cell is shown in Fig. 4 where *Rs,* is the solution resistance, *Ru,* is the uncompensated resistance, *Rt,* is the charge-transfer resistance, *Rr,* is the resistance of the reference electrode, Cd, is the electrode double-layer capacitance and Cr, is the parasitic loss to the ground in the leads. To select the correct equivalent circuit and to obtain the values of the elements in the circuit have been used various methods. Circuits with one time constant present no problem as the circuit and the values of the elements can be easily obtained graphically either from the Bode plot, or more commonly, from the Nyquist plot. For example, a semi-circle plot may indicate the presence of only one time constant with the circuit consisting of a resistor and capacitor in parallel [121]. As stated in [122], the equivalent circuit for simulation must be chose having in mind the processes and metals used in sensor fabrication. If we consider that only 2 electrodes out of three are in direct contact with the solution to be tested, the

schematic for the sensor, as seen by Gomez et. al. in their work [123] can be approximated as:

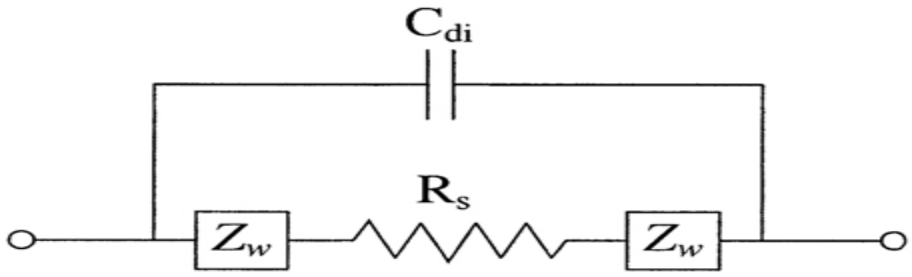

Fig. 3.5. Equivalent schematic design for a 3 electrode cell as designed by Gomez et. al. [123].

Equivalent circuit of a pair of electrodes immersed in an electrolyctic solution (Cdi= Dielectric capacitance, Rs=bulk solution resistance, Zw=Interfacial impedance) [123]. Another alternative design for an equivalent electrochemical cell model is reported in [124], a more complex design, suited for big arrays of electrochemical sensors.

Chemical sensors are increasingly used as arrays. Chemical sensor array can eliminate the interference from similar chemicals during the detection and quantification. Nowadays chemical sensor arrays have become important tools in many analyses such as: volatile analytes online monitoring of biological liquids, toxin detection and so on. Usually, but not always, a chemical sensor array is made up of a group of chemical sensors of same type, each chemical sensor having a partially selective material to provide a pattern of response to a given chemical analyte. There are thus arrays that combines 2 ore more types of sensors that are based on the same type of bacteria or principle but witch detect the targeted substance in the analyte in different ways. Furthermore biochemical sensor array takes the advantages of several different transduction principles to offer so called higher order sensing, so the response pattern as a whole provide the desired 2-D or 3-D information about the analytes.

3.3. Mathematical algorithm

First of all, a few data about Randles circuit to understand better the concept. A Randles circuit is an electrical equivalent circuit consisting in an active electrolyte resistance R_S in series with the parallel combination of the double-layer capacitance Cdl and an impedance of a faradaic reaction. It is commonly used in electrochemical impedance spectroscopy (EIS) for interpretation of impedance spectra, often with a constant phase element (CPE) replacing the double layer capacity (C_{dl}). Figure 1 shows the equivalent circuit initially proposed by Randles for modeling of interfacial electrochemical reactions in presence of semi-infinite linear diffusion of electroactive particles to flat electrodes. In this model, the impedance of a faradaic reaction consists of an active charge transfer resistance R_{ct} and a specific electrochemical element of diffusion W, which is also called Warburg element ($Z_W = A_W/ (j\omega)^{0.5}$, where A_W is Warburg coefficient, j – imaginary unit, ω – angular frequency).

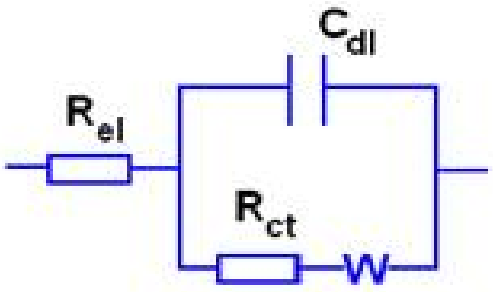

Fig. 3.6 Randles Circuit.

In a simple situation, the Warburg element manifests itself in EIS spectra by a line with an angle of 45 degrees in the low frequency region. Values of the charge transfer resistance and Warburg coefficient depend on physico-chemical parameters of a system under investigation [117]. To obtain the Randles circuit parameters, the fitting of the model to the experimental data should be performed using complex nonlinear least-squares procedures available in numerous EIS data fitting computer programs. The Randles equivalent circuit is one of the simplest possible models describing processes at the electrochemical interface. In real electrochemical systems, impedance spectra are usually more complicated and, so, the Randles circuit may not give appropriate results.

One of the most fundamental formula in electrochemistry is the Butler–Volmer equation. The equation describes how the electrical current on an electrode depends on the electrode potential, considering that both a anodic and a cathode reaction occur on the same electrode. The equation is valid when the electrode reaction is controlled by electrical charge transfer at the electrode.

$$I = A\, i_o \left\{ exp\left[\frac{(1-\alpha)nF}{RT}\,(E - E_{eq})\right] - exp\left[-\frac{\alpha nF}{RT}\,(E - E_{eq})\right]\right\} \qquad (3.1)$$

Where

I: electrode current, A

i_o: exchange current density, A/m^2

E: electrode potential, V

E_{eq}: equilibrium potential, V

A: electrode active surface area, m^2

T: absolute temperature, K

n: number of electrons involved in the electrode reaction

F: Faraday constant

R: universal gas constant

α: so-called charge transfer coefficient, dimensionless

Electrochemical impedance spectroscopy (EIS) also called AC impedance is an electrochemical technique that appeared in the late 1960's but have not been extensively studied until the late 1970's and early 1980's when computer controlled

laboratory equipment registered innovations and progress in all computer fields. The reason is that the technique is most easily controlled with a laboratory computer. While many of the idiosyncrasies of the technique are now reasonably understood, the ability to use the technique to model all corrosion systems remains quite a challenge. The technique itself is conceptually simple. A low amplitude alternating current (or potential) wave is imposed on top of a DC potential (often the corrosion potential with zero imposed current). The frequency is varied from as high as 10^5 Hertz to as low as about 10^{-3} Hertz in one experiment in a set number (often between 5 and 10) steps per decade of frequency. The corrosion process usually forces the measured current to be out of phase (denoted by the phase angle) with the input voltage. Dividing the input voltage by the output current furnishes the impedance. The variation in impedance (magnitude and phase angle) is used for the interpretation. This technique is in essence built on the DC polarization resistance technique in which a direct current voltage (or current) ramp is imposed. The used electrochemical methods were Cyclic Voltammetry (CV) and Electrochemical Impedance Spectroscopy (EIS). The main characteristic to establish by EIS is electron (charge) transfer resistance, CTR, in protecting film presence. The CTR concept follows from the Volmer-Butler equation,

$$I = I_0 \left\{ e^{[(1-\alpha)nf\,\Delta E - e^{-\alpha nf\,\Delta E}]} \right\} \tag{3.2}$$

for electrochemical kinetics, in which I stands for current**,** I_0 is exchange current, the key kinetics parameter, proportional to heterogeneous rate constant k, E is potential, while a, n, and f are constants. For small polarization $\Delta E = |E - E^0|$, charge transfer resistance $R_{ct} = \Delta E/I = RT/nFI_0$ – actually "ohmic" entity – may be defined. This makes possible to approach the electrode dynamic properties by equivalent scheme, presented in Fig. 5.3, in which, in addition to R_{ct}, the electrolyte resistance R_{el}, interfacial double layer capacitance C_{dl}, and diffusion impedance W are also involved (provided that low amplitude sinusoidal potential is applied). Such Randles' circuit well simulates AC response of Au or Pt in Fe2/Fe3 solution.

For $R_{el} + (C_{dl} / (R_{ct} + W))$ circuit, EIS spectrum in Nyquist plot, imaginary Z_{im} vs. real Z_{re} impedance parts, in which lower impedance corresponds to higher frequencies f, presents a semicircle continued by straight line with 45° slope. Diameter of the semicircle is interpreted just as R_{ct}. On Fig. 3, EIS spectrum of 10 mM ferri/ferrocyanide system on 1 cm^2 electrode is presented [125].

The resistance of the electrolyte (R_{el}) is always of the order of magnitude of several Ohm. However, if WE has its own high internal resistance (being, for example, semiconductor, or very thin metal film), R_{el} may increase up to tens kOhm. R_{ct} depends on reaction rate and electro-active material concentration. With moderately (10 mM) concentrated and fast reacting material (as Fe2/Fe3), "specific" R_{ct} may be as low as several $Ohm \cdot cm^2$. However, for slow reactions and low concentrations it may reach $MOhm \cdot cm^2$. C_{dl} in electrolytes on metals is always in the range of *5 to 50μF/cm²*.

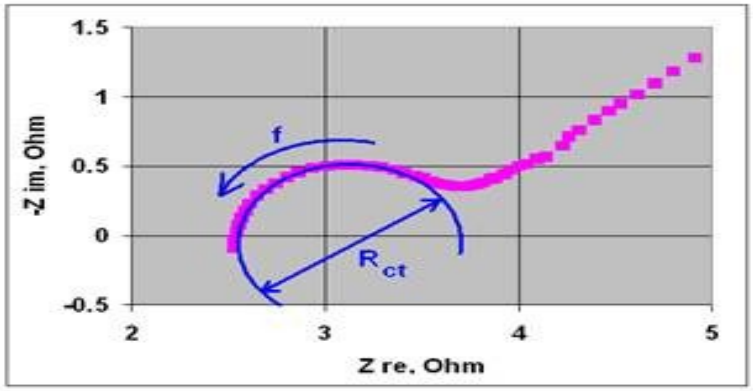

Fig. 3.7. EIS spectrum in Nyquist plot.

Warburg (diffusion) impedance is defined by the following equation:

$$W = a_w \left(\frac{1}{\omega^{1/2}} + \frac{1}{j\omega^{1/2}} \right) \tag{3.3}$$

where ω is angular frequency, and j – imaginary unit. Warburg constant [125] (for $T = 25^oC$) is

$$a_w = \left(\frac{1{,}87 \cdot 10^{-7}}{n^2} \right) \cdot \left(\frac{1}{D_0^{1/2} \cdot C_0} + \frac{1}{D_R^{1/2} \cdot C_R} \right) \tag{3.4}$$

where n, the reaction "electronity", equal to 1 or 2, D_o and D_R – diffusion coefficients, which are always about 10^{-5} cm^2/sec, and C_O and C_R – Ox and Red material concentration, respectively. D for most materials is close to 10^{-5} cm^2/sec and C may just vary in wide range from 10^{-4} to 10^{-9} mol/cm^3. The Warburg impedance usually dominates at low frequencies (~1 rad/sec), so that, for example, for $C_O = C_R = 10^{-5}$ mol/cm^3 (10 mM) and n = 1, /W/ is about 10 Ohm·cm^2. Impedance of single electrode (WE) is measured with 3-electrode scheme. With this scheme, current I flows through WE, electrolyte and CE. RE electrode serves for WE potential measurement (with respect to RE).

3.4. Electrochemical cell - proposed model

In Fig. 5.5, the author presents his original proposed model. This model is based on its needs and has been developed having in mind the simplicity needed in simulation and in the same time all the factors that affect the behaviour of the sensor.

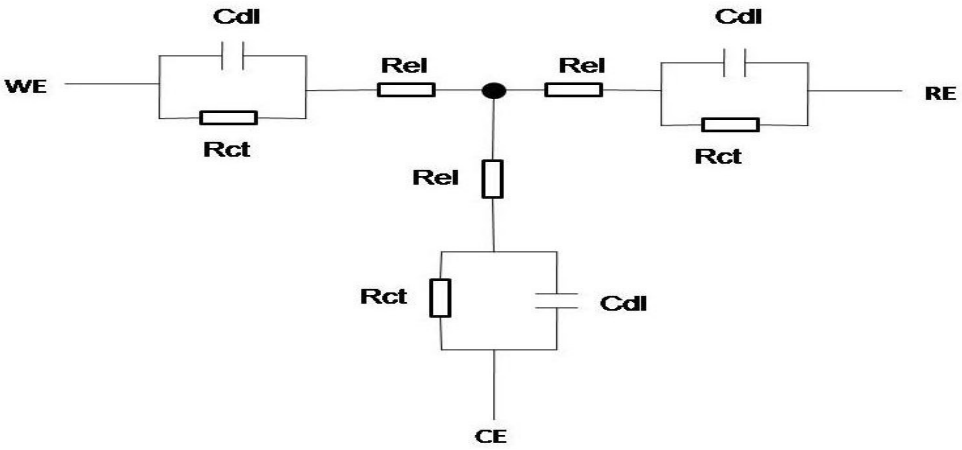

Fig. 3.8 Proposed electrochemical cell model for simulation.

For this design, the values have been chosen for our purpose and system applications and the model will be included in an array of sensors. Rct have a varying value between 1 ohm and several kilo Ohms while Rel=1-10 ohm and Cdl ~0.65uF.

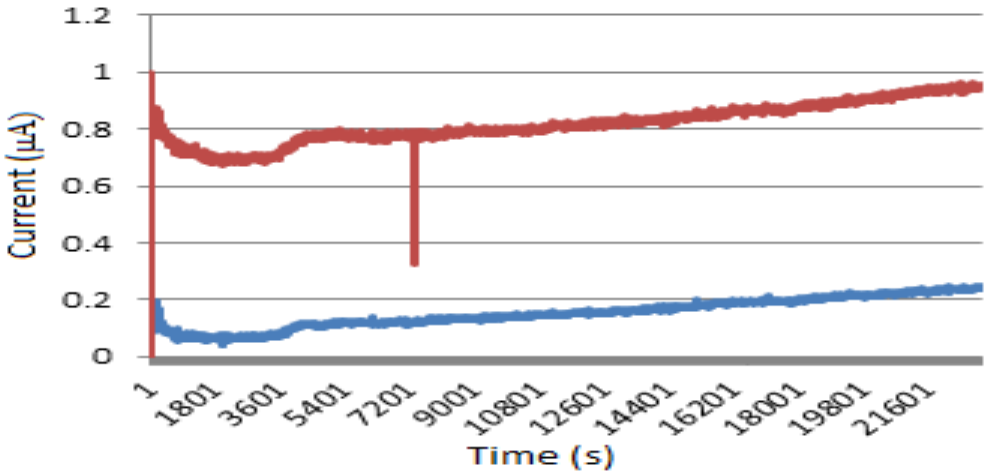

Fig. 3.9 Experimental results for electrochemical cell.

3.5. Experimental validation for simulation results

We have simulated the circuit maintaining a 300mV constant potential between counter electrode CE and reference electrode RE, in the same time measuring the current flow between working electrode WE and ground.
As one can see, the form and values of the signal obtained in the simulation approximate very well the signal obtained using the classical method, previously presented in Fig. 2. Good results can be also obtained without varying resistors, in this case the signal will be a straight line, at 0.2 μA. The signal presented in Fig 7 emulate the signal obtained in the absence of toxicants in simulation, presented in Fig.6. The simulation for the case with presence of toxicants, Fig. 2, chart A, can be simulated by adjusting the resistors of the model or using variable resistors. The simulation has been made using Tanner Tools, S-Edit for schematic editing and T-Spice for simulation. The proposed electrical circuit was designed for the electrochemical micro-chip whole-cell biosensor presented by Ben-Yoav and colleagues [126].This bio-chip comprised of four cylindrical electrochemical 50 μm deep micro-chambers with different radii: 1 mm, 0.5 mm, 0.25 mm, and 0.125 mm. The corresponding volumes were 157 nl, 39 nl, 9.8 nl, and 2.5 nl. Each chamber contains three electrodes: working electrode (WE), counter electrode (CE) and reference electrode (RE). The electrodes are made of thin evaporated gold (300 nm)/Cr (15 nm). The open reference electrode was coated with Ag/AgCl layers (Fig. 2B). The Ag/AgCl open reference electrode was manufactured by a two-step electrochemical process:
a) Ag electroplating (Standard Ag nitrate bath) at a rate of 0.8 μm/min;
b) Anodization of the Ag in a bath containing chlorine ions.

The presence of toxicants induces a cascade of biological reactions in the genetically engineered bacteria, producing an increased concentration of the enzymatic bio-reporter alkaline phosphatase. This enzyme catalyzes the reaction converting the substrate para-aminophenyl phosphate (pAPP) to the electro-active species para-aminophenol (pAP). Therefore, by using an appropriate electrochemical transducing system, the generated electrochemical bio-signal can be detected. Fig. 6 presents chrono-amperometric results of the response of *E. coli* bacteria in the presence and the absence of the model toxicant NA.

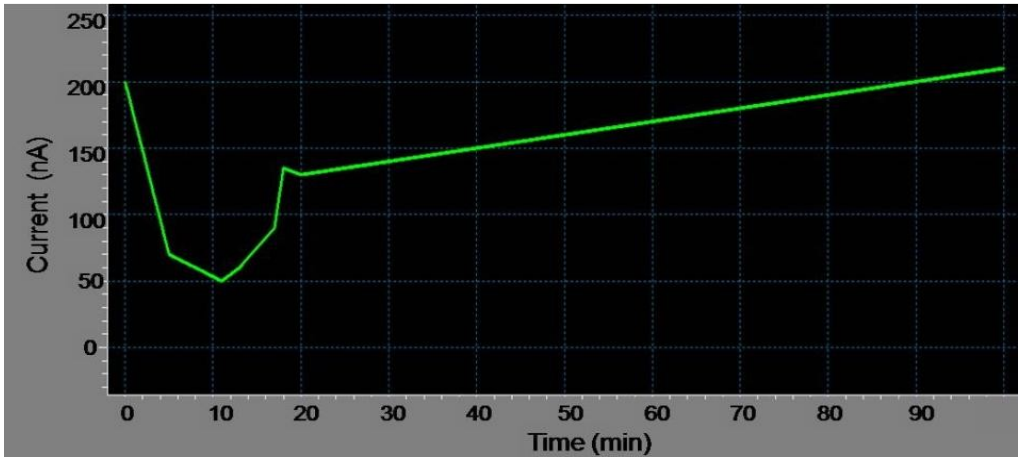

Fig 3.10 Simulation results for electrochemical cell equivalent model.

The response of the bacteria in the presence of NA showed an increasing electrochemical current after pAPP was added. As seen in Fig. 3, there is an important difference between the signal generated by bacteria in the presence of the pollutants and the signal generated in the absence of the pollutants. This will be translated by the circuit we proposed here in a lower frequency for the absence of pollutants and in a much higher frequency for the presence of the pollutants.

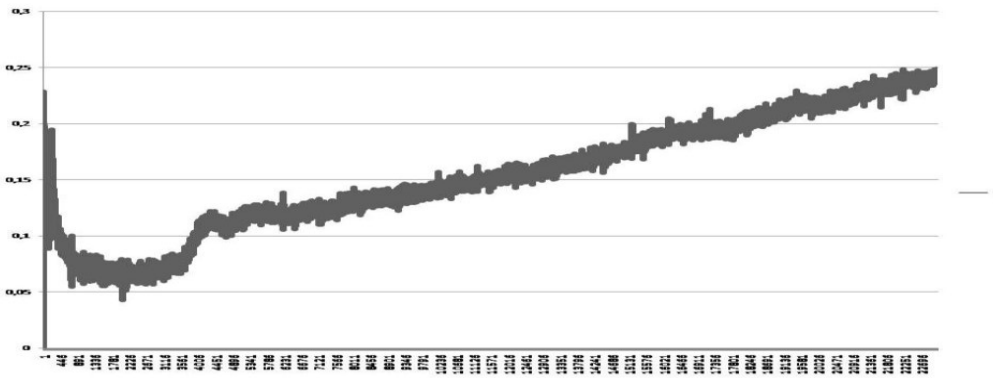

Fig 3.11 Experimental results for 3 electrode cell.

In the future, because of the fast development of the biotechnology and biochemistry, the measurements and analysis will be made faster, the circuit being capable to detect changes in the current value much lower than bio-technology is able to analyze today. The goal is to integrate as many components of the circuit as possible, to make it reusable, despite the disposable electrochemical sensors present on the market today.

The shape of the signal, shown in Fig. 3.10, was obtained using varying resistors while keeping Cdl at a constant value [127].

4. A LITERATURE SURVEY OF POTENTIOSTATIC DEVICES

This chapter is a literature survey that introduce the reader in the field of electronic parts of biosensors. The author is presenting here the concepts of potentiostatic devices, requirements and qualities requested for a potentiostat. Next the author is presenting a few potentiostatic devices with major role in his research. The first potentiostat dating from 1953 is also illustrated. In the last section of this chapter the author makes a review of equivalent electronic models for simulation for electrochemical cells, from the simplest designs to more complex architectures.

4.1. Signal conditioning systems for electrochemical cells

The firsts electrochemical devices started to emerge approximately in the second part of the 20th century and were used for oxygen monitoring. In the last years, as the Occupational Safety and Health Administration (OSHA) has began asked for monitoring of toxic and combustible gases in closed space applications, new and diverse electrochemical sensors have been discovered. By the mid-80s, miniaturized electrochemical sensors for detection of many different toxic gases in PEL ranges with good selectivity, accuracy and reliability became available.

Currently, a vast variety of electrochemical sensors are used extensively in many stationary and portable applications for personal safety, environment monitoring and military applications. The physical size, geometry, selection of various components, and the construction of an electrochemical sensor usually depends on the application it has been designed for. Now, the design of an electrochemical sensor, physical and electrochemical properties depend on the applications they are intended for and represent a compromise between its functions. An usual mistake commonly made is the idea that all electrochemical sensors are the same. In fact, the appearance of the electrochemical sensors used to detect various components may be similar, but their functions are different in an vast area of domains. In summary, different electrochemical sensors may appear quite similar, but are constructed with different materials including critical elements as sensing electrodes, electrolyte composition, porosity of hydrophobic barriers or biosensing element ranging from cells, tissues to bacteria. Additionally, some electrochemical sensors use external electrical energy to make them reactive to the target component. All parts of the sensors play a crucial role in determining the overall characteristics of the sensors [128].

4.2. Technical requirements of potentiostats

Potentiostats are very simple circuits, amplifiers, in classical designs, usually 2, used to control a voltage between two electrodes, the working electrode (WE) and the reference electrode (RE), maintaining it to a constant value regardless of the current flow in the cell. Potentiostats combine several technologies from

different fields, ranging from electronics, MEMS technologies, electrochemistry and so on. To understand how a signal conditioning system for electrochemical sensors or 3 electrode cells, as it is also known in literature work, you first need to understand the chemical or electrochemical reactions that take place.

In electrochemical reactions, you generally either want to know, to maintain at a constant value or to control the potential at the working electrode (WE). Directly measuring the potential of the electolyte side of the double layer of the WE is difficult. Usually, a well known and commonly accepted technique is to measure the potential of the electrolyte using a well-behaved electrode called a reference electrode (RE), the sencond electrode. In order for the RE to maintain a constant potential over all conditions, no metter what the voltage or the current generated in the reaction, no current should flow through it. For that reason, a third electrode was added. This third electrode sole purpose is to conduct current trough the cell. This current has to balance with great accuracy the current generated at the working electrode. The third electrode is called the counter electrode (CE) or auxiliary electrode (AE). A more detailed explanation of 3 electrode sensors will be also presented. A cell of this kind is called a three-electrode cell or electrochemical sensor [129].

The current generator, usually bacteria or mammalian cells, responds to the analyte chemical reacting at the WE. The capacitor represents the double layer capacitance, which can be very large for some sensors. The resistor at the counter electrode represents the solution resistance between the counter electrode and the current source. Usually, there is another resistor in series with the reference electrode, although the reference electrode does not generally conduct current, being isolated from the reaction. With this background, it follows that a circuit that manages a cell of this kind, including a three-electrode electrochemical sensor, has to have special properties:

* It has to maintain with great accuracy a fixed potential between the WE and RE
* It is bipolar and will operate regardless of whether the current flows to or from the WE
* It must measure the current from the WE, delivering a usable signal to an output terminal.

At the inputs of an operational amplifier usually there is no current. Though the working electrode is connected directly to the inverting input. This can be explained by the fact that the current has to come through a feedback resistor. The positive-going potential feeds back to the inverting input and forces the voltage back down if the output voltage rises too high; the reverse happens if the output falls too low, forcing the voltage back up. The output voltage is therefore proportional, with great accuracy, to the current; the proportionality factor is the value of the resistor' feedback in ohms. The inverting input is held very close to ground, virtually grounded by the operational amplifier, thus the working electrode appears to be grounded. It is imperative to remember that if the potentiostat power is cuted off, this active forcing of the ground no longer occurs. Sensors may therefore require some time to come to equilibrium after being powered down for a time. High-surface area electrodes, such as those in a carbon monoxide sensor, may require up to 24 hours or more to stabilize.

The other operational amplifier actually has the role to perform the potentiostatic action. Let's suppose, for example, that a potential of +0.5 V is applied to the bias input. In order for the output voltage of the op amp to be within a reasonable output range, the inverting input of the op amp has to be very closely to +0.5V, the input bias voltage. The inverting input is connected directly to the RE,

but should not draw any current from it. The operational amplifier delivers a voltage to the CE that is sufficient to keep the electrolyte (and the RE) at the established bias voltage, +0.5V. Consider that the reference electrode is driven to a voltage that is higher than the bias input. The inverting input is greater than the bias input, so the operational amplifier output will be decreased. The decreased voltage conduct less current into the cell, and the electrolyte voltage will go down. If the reference electrode voltage falls, the op amp will increase the voltage of the electrolyte. The electrons are attached to the electrode, which tends to force the inverting input of U1 negative. A positive voltage appears at the output of U1, proportional to the oxidation taking place on the WE.

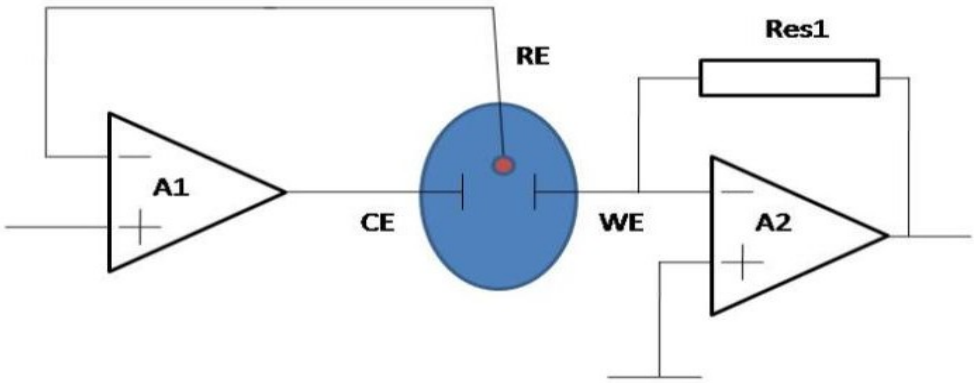

Fig. 4.1 Basic structure of an amperometric sensor with three-electrode potentiostat device.

In 1950, metallurgists and physico – chemists scientists tried to explain a strange electrochemical phenomenon. If you submerge an iron bar (an iron electrode) into diluted sulphuric acid (electrolyte), it will start to disintegrate, to dissolve - the phenomenon of corrosion appear. If another electrode is now inserted, one that do not corrode, e.g. platinum, and connect the iron electrode to the negative output of a source current, and the platinum wire to the positive output, the iron corrosion will slow down and eventually will stop, in close relation with the voltage applied. This phenomenon was reported by Sir Humphrey Davy (1778 – 1829) in the 17th century. If an iron electrode is connected to the positive pole, and rise the values of the voltage beginning from very low up to higher ones, the dissolution will grow exponentially with the rising voltage. Above a certain current limit, depending on the electrode area and the electrolyte composition and the temperature, the current suddenly drops to very low values, and the iron electrode stops the corrosion process.

Michael Faraday (1791- 1867) detected this phenomenon and called it "passivity". Since then this phenomenon has been object of controversy. The phenomena have been explained only in the middle of 20th century. A better understanding was possible after invention of the potentiostat. The nature of the phenomenon imposes an electrochemical method to investigate. The idea was to record the characteristic current - voltage curve of the iron dissolution in the electrolyte. However, there was one difficulty: According to the applied method, the results varied strongly [130].

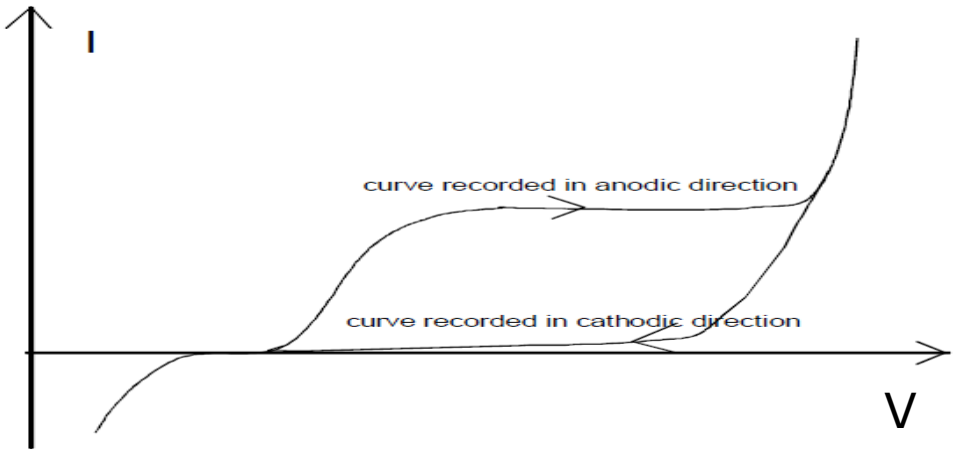

Fig. 4.2 I-V Curve for a potentiostatic device.

The stable reference voltage difference is formed between the grounded (WE) and the (RE). This difference is now inverted and amplified. The resulting signal, the current, control the counter electrode. Thus a residual error remains. As higher the amplification is as smaller the residual error will be. Such instruments were built in Goettingen, Germany, and at the same time also, in the UK, in Italy and the USA.

Each sudden voltage rise includes a frequency spectrum, with upper frequency limited by its slope. At the time when the first potentiostatic amplifiers had reached this state, a group of physico - chemists worked in Goettingen with professor Bonhoeffer and his assistant Weil. A young physicist, Hans Wenking, joined this group [130]. His task was to manage the institute's scientific instruments. This young phisicist became familiar with the problems of the electrochemists. Analysing the available amplifiers, the first properly working potentiostat was developed. Wenking's merit was to introduce new features: The phase correction and the differential amplifier. The first real potentiostat built by Hans Wenking already showed the features which can be found today in a common solid - state operational amplifiers. This basic potentiostatic principle is used in many instruments until today.

Characteristics of a potentiostat as seen in [130]:

Speed Control

Chemical reactions can be very fast. The potentiostat must be able to react at appropriate speed: The speed of a potentiostat is measured in terms of small - signal rise - time, bandwidth and slew rate. The bandwidth depends on the the output power and principe of the circuitry. Usual potentiostats have bandwidths from 100 kHz to some MHz. The slew rate ranges from 105 to 107 V/s, the small - signal rise - time is in the order of some microseconds or below. Fortunately, in electrochemical sensors with living organisms cells, the reactions are quite slow so the author do not encountered this challenge.

Current range and dynamics

High currents are sometimes required from the potentiostat. Investigations in biotechnology science demand usually some 10 uA to 1 A, for other purposes ten

or even hundred amperes are required. A good laboratory potentiostat may have for example an 1 A current output, and a current resolution of 100 nA or much less. State of the art are one - ampere - potentiostats which are capable to measure less than 1 nA. The relative accuracy of the measurement may be less than 0.1%, anyhow better than 1-1.5 %. Dynamic is the usable span of current between full range and the lowest detectable current in the same range. The dynamic of a good potentiostat may reache 5 decades. From the highest current range to the lowest threshold current, the overall span covers 9 or more decades.

Accuracy

The voltage difference between the reference voltage in the cell and the existing voltage in the cell needs to be balanced so the electrochemical sensor to work properly. This balance is made by the potentiostat. Regardless the quality of the potentiostatic device, it can not make a perfect compensation due to time and technology constrains and always will remain a residual error. This residual error is reciprocal to the open loop gain of the potentiostat: Suposing an open loop gain of 106, a control voltage of 1 V can be approximated to 1 μV error. Thus the total error has other and more influencing sources, e.g uncompensated cell cable resistances and resistance effects in the cell. This is a reason for the decision of integrating all the circuits on the same chip with the sensor array.

Noise

Electronic noise is the sum of all statistic current fluctuations produced in a circuitry. Most of the noise is produced by thermal effects in resistors, another main part in semiconductors. The most sensitive circuit in potentiostats is the input stage, producing noise in the input resistor and the first amplifier stage, if one will decide to use this approach. Good potentiostats are equipped with low-noise amplifiers or convert current in frequency. In electrochemistry, unfortunately there are more sources of noise other then electronic components, sources as biologic parts, chemical and electrochemical and so on. These noise sources are more problematic and quite difficult to compensate.

Stability

A potentiostat used for a variety of electrochemical tests must have good stability, as the electrodes act in the control circuit, with all their variety of capacities (mainly parasitic), resistances, and frequency - dependent impedances. A potentiostat can be tested quite easy, by feeding a 1 kHz -rectangle wave of e.g. 100 uV amplitude into the control input. Connecting a fake cell with different capacitors to the potentiostat, and an oscilloscope at the potential output. The rectangle wave should be transferred to this output with a) a high slew rate and b) oscillations caused by high capacities should be properly damped [130].

Phase correction

By connecting a dummy cell with pure ohmic load, current and potential should be in phase as close as possible to the theoretical limits. If this property or result is not achieved, several experiments as measurement of a.c. impedance will generate wrong results.

On the market there are a lot of signal conditioning systems for all kind of sensors. Signal conditioning systems for electrochemical cells are divided in many categories based on type of sensors they are working with, number of electrodes, precision demanded by the applications, concept of functionality etc. The field of electrochemical study often involves sensor devices that are used to measure quantity or presence of toxicants in a given solution. In the case that sensor detect the toxic agent or substance it has been designed for, a chain of reaction will take place in the algorithm presented in chapter 3 and a signal will be generated. This

signal is usually a current or a voltage. Fortunately, the concentration of foreign substance can be quantify, signal being proportional in strength with the concentration.

One of the most common used and generally accepted algorithm of detecting analytes is the usage of amperometric sensor, This method utilize a potentiostat hardware, which is used to control the electrode cells for running electroanalytical applications. A structure of potentiostat hardware utilized in amperometric cells design contains three kinds of electrode cells. The first electrode cell is the working electrode (WE). This electrode serve as a platform on which the electrochemical reaction takes place. The second electrode is referred in literature as reference electrode (RE). Reference electrode function is to measure any potential, as low as the technology allow, present in WE electrode. The voltage at the reference electrode of a potentiostat will be affected by current that might flow through this terminal. In a well designed and fabricated cell, it is forbidden to have any current flowing trough the reference electrode. A highest input impedance is recommended to maintain this requirement which may be implemented by connecting a MOSFET trough its gate to the reference electrode. Again, having the potentiostat integrated into CMOS chip will keep the system price down and will miniaturize the hardware size. This is mandatory for a lab-on-chip due to the combination of this function with some other applications. Counter electrode (CE) or auxiliary electrode (AE) as some scientist named it is the third electrode. This third electrode serves as a conductor, supplies current required for electrochemical reaction at WE electrode and it is also used to measure currents [131].

In typical configuration, the value of the cell potential can be controlled in three different methods:

1. grounded counter electrode [132],
2. grounded working electrode [133], [134] and
3. virtual grounded working electrode [134].

Even if the virtual grounded WE configuration can stop current from flowing into RE, the WE has no direct connection to the true ground. Any connection present in the potentiostat that is not safely shielded may cause environmental noise and interference to flow trough unshielded wires that will act in this case as antennas and this will produce significant noise levels at the output of the transimpedance amplifier. The output connection between control amplifier and CE produces a very large parasitic capacity that may contribute to instability factor on the control amplifier. This situation is similar for grounded CE. Moreover, the grounded CE situation has obviously several more complex issues and necessitates more electronic parts, conducting to more vulnerabilities as common interferences and more often prone to component mismatches.

Another style designing three electrode cells is by controlling the current. There are, generally , two main configurations used to measure the amount of electrochemical cell current:

1. readout current through working electrode
2. readout current through counter electrode.

In the first configuration, literatures reports [132], [134] have employed transimpedance amplifier to read out current from WE. The read-out current configuration offers a number of advantages over the second configuration: it is easier to implement and fewer currents are measured due to higher values resistor switching current measurements. Thus, there are also disadvantages, anyhow, includes no direct connection between working electrode and real ground, which may determine the acquirement of environmental noise and some form of

interference that produces significant noise level at the output of transimpedance amplifier. Also, another drawback is instability and oscillation in the potential control loop due to the inductive behaviour of input resistance present in the transimpedance amplifier. Also, the connection in series of electrochemical cell and transimpedance amplifier, electrochemical cell having very large capacitive components has major contributes to the amplifier inductivity [135]. Although, literatures [136-141] reports utilization of two-electrode current conveyor sensor, with a working electrode still coupled at virtual ground, picking any presence of interference and environmental noise. Anyhow, the nonlinear property of the transistor resistance between drain and source terminals degrades the performance of linearity of the potentiostat.

In the second configuration, the three-electrode current conveyor has been fully experimented with in [133] and [142], but constrains on saturated voltage and nonlinearity problems have been encountered. But working electrode is held at a true ground preventing noise and interference. Moreover, it has been reported [142] current mirror conveyor usage as an alternative topology of three-electrode sensor. Unfortunately, the presence of current mirror mismatch has caused the potentiostat linearity to degrade as seen in [131].

4.3 Concepts and designs for potentiostatic devices in literature

To pay his respect to G. Schouten, J. G. F. Doornekamp, first scientist who designed and reported one of the firs designs for potentiostatic devices (1953) for in lab applications, the author used their exact schematic without any alteration or modification. In the early stages of electrochemistry (year 1953)there ware used potentiostats based on electronic tubes [143].

In the electronic tubes potentiostat, four parts can be distinguished. These parts are the supply-system, the chopper circuit, the amplifier, and the phasesensitive rectifier with the subsequent RC-circuit [143].

Even if the technology was very young those years and various concepts and techniques seems impossible those times, the authors managed to achieve precision of 0.5 V, using resistors up to 60 Mohms for amplification stages

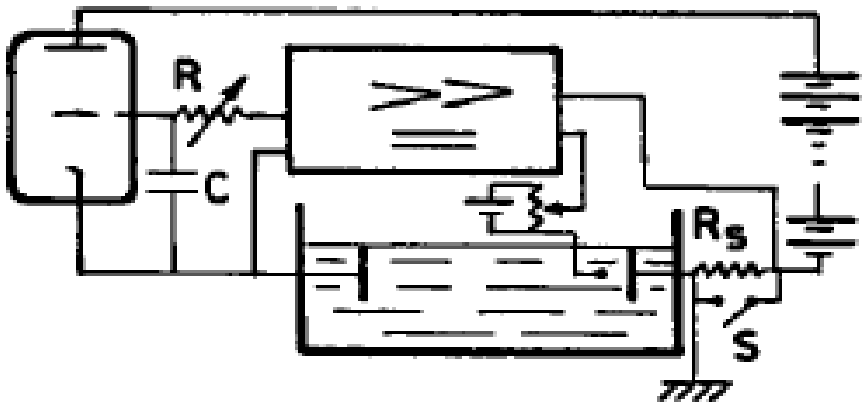

Fig. 4.3 Early stage potentiostat with electronic tubes [143].

A more recent potentiostat design based on OTA converter is reported in [144]. Amperometry and cyclic voltammetry detection techniques are based, as already presented on the accuracy of the potential difference between the WE and RE. The negative capacitive feedback around an operational transconductance amplifier (OTA) and the input common-mode feedback circuit impose a fixed voltage at the two WE. An external voltage source drives the reference electrode to set the potential of the redox reaction [144]. This design is very interesting because of the usage of OTA and conversion of the obtained electrochemical signal into impulses, making the frequency the main carrier of the information. It apply the same principle author base its research on but, on the other hand, the sensor concept used is different, in [144] being used an multi WE sensor.

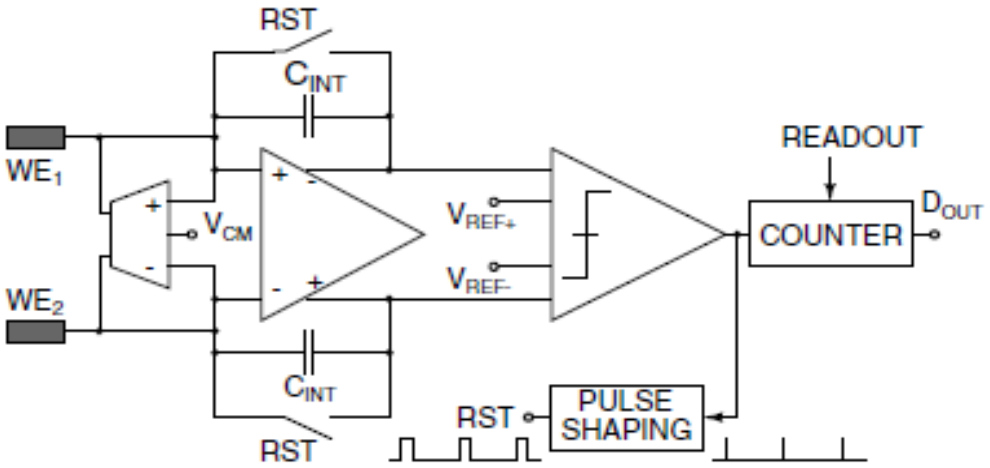

Fig. 4.4. Schematic design for bidirectional electrochemical sensors [144].

The potentiostat reported in [144], Fig. 3.4, measures electrochemical redox currents from electrochemical sensors with noise margin in pico amperes range. This fully differential architecture with differential recording electrodes rejects the common mode interference. Authors also reported an experimetal prototype in 0.35 um CMOS technology, with a 16 bit current to frequency conversion.

In [145] is reported a new concept on which author based its design and work. The principle reported is to convert very small, hard to measure currents into impulses, without any amplification stages. This design apply the same principle, being able to work only with classic 3 electrode electrochemical sensors.

The concept presented in [145] does not use amplifiers that need a lot of circuitry for amplification, cleaning the signal, circuits that deal with noise and so on and also do not need clock circuits that also take area on chip so it is a very good concept that author have decided to use and improve. By converting input currents into impulses, as seen in [127] and [145], so into time, amplifying circuitry has been eliminated, avoiding matching problems and save on area on chip and power consumption. The concept is to design a potentiostat circuit that accepts an electrochemical signal, in case studied here, proportional to current flowing through the electrolyte (in the electrochemical cell principle) and measure the time it takes to charge or discharge a capacitor. The proposed design is more sensitive, portable, inexpensive and consumes lower power than earlier designs.

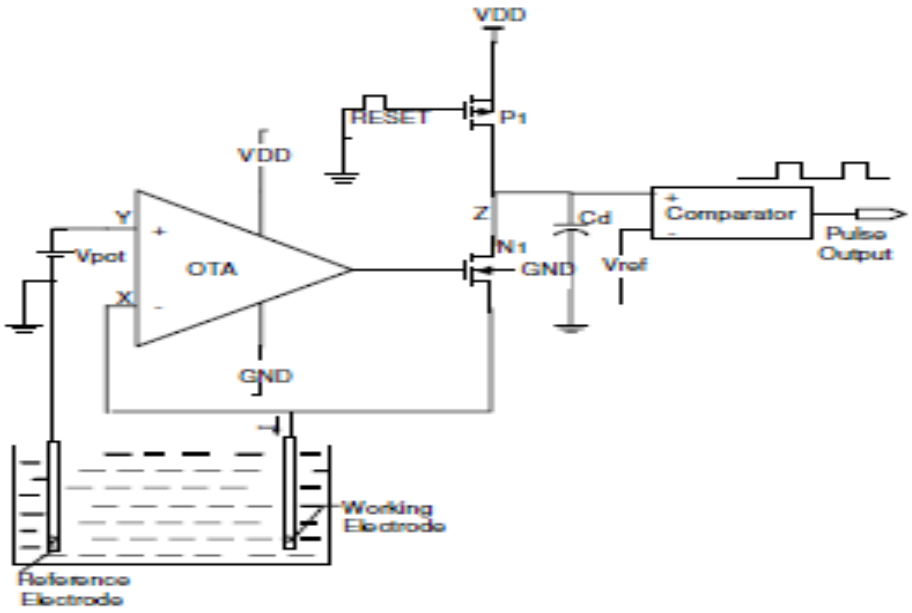

Fig. 4.5. Design of a potentiostatic device base in current-time conversion [145].

In [131] a different architecture has been reported. Wei-Song Wang et al reported a single-ended classic potentiostat topology with a new connection interface between potentiostat circuit and sensor electrodes so avoiding deviation of cell voltage and converting linearly the cell current into voltage signal. Because the increased quantity of harmonic distortion when low-level current from the sensor is detected, so decreasing the performance of the potentiostat linearity, decrease that limits the detectable current and dynamic range. So, to minimize these irregularities, a fully differential potentiostat is designed with a wide output voltage swing compared to single ended potentiostatic devices. Two proposed potentiostats were implemented by the Wei-Song Wang and team, using TSMC 0.18-μm CMOS process for biomedical application. They ware able to measure current from 500 pA to 10 uA with the dynamic range value can reach a value of 86 dB.

The last example that the author presents in its literature survey is a potentiostat as seen in [129]. This is a cell using thin-film transistors (TFTs) integrated potentiostat. The integrated potentiostat reported by Mutsumi Kimura and his team consist of three operational amplifiers composed of poly-Si TFTs, while the electrochemical cell was fabricated in printing technology. These microsensor cmponents have been integrated on a glass wafer to compose a micrototal analysis system (uTas). A cyclic-voltammetry measurement was performed as a standard biosensing experiment to confirm the elementary function of the integrated potentiostat. The expected characteristic has been acquired by an amperometric enzymatic redox reaction using glucose oxidase and ferrocene mediators, and a glucose concentration of as low as 0.7 mM was detected, which is sufficient sensitivity for some medical applications including diabetic diagnosis.

The reported system [146] consists in a waveform generator to generate the triangle waveform applied to voltage input, a sample and hold circuit to extract the maximum out voltage, and an analog–digital converter to convert it to a digital signal as peripheral equipment to complete a detection system. On the market there are massive numbers of signal conditioning systems for electrochemical cells, based on different principles [147]- [153], from measuring time between impulses to amplifying the currents or transforming the currents into voltages.

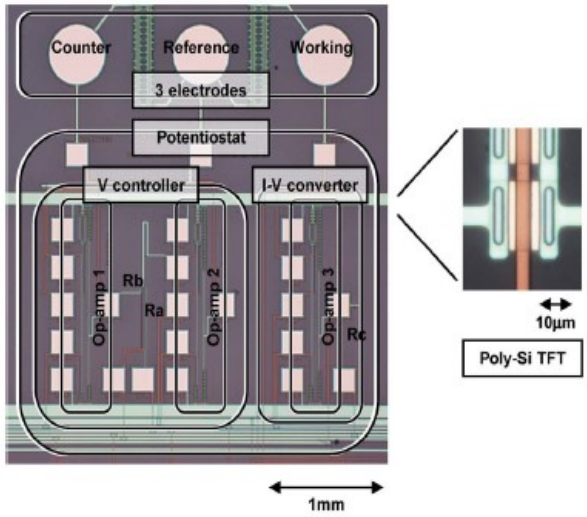

Fig. 4.6. Experimental integrated potentiostat [146].

5. PROPOSED SIGNAL CONDITIONING CIRCUIT

Chapter 5 presents the new and original universal signal conditioning system for electrochemical and bioluminescent sensor array. Here the author details the working principle and functionality of the circuit. In this chapter is also presented a simplified OTA design with fewer transistors that maintain the characteristics of more complex designs. An important part of this chapter is for detailing the calculus algorithm for OTA circuit. Also the new keys that replaced the simple transistors are presented. Tsi new and complex keys are fast current switches from literature. The novelty is their integration in this original design.

Integration of various chemical devices and complex operations onto a micro-chip, which is often referred to as a micro-total analysis system (μ-TAS) or "lab on a chip", is currently generating major interest due to the promising characteristics of such systems. Over the last few years, the dimensions of these systems have decreased, resulting in the ability to accommodate biological sensors on solid-state platforms with micron scale features. There are few methods to detect the generated signal from the microbial cells, e.g. optical, electrochemical, electrical and mechanical.

There are, as seen in previous paragraphs, many designs available on the market, designs suitable for electrochemical sensors, bioluminescent sensors or both. From Sigma-Delta converters to full integrated capacitors or resistors batteries. The author conducted a full and comprehensive 2 semester study of those designs. The main problem that needed to be overcome in classical design that deal directly with currents and voltages is that it is imperative to amplify the signal prior to the measurement and interpretation. The main issue of amplification stages is their big area on chip. Resistors are quite big, area on chip is expensive so to integrate resistors is not cheap at all. The goal of the research is to model a circuit for very limited or single use sensor array so to have a competitive product on the market, price is an essential quality and decision factor. Another approach could be with Delta Sigma converter but the circuit is quite complex and not quite suitable for our application. Delta Sigma converters are mass produced in audio-video systems where the rules that must be followed are more complex than in our case where the variation of the input signal is small, slow and usually fallow a linear pattern.

Another reason for choosing this approach is that the integrator must be able to integrate in both directions, up and down. This bi -directional integration is because of the large excursion of signals that we deal with, from a few nano Amps to several hundreds micro Amps. The direction of the current flowing from the sensors differ, one type inject current into circuit and the other one subtracts current from the circuit. This further narrows the options what circuits could be used for. For combining these two types of sensors into one single matrix, the first idea that the author tried was to use two separate circuits, one for each type of sensor but the number of components exceeded the maximum number the design could have being proficient at the same time. Another solution that the author has studied was to use a single circuit, simpler one and to convert both signals, to bring them both in the same field of values. It would have had no sense to divide the

powerful signal from the electrochemical sensor so as to be closer as value to the values provided by the bioluminescent sensor, it was also a bad solution to build an amplifier just for the signals from bioluminescent sensors. Even if one of this solution was selected, it was still needed to overcome the problem with the direction of the signals.

But why to measure an electric signal? Actually, time is the element that is measured and quantified with the greatest precision now so why not to convert both signals into time, making the frequency the main carrier of the information. There are designs in literature that do this for each type of sensors but we decided to implement the concept for a circuit able to work with both kind of sensors. A circuit that is able to work with both electrochemical and bioluminescent sensors is one that is able to work with sensors regardless the direction of the current. This way we end up designing an original signal conditioning system for amperometric sensors. Even after the decision on a concept was made, the problem with the direction and big difference between the two signals remained. The integration of a multiplexer was the solution for the problem. Actually, at the beginning the first solution was with 2 multiplexers but we gave up one because only one was enough for our purpose. Another challenge was designing an One Shot circuit that is able to fire the signals for both types of signals that come from the Operational Transducer. OpAmp is also a very important part of the design because of, as we previously stated, the directions of the current and the large excursion of values.

The circuit the author proposes is based on the concept presented in [154] and [155]. The main idea is to eliminate the amplifying stages and to convert the small currents, either electrochemical or bioluminescent, but mainly electrochemical currents into time, making the frequency the carrier of the information. The author is also proposing an universal signal conditioning circuit for 8X8 sensors array. Eliminating amplifying stages author reduced area on chip, lowering the cost and complexity of the chip in the same time.

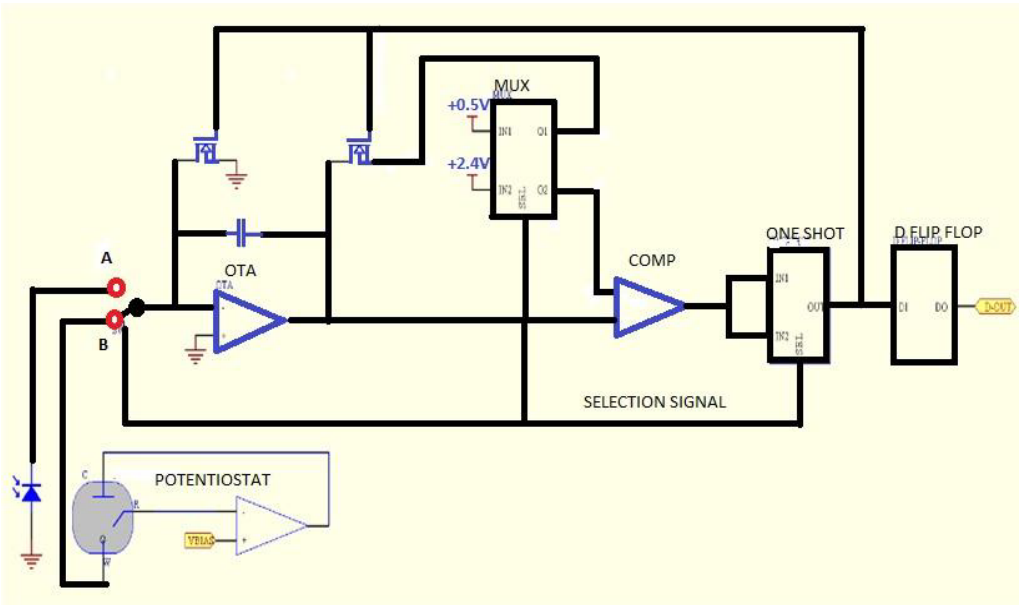

Fig. 5.1. Simplified proposed universal signal conditioning system.

In the schematic the concept is presented, at the entrance of the system it will be a 8X8 array of both electrochemical and bioluminescent sensors linked to the main circuit by a control circuit that decide which sensor in the matrix will be activated. Each cell will be able to perform both as electrochemical and bioluminescent sensor. This is an original design based on [154] and [155]. Decision was made after author has studied the designs and possibilities on the market [156] at the time when the research took place. At the entrance of the circuit we have, Fig.5.1, a switch that commute between the electrochemical sensor and the bioluminescent sensor, point A and B in the design. The sources used in design and calibration of the circuits have been reported by the author in [10]. First, we assume that point A is connected. In this case, the multiplexor MUX will send at the entrance of the operational transducer OTA 0.5 V and at one entrance of the comparator COMP 2.4 V. The current from the sensor will start to charge the 1 pF capacitor, until the voltage will reach 2.4 V. When this value is obtained, the comparator will send a signal to the ONE-SHOT circuit. The role of this circuit is to amplify the signal enough to reset the two keys of the circuit discharging the capacitor to 0.5 V and bringing 2.4 V at the entrance of the comparator COMP. The same impulse will be send to the D Flip-Flop circuit that transforms the impulses into the OUT signal of the design. More toxic agent into the water will be translated in more light, a bigger input current which will charge the capacitor faster, so the comparator will fire faster to the One-Shot circuit, which will reset faster the circuit so the frequency of the signal will increase proportionally with the concentration of pollutants. In the other case, the entrance of the circuit is on point B, at the exit of the electrochemical sensor. In this case, the OTA integrates the signal downwards, from 2.4V to 0.5 V. The MUX will provide 2.4 V to the entrance of the OTA, charging the capacitor to 2.4 V and bringing 0.5 V to the entrance of comparator COMP. The current from electrochemical sensor will start to discharge the capacitor until it will reach 0.5 V. In this moment, comparator will send a signal to ONE SHOT.

This signal, which resets the keys, is also the output signal of the circuit. Also, in this case, the frequency is proportional with the pollutants concentration. In the initial schematic, the keys ware simple transistors. In this case, the results of simulation ware less than satisfactory, the voltages being either too big or to small. One case was that the voltage was not big enough to open the transistors in one case, the other case was that voltage was to big all the time on transistors so it was impossible for them to close, no matter what dimensions was chosen for the transistors. The author decided to replace the simple transistor with more complex schematics.

The main goal the author have had in mind was to use circuits as simple as possible, common used blocks, so to reduce the complexity of the circuit as much as possible, maintaining in the same time the integrity of the signals, lowering the noise and errors inserted by the electronic part [173]. There are also noises that affect the functionality of the system, noises that not enter into field of activity of the author, electrochemistry, biology, chemistry etc. The main blocks will be detailed in next paragraphs.

5.1. Operational Transductance Amplifier

The integrator used in the schematic represent the interface between the sensors and the signal processing blocks, so this circuit is the core of the entire module and the performance of the module is highly connected with the overall

performance, so the architecture and the dimensions of the transistors should be done in order to obtain low noise, low offset and high gain and a good common mode voltage range.

5.1.1. Requirements and calculus algorithm for OTA design

To obtain high gain using CMOS technology is necessary for the amplifier to be with at least two stages. The basic two stage CMOS operational amplifier is shown in Fig.4.2.

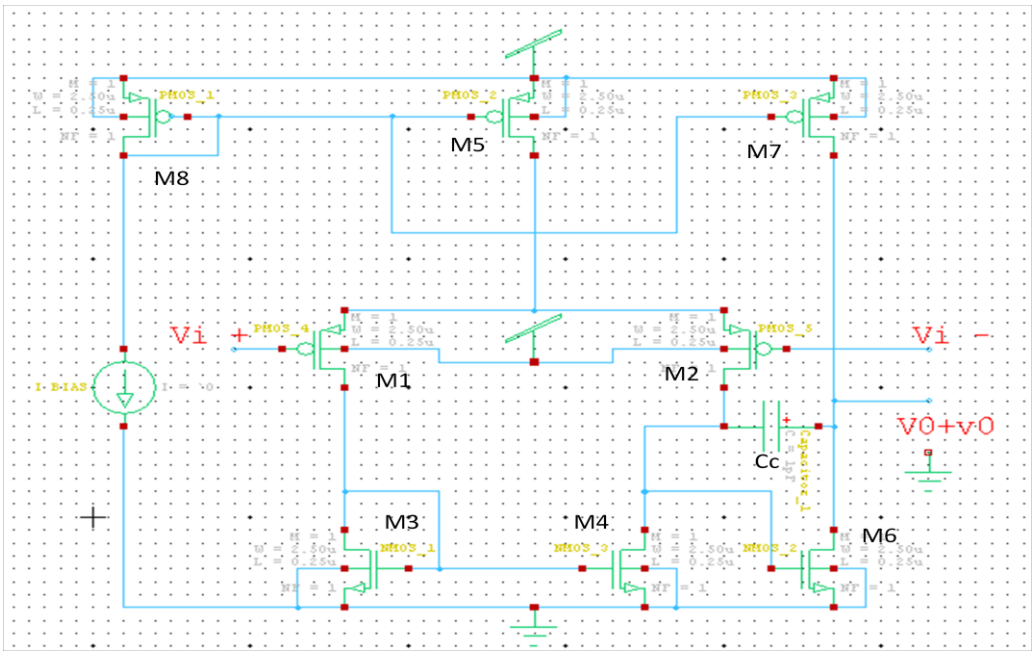

Fig. 5.2. The basic two stage CMOS operational amplifier design [158].

A differential input stage drives an active load followed by a second gain stage. This circuit provides good common mode range, output swing and voltage gain and has only one capacitor used for compensation.

The first stage consists in a two PMOS pair M1-M2 with a NMOS current mirror load M3-M4 and also a current source made by a PMOS transistor M5. The second stage consists of an NMOS common source amplifier (M6) with a PMOS current source load (M7).

The output resistance is the resistance looking back into the second stage with the op-amps inputs connected to the ground.

$$Ro = ro6||ro7 \tag{5.1}$$

The voltage gain of the first stage is :

$$Av1 = Gm1*Ro1 \tag{5.2}$$

where Gm1 and Ro1 are the transconductance and the output resistance of the first stage, so, the gain of the first stage becomes :

$$Av1 = gm1^* (ro2||ro4) \quad (5.3)$$

The second stage voltage gain can be obtain in similar mode :

$$Av2 = -gm6^*Ro \quad (5.4)$$

So, the overall gane of the thw stage ampliefier becomes:

$$Av=Av1^*Av2 = - gm1^* (ro2||ro4)^* gm6^*Ro \quad (5.5)$$

The output swing of the amplifier represents the output voltages for which all transistors operates in active region and can be increased by reducing the overdrives of the output transistors.

5.1.2. Input offset parameter

Another important parameter is the input offset as presented in [158]. The input offset is defined as the differential input voltage for which the differential output voltage is zero, on the other hand in the situation where the output is single ended and VSS equals GND is defined as the differential input voltage for which the output voltage is midway in the supply voltage and Gnd range, Vdd/2 if Gnd is considered 0, and in this way we maximize also the output voltage swing. In case of *VDD ≠ Vss,* anyhow, the output voltage should be set between the supply voltages to maximize the output swing. Therefore, the input offset voltage of op amps with differential inputs and single-ended outputs will be define as the differential input voltage for which the dc output voltage is midway between the supplies. Two components compose the offset voltage of an op amp: the first component is the systematic offset and the second component is the random offset.

The systematic offset voltage is another important parameter that needs to be studied. In bipolar technologies, the gain of each stage in an op amp can be quite high (on the order of 500) due to the product $g_m r_o$ that is usually greater than 1000. In consequence, the input-referred offset voltage of a bipolar operational amplifier usually have high dependency mainly on the first stage design. In CMOS technologies, anyhow, the $g_m r_o$, product is usually in *20* to 100 range, sometimes causing the offset of the second stage to play an major role in determining the op-amp offset voltage by reducing the gain per stage.

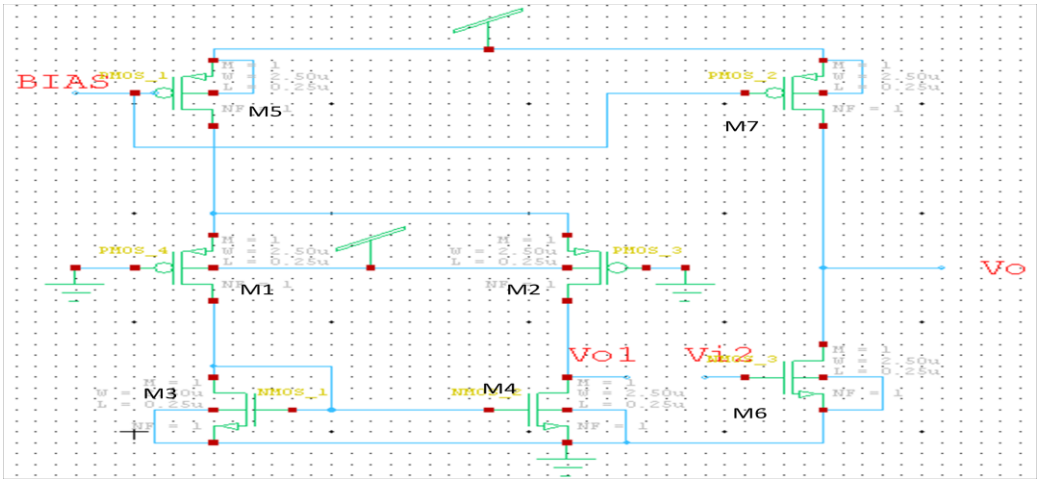

Fig. 5.3. Two stage amplifier with stages disconnected [158].

To study the systematic offset, the operational amplifier from Fig. 5.2 was split into two separate stages as shown in Fig. 5.3. Assuming the inputs of the first stage grounded, and considering a perfect, the dc drain-source voltage of *M4* must be equal to the dc drain-source voltage of M3**.** This result stems from the observation that if *VDS3 = VDS4,* then $V_{Ds1} = V_{DS2}$ and I_{D1}, = I_{D2} = I_{D5}/2. And so, with V_{DS3} = VDS4 and so $I_{D\,3} = I_{D4} = -I_{D5}/2$. AS a result, V_{DS3} should be equal to V_{DS4} because this operating point is the only point where the current flowing out of the drain of M2 is equal to the current flowing into the M4drain**.**

For instance, increasing voltage in the drain-source of *M4* will produce the increase the current flowing into the drain of M4 in the same time decreasing the current flowing out of the M2drain as a consequence of the effects of modulation of channel-length and for this reason the dc drain-source voltages of M3 and M4 pair of transistors must be equal under given conditions. Thus, the value of the M6 gate-source voltage required to set the amplifier output voltage midway between the supplies may be different from the dc output voltage of the first stage. If the first stage gain is, let's say 100, each 0.1-V difference in these voltages results in input-referred systematic of offset 10 mV. Ignoring channel-length modulation in *M5* and M7, the current in this pair of transistors do not depend on their drain-source voltages with the condition that the pair operate in the active region [158]. To set the output voltage midway between the supplies, both transistors should operate in the active region and the gate-source voltage of *M6* should be chosen so that its drain current is equal to the drain current of M7.

When the output of the first stage is connected at the input of the second stage, V_{GS6}= V_{DS4}. With perfect matching and zero input voltages, V_{DS4} = V_{DS3}= V_{GS3} and V_{t3} = V_{t4} = V_{t6}.

$$V_{ov3}=V_{ov4}=V_{ov6} \tag{5.6}$$

$$\frac{|Id3|}{2\,(W/L)3}=\frac{|Id4|}{2\,(W/L)4}=\frac{|Id6|}{2\,(W/L)6} \tag{5.7}$$

$$\frac{|\mathrm{Id}5|}{2\,(\mathrm{W/L})3}=\frac{|Id5|}{2\,(W/L)4}=\frac{|Id7|}{2\,(W/L)6} \tag{5.8}$$

$$\frac{Id5}{Id7}=\frac{(W/L)5}{(W/L)7} \tag{5.9}$$

$$\frac{(W/L)3}{(W/L)6}=\frac{(W/L)4}{(W/L)6}=\frac{1}{2}\frac{(W/L)5}{(W/L)7} \tag{5.10}$$

Having the aspect ratios chosen to satisfy (5.10), M3, M4, and *M6* operate with equal densities of current. The current density of a device not only depends on its gate-source voltage while working into active region, but also to some degree on its drain-source voltage. Knowing current densities and the gate-source voltages of M3, M4, and M6 have the same value, the drain-source values of voltages of this group of transistors must also be the same. Thus, the output dc voltage in this case is (5.11)

$$V_0=V_{DS6}-V_{SS}=V_{DS3}-V_{SS}=V_{GS3}-V_{SS}=V_{t3}+V_{OV3}-V_{SS} \tag{5.11}$$

To determine the systematic op-amp output offset voltage, from the output voltage a voltage midway between the supplies should be subtracted (5.11). To refer the systematic offset voltage to the op-amp input, this difference should be divided by the op-amp gain.
The result is

$$Vos(sys) = \frac{Vt3+Vov3-Vss-\frac{VDD-VSS}{2}}{Av} \quad (5.12)$$

where A is the op-amp gain given in (4.5). DC output voltage will not be midway between the supplies in most cases due to the fact that $V_{GS3} = V_{t3} + V_{ov3} \neq (V_{DD} + V_{SS})/2$ so the systematic offset is nonzero. Thus the systematic offset voltage is in general nonzero, the aspect ratios choice is given by (5.11) and can result in an operating point that is insensitive regardless the process variations.

It has been proven in literature that the channel effective length of a transistor MOS differs from its drawn length by offset terms caused by the diffusion side of the source and drain (Ld) and the depletion region width around the drain (*Xd).* In the same way , the effective width of a transistor MOS type differs from the width drawn by an offset term *dW* caused by the effect of so called bird's beak in the oxide. To keep constant the ratio in (5.11) in the presence of process-induced variations in Ld, Xd, and dW, the drawn channel lengths and widths of the ratioed transistors each should be chosen to be identical. This statement being accomplished, the ratio in (5.11) can be set equal to any rational number J*I*K by connecting J identical devices called n-channel units in parallel to form M4 and M3 while the K n-channel units in parallel form M6**.** After this, consider that M5 is constructed of 2J devices, selfsame, called p-channel units, M7 must be designed from K p-channel units. In day to day practice for appropriate devices, the channel lengths are almost never ratioed directly due to the use of small channel lengths for high-speed operation would result in a large to process sensitivity modification. Otherwise, the matched device channels widths are occasionally related in a straight forward way when sensitivity to process variations resulted is insignificant due to the large enough width.

5.1.3. Random input voltage parameter

Random input offset Voltage is another important parameter of OTA design. Generally, source-coupled pairs display a higher random offset than their bipolar counterparts. Not paying attention to the contribution of the second stage in the op amp to the input-referred random offset, a direct analysis for the voltage offset of the circuit presented in Fig. 5.2, gives the (5.13) equation.

$$V_{OS}=\Delta V_{t\,(1\text{-}2)}+ \Delta V_{t\,(3\text{-}4)} \left(\frac{gm3}{gm1}\right)+\frac{Vov\ (1-2)}{2}\left[\frac{\Delta\left(\frac{W}{L}\right)_{(3-4)}}{\frac{W}{L}_{3-4}}-\frac{\Delta\left(\frac{W}{L}\right)_{(1-2)}}{\frac{W}{L}_{1-2}}\right] \quad (5.13)$$

In (5.13) the first term the threshold is mismatched of the input transistors. The second represents threshold mismatch of the current-mirror-load devices and drop down by choosing the load devices W/L ratio in such way that their transconductance will be smaller than that of the transistors present at the input.

Therefore, selecting a channel length longer for M3 and M4 compared to M1 and M2 will reduces the random offset voltage input. The third term is the effects of W/L mismatches in the input transistors and loads and is minimized by operating the input transistors at low values of overdrive, usually on the order of 50 to 200 mV.

$$\text{CMR} = \left| \frac{A_{dm}}{A_{cm}} \right| = \left| \frac{\frac{v0}{v01} X \frac{v01}{vid}}{\frac{v0}{v01} X \frac{v01}{vic}} \right| = \text{CMR1} \qquad (5.14)$$

The second stage do not contribute to the common-mode rejection ratio of the op amp because the second stage has a single-ended input and a single-ended output.

$$\text{CMR} = (2g\ (dp)\ rtail)\ gm\ (mir)\ (r0\ (dp)\ ||\ ro\ (mir)\ ) \qquad (5.15)$$

where gm (dp) and $r_{0\ (dp)}$ are the transconductance and output resistance of M1 and M2**,** while $g_{m\ (rnir)}$ and $r_{o\ (mir)}$ are the transconductance and output resistance of M3 and M4, and R tail is the output resistance of Ms**.** By a process similar to the derivation of (5.3), this equation can be simplified to give (5.16).

$$\text{CMR} = \left| \frac{2}{V_{ov\ (dp)}} \frac{2}{V_{ov\ (dp)}} \left(\frac{V_{a\ (dp)} V_{A\ (mir)}}{|V_{A\ (dp)}| + |V_{A\ (mir)}|} \right) \right| \qquad (5.16)$$

In (5.16), Vov (dp) and VA (dp) are the overdrive and Early voltage pair differential, and Vov (mir) and VA (mir) are the overdrive and Early voltage of the mirror. Equation (5.16) shows that the common-mode rejection ratio of the op amp can be increased by reducing the overdrive voltages.

A different way to increase the common-mode rejection ratio is by replacing the simple current mirror M_5 and M_8 with one of the high-output-resistance current mirrors.

On the other hand, such a replacement would also make the common-mode input range worse. It is commonly accepted that common-mode range input is the range of dc common-mode voltage inputs for which all first stage transistors operate in the active region. To be able to operate in the active region, the NMOS gate-drain voltages of transistors must be smaller than their thresholds therefore their channels do not exist at their drains. Similarly, PMOS transistors will operate in the active region only if their voltages of gate-drain are larger compared to their thresholds, similarly that their channels do not exist at their drains [158]. With a pure common-mode input V_{ic} applied to the inputs of the op amp in Fig. 5.2, will obtain :

$$V_{DS4}=V_{DS3}=V_{GS3}=V_{t3}+V_{ov3} \qquad (5.17)$$

$$V_{GD1}=V_{GD2}=V_{ic}-V_{t3}-V_{ov3}+V_{SS} \qquad (5.18)$$

When V/c is reduced to the point of *VGD1* = VGD2 = Vt1 = Vt2, M1 and *M2* operate between the the triode and active regions, at the edge. This point defines the common-mode range at the lower end, which will be defined as in (5.19).

$$V_{IC} > V_{t1} + V_{t3} + V_{ov3} - V_{SS} \qquad (5.19)$$

If V_{lc} is too high, however, *M5* operates in the triode region. The drain-source voltage of M5 is:

$$V_{DS5} = V_{IC} - V_{GS1} - V_{DD} = V_{IC} - V_{t1}.- V_{ov1} - V_{DD} \quad (5.20)$$

From the point of view of drain-source voltages, NMOS transistors will operate in the active region only if their drain-source voltage is bigger than their overdrive. Thus, PMOS operate in the active region only if their drain-source voltage is less than their overdrive. Therefore, the upper end of the common-mode input range will be:

$$V_{IC} < V_{t1} + V_{ov1} + V_{ov5} + V_{DD} \quad (5.21)$$

M1 and M5 are PMOS , their overdrives are negative, *M1* is an enhancement-mode device, its threshold is negative due to its PMOS properties. The common-mode range limits becomes:

$$V_{t3} - |V_{t1}| + V_{ov3} - V_{ss} < V_{IC} < V_{DD} - |V_{t1}| - |V_{ov1}| - |V_{ov5}| \quad (5.22)$$

(5.22) is an inequality that represent the necessity that the magnitudes of the overdrive terms should be diminished to maximize the common-mode range. In the same way, the body effect on the input transistors could be used to increase the range. If the M1 and M2 bodies are connected to *VDD* as showed in Fig. 6.16, these transistors source-body voltage is low when V_{ic} is high. So, by using the zero-bias value of Vt1, the upper limit in (5.22) can be found with satisfactory approximation. When value of V_{lc} goes down, the *M1* and *M2* source-body voltages becomes more negative, enlarging the depletion region around the source and making more negative the threshold voltage of these transistors.

5.1.4. Power Supply Rejection Ratio

To determine the Power Supply Rejection Ratio, (PSRR) from the *Vdd power* supply for the op amp in Fig. 4.2, the small-signal gain A^+ = Vo/Vdd will be divided into the gain from the input. For this equation, assuming that supply voltage Vss is constant and that both op-amp inputs in Fig. 4.2 are connected to small-signal grounds. The current in *M8* is equal to I_{BIAS}**.** If I_{BIAS} is constant, the *M8* gate-source voltage must be also constant due to the fact that *M8* is connected as a diode.

To determine the gain with finite Rtail and r_{07}, assume the small-signal diagrams shown in Fig. 5.4 and Fig. 5.5, where the *M5* and *M7* gm generators are ignored for they are inactive. In Fig. 4.4 , the output is defined as v_{oa}, and *Vdd* variation is set equal to zero at the point where Rtail is connected. In Fig. 4.5, the output is defined as v_{ob}, and the variation of *vdd* is set equal to zero at the point where is connected r_{o7}. v_{oa} and v_{ob} can be calculated separately and use superposition to find the total gain Vo/Vdd = (voa + vob)/vdd. In Fig. 5.4, no variation can be detected in first stage, and v_{gs6} = 0. For this, g_{m6} is inactive and the output stage is seen as a simple voltage divider to the supply variation. Since the M6 dc drain current is equal but opposite to that in *M7,*

$$\frac{v_{oa}}{v_{dd}} = \frac{r_{o6}}{r_{o6}+r_{o7}} = \frac{\frac{V_{A6}}{I_{D6}}}{\frac{V_{A6}}{I_{D6}}+\frac{|V_{A7}|}{I_{D6}}} = \frac{V_{A6}}{V_{A6}+|V_{A7}|} \tag{5.23}$$

$$\frac{V_{ob}}{V_{dd}} = \frac{v_{gs6}}{v_{dd}} \frac{v_{ob}}{v_{gs6}} \tag{5.24}$$

where the first term on the right side is the gain of the first stage, and the second term is the second stage gain.

The vdd input to the first stage in Fig. 5.5 is applied between the top of r_{tail} and ground while the *M1* and *M2* gates are grounded. This case is equivalent to grounding the top of r_{tail} and applying a voltage of *–vdd* between the *M1* and *M2* gates and ground.

The gain of the first stage becomes:

$$\frac{v_{gs6}}{v_{dd}} = -\frac{v_{gs6}}{v_{ic}} = --Gs\ [cm]Ro1 \tag{5.25}$$

Where Gs [cm] is the first stage common mode transductance and Ro1 is the output resistance of the first stage.

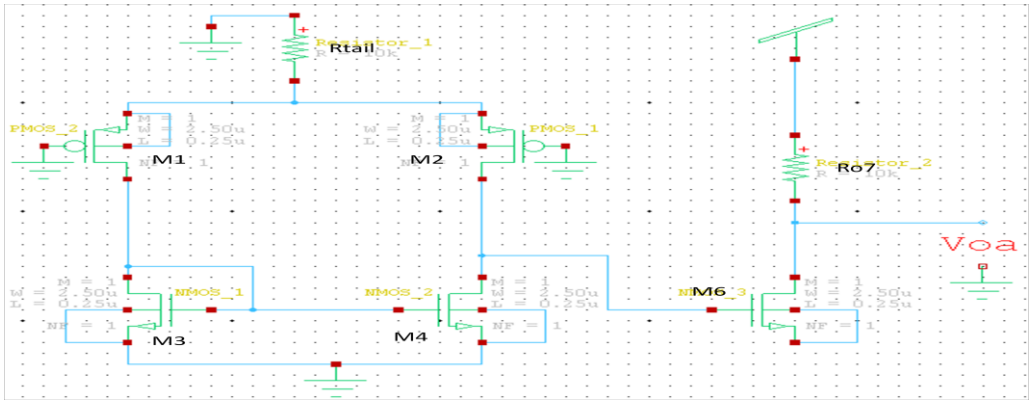

Fig. 5.4. Small signal diagrams of two stage amplifiers used to determine the relation between Vdd and the output through the second stage.

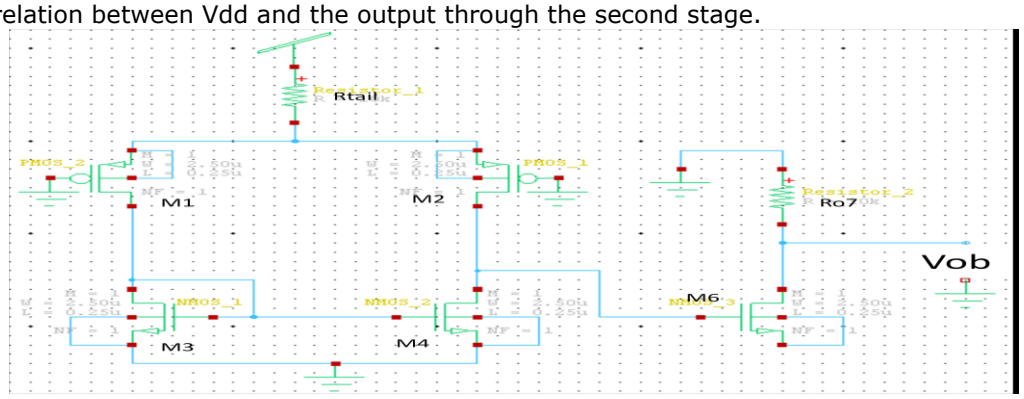

Fig. 5.5. Small signal diagrams of two stage amplifiers used to determine the relation between Vdd and the output through the first stage.

$$\frac{v_{gs6}}{v_{dd}} = \frac{gm\ (dp)\ (r_{o(dp)}||r_{o(mir)})}{1+2g_{m\ (dp)}\ r_{tail}}\left(\frac{1}{1+g_{m\ (mir)}r_{o\ (dp)}}+\frac{1}{1+g_{m\ (mir)}r_{o\ (mir)}}\right) \quad (5.26)$$

$$\frac{v_{gs6}}{v_{dd}} = \frac{r_{o\ (dp)}||r_{o\ (mir)}}{2\ r_{tail}\ g_{m\ (mir)}\ (r_{o\ (dp)}||r_{o\ (mir)})} = \frac{1}{2g_{m\ (mir)}r_{tail}} \quad (5.27)$$

$$\frac{v_{ob}}{v_{dd}} = -\frac{g_{m6}\ (r_{o6}||r_{o7})}{2g_{m\ (mir)}r_{tail}} \quad (5.28)$$

$$\frac{v_{ob}}{v_{dd}} = -\frac{V_{A6}}{V_{A6}+V_{A7}} \quad (5.29)$$

Due to the fact that $V_{A5}=V_{A7}$ and $|I_{D5}|=2I_{D3}$,

$$A^{+}=\frac{v_o}{v_{dd}}==0 \quad (5.30)$$

For the reason that the coupling from Vdd to the output through the first stage cancels that perfect matching through the second stage, PSRR→±∞ for low frequencies.

For to determine PSRR assume that the Vdd power supply at a constant value and that both op-amp inputs in Fig. 5.2 are connected in small-signal grounds configuration. With these constrains, M1 and M2 are acting as common-gate amplifiers, trying to keep the M3 and M4 bias current at constant values. If we consider the drain current of M3 constant, the gate-source voltage of the M3 transistor should be constant due to the fact that M3 is connected in diode configuration. Therefore, vgs3 = 0. Because vds = vgs3 and since vds4 = vds3 in this case, vds4 = vgs6 = 0. So, gm6 is inactive, the output stage appears as a simple voltage divider to the supply variation. Because the current drain of M6 is equal but opposite to that in M7,

$$A^{-}=\frac{v_o}{v_{ss}} = \frac{|V_{A7}|}{V_{A6}+|V_{A7}|} \quad \frac{v_o}{v_{ss}} = \frac{|V_{A7}|}{V_{A6}+|V_{A7}|} \quad (5.31)$$

$$\text{PSRR-}=\frac{A_{dm}}{A-} \quad (5.32)$$

Low-frequency supply rejection from the negative supply is given by this equation. As the frequency increase this rejection becomes worse.

If the applied frequency increases, the impedance of the compensation capacitor decreases, for high-frequency ac signals shorting the M6 gate to its drain. In the case that the gate-source voltage on M6 is constant the variation on the negative supply is fed directly to the output at high frequencies. A^{-} = 1 at frequencies high enough to short circuit Cc, considering that Cc >> CL, where the load capacitance of the op amp connected between the op-amp output and ground is represented by CL [158].

The same phenomenon causes the gains Adm and A^{+} to decrease as frequency increases, so that the PSRR+ remains relatively constant with increasing

frequency. Since A⁻ increases to unity as Adm, decreases, however, PSRR- decreases and reaches unity at the frequency where |Ad| = 1.

In figure 5.6 two cascode circuits are presented with, for simplicity, VDD = 0. In Fig. 5.6a, both M1 and M1A are p-channel devices. In Fig. 4.6b, M1 is still a PMOS e but M1A is now an NMOS. In both cases, anyhow, M1 is connected in a common-source configuration, and M1A is connected in a common-gate configuration. Small-signal variations in the drain current of M1 are conducted primarily through M1A in both cases because I_{BIAS} is a constant current source. Therefore, both circuits are examples of cascodes. The cascode in Fig. 5.6b is said to be folded.

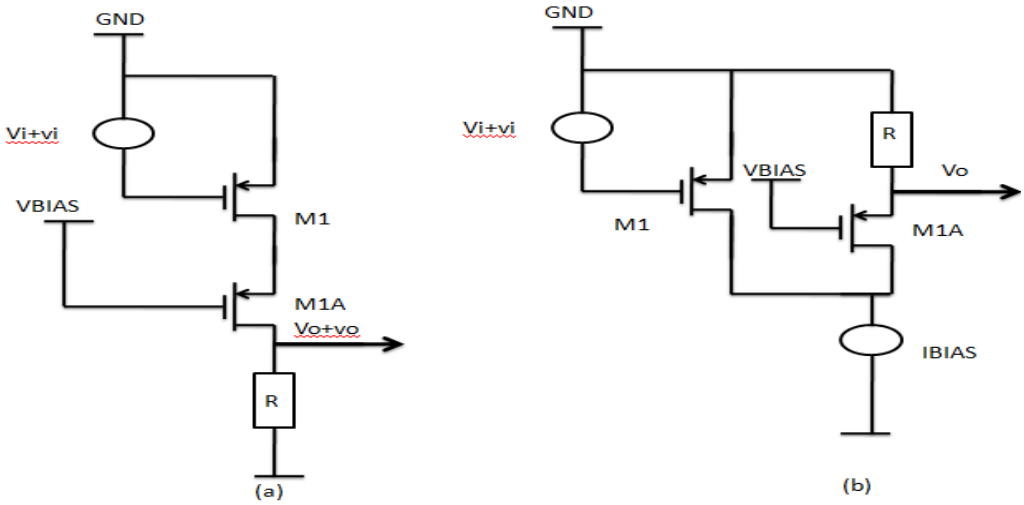

Fig. 5.6 (a) Standard cascode configuration (b) Folded cascode configuration [158].

Figure 4.7 presents a simplified schematic of a circuit that applies the folded- cascade structure to both sides of a differential pair. The current mirror is converting, as seen in [158], into a single-ended output, the differential signal by sending to the output variations in the drain current of M1A. The resulting op amp is called a folded-cascode op amp.

$$ID1A = ID2A = ID11 - \frac{I_{D5}}{2} = ID12 - \frac{I_{D5}}{2} = IBIAS - \frac{I_{TAIL}}{2} \qquad (5.33)$$

Compared to the other op-amp configurations, the folded-cascode configuration improves dramatically the input range for the common-mode. The upper end of the range is the same as in the basic two-stage op amp and the telescopic cascode op amp. The lower end of the range can be reduced significantly compared to both other configurations if V_{BIAS2} is adjusted so that M11 and M12 operate at the edge of the active region. Under this condition, the bias voltage from the drain of M1 to - Vss is Vov11, which can be much less than in the other configurations.

To calculate the output swing, first consider the PMOS cascode current mirror by itself. *M3* and *M4* are diode connected.

$$V_{OUT\ (max)} = V_{DD} - |Vtp| - 2|Vov| \qquad (5.34)$$

The threshold term in this equation can be eliminated by using a p-type version of one of the high-swing cascode current mirrors. The result is:

$$V_{OUT\ (max)}=V_{DD}-2|Vov| \tag{5.35}$$

To determine the output minimum voltage, if the V_{BIAS2} is adjusted so MI2 operates at the edge of the active region. Then the M12 drain-source voltage of is Vov and the minimum output voltage for which both M2A and M12 operate in the active region is (5.36).

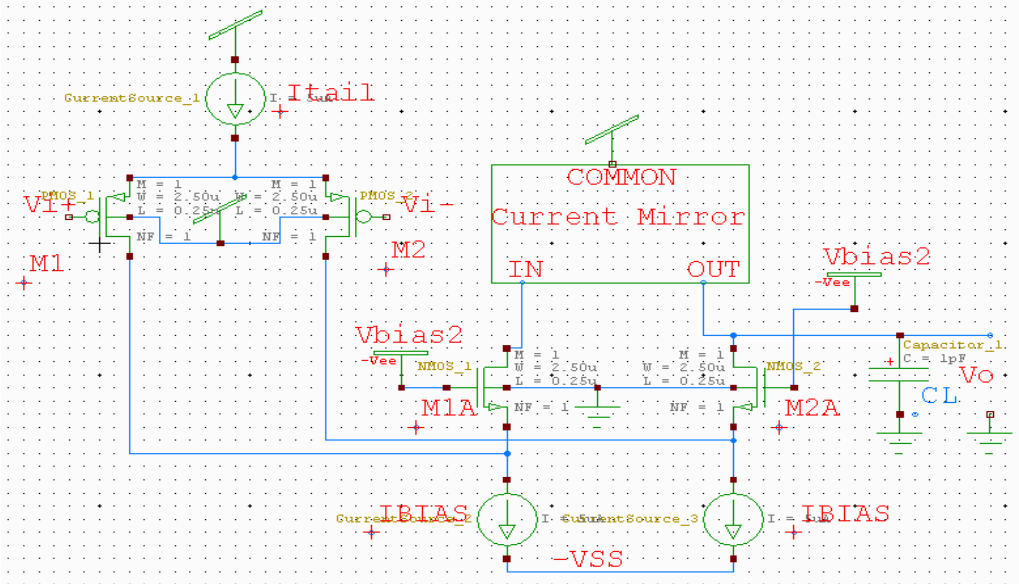

Fig. 5.7 Simplified folded cascode amplifier [158].

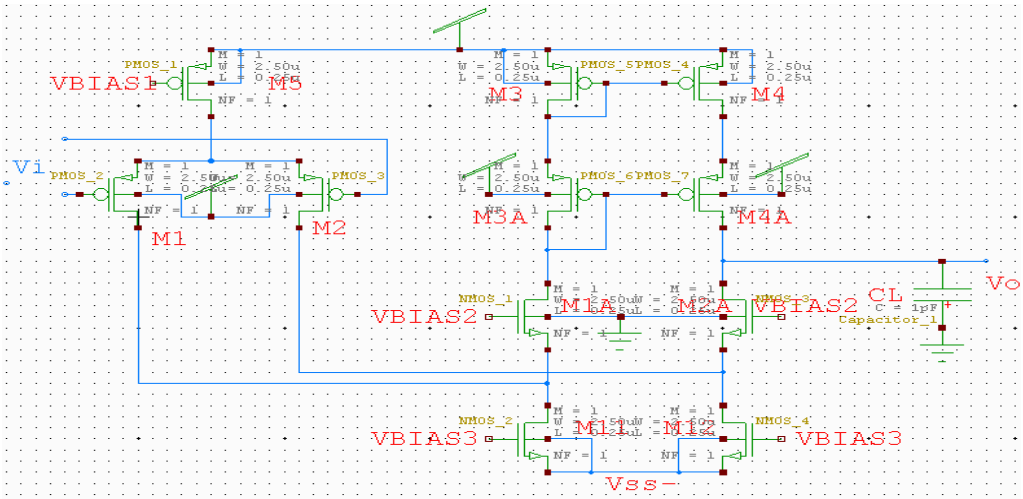

Fig. 5.8 Detailed Folded cascode amplifier [158].

$$V_{OUT\ (min)}=V_{SS}+2|Vov| \tag{5.36}$$

A folded-cascode operational amplifier can provide nearly constant voltage gain while its output swings into two overdrives of each supply. On the other hand, the telescopic cascode op amp output can swing within two overdrives of one supply and three overdrives of the other thus providing almost constant gain. The small-signal voltage gain of this circuit at low frequencies is:

$$A_V=GmRo \tag{5.37}$$

where Gm is the transconductance and Ro is the output resistance [158]. Supposing all the transistors operate in the active region, the range of typical gain magnitudes is varying from several hundred to several thousand. Variation in the drain current of M1 and M2 contribute constructively to the transconductance due to the action of the current mirror M3 - M4.

$$Gm=gm1=gm2 \tag{5.38}$$

To determine Ro both inputs must be connected to GND. Even if the input voltages do not move in this situation, the sources of M1- M2 are not operating at ac ground. Anyhow, connecting this node to small-signal ground as shown in Fig. 5.9 a consume little change in Ro, due to the action of the current mirror M3 - M4. Assuming $r\rightarrow\infty$, $\Delta id_1 = \Delta id_2$ for the reason that this connection imply equal changes in the gate-source voltages of M1 and M2. After, Δidl flows in the source of M1A, where it is mirrored to the output with a gain of unity if $r\rightarrow\infty$ in M3 - M4. As a consequence, KCL at the output shows that Δid1 and Δid2 cancel, causing no change to the output current *ix,* or the output resistance Ro. As a consequence, Ro can be found, only if the sources of M1 - M2 operate at ac ground.

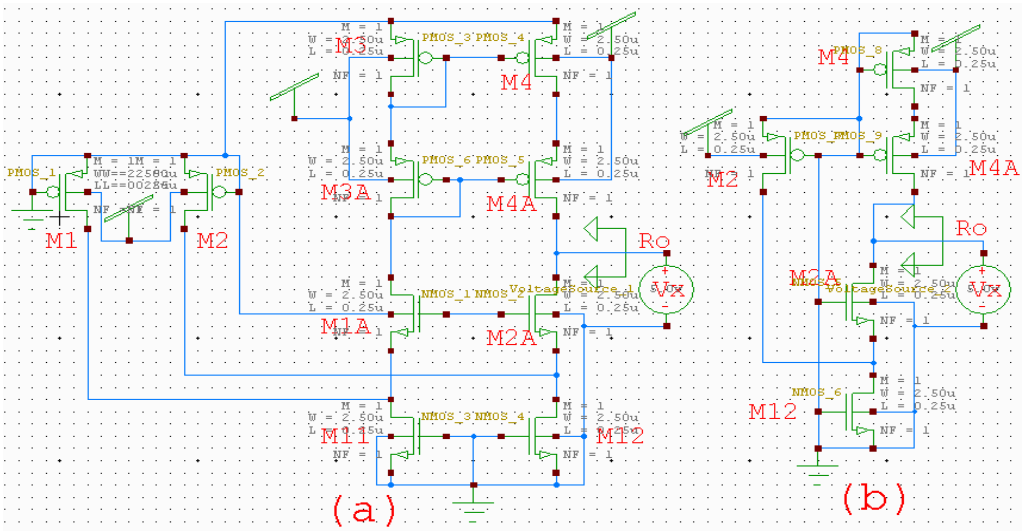

Fig. 5.9 (a) Test voltage source applied to the output to calculate resistance (b) Simplified circuit [154].

Usually, ro, in all the transistors is finite, and Ro, by connecting this point to ac ground, is slightly altered for two reasons. First reason is that Δid1 and Δid2 are unequal with finite ro, because vds1 and vds2 are not exactly equal. Differences between vds1 and vds2 stem from finite ro*,* in M1A and M2A for the reason that pair M3 and M3A are connected in diode configuration but their counterparts , pair *M4* and M4A are not diode connected. Second, the current gain small-signal of the current mirror is not exactly unity with finite ro, because Vds3 and Vds4 are not quite equal. Anyhow, the change in the output resistance introduced by these considerations is usually negligible.

Considering M1 - M2 sources connected to ac ground, the M1drain current is at a constant value. On the other hand, the Thevenin equivalent resistances on the gates of M4 and M 4A are small due to the fact that M3 and M 3A are connected in diode conffiguration. So, little error is introduced by assuming that the gates of M4 and M 4A are small-signal ground connected. Thus, the calculation of Ro can be made using the circuit of Fig. 5.9b.

$$Ro = (Rout|M2A)\,||\,(Rout|M4A) \tag{5.39}$$

The result is similar to a source degeneration common-source amplifier.

$$Rout|M2A = (r_{o2}||r_{o12})+r_{2oA}\,[1+(gm_{2A}+gmb_{2A})\,(r_{o2}||r_{o12})] = [gm_{2A}\,(r_{o2}||r_{o12})]r_{o2A} \tag{5.40}$$

$$Rout|M4A = r_{o4}+r_{o4A}\,[1+(gm_{4a}+gm_{b4A})\,(r_{o4})] = (gm_{4A}\,r_{o4})r_{o4A} \tag{5.41}$$

5.1.5. Proposed simplified ota design

An mandatory advantage of this circuit is that the load capacitance CL is performing the compensation function. So no additional capacitance is need be added to keep the amplifier when connected in a feedback loop from oscillating. In the basic two-stage op amp, Cc feeds the variation from one power supply forward to the op-amp output at high frequencies. Improving their high-frequency power-supply rejection ratios from the Vss supply, this feedforward does not occur in one-stage op amps such as the folded cascode and telescopic cascode structures.

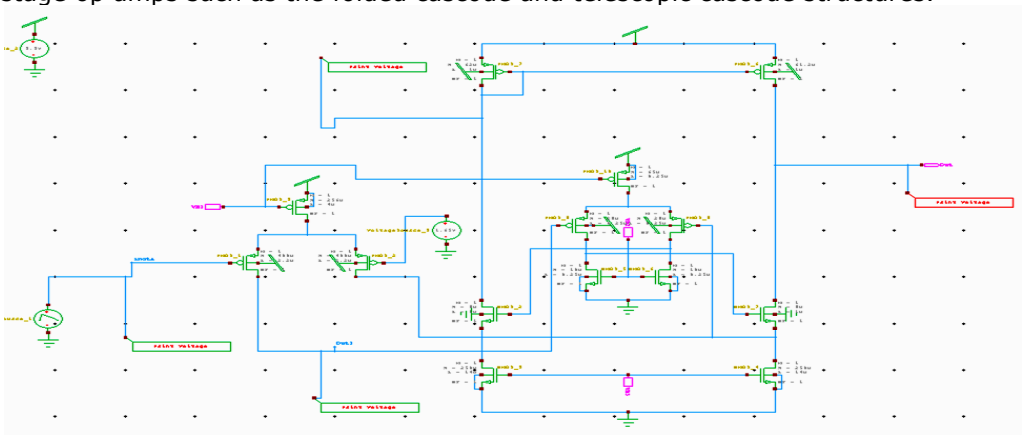

Fig.5.10 OTA simplified proposed model.

To determine the DC input offset, one of the inputs was connected to Vdd/2 and at the other input, a linear ramp voltage was connected. The difference between inputs was measured. Here the author will present the results obtained in Typical case of technology.

The graphic below present the variation of DC Offset Input variation for Typical, Slow and Fast cases, the simulation results and values are attached at the end of the thesys.

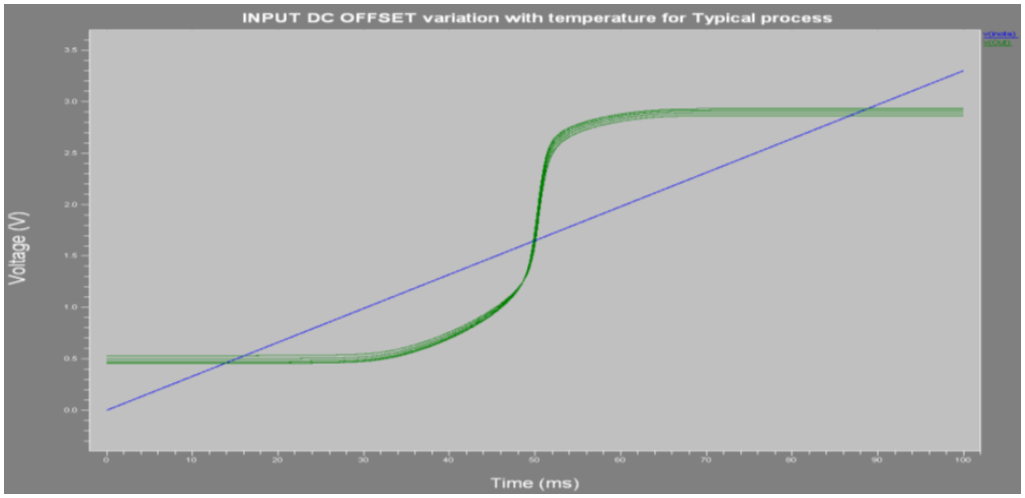

Fig. 5.11. Input DC OFFSET variation with temperature for Typical case process.

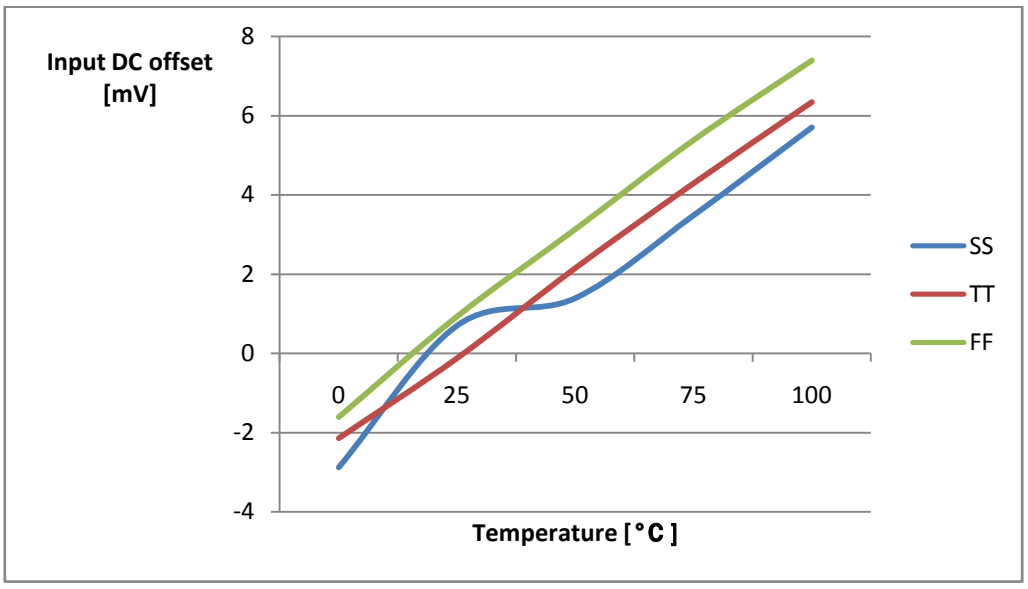

Fig. 5.12 DC Offset Input variation, Temperature and process variation.

To determine Bandwidth, one input is connected at DC voltage Vdd/2 and the second input is connected at an AC source, offset DC voltage Vdd/2. To calculate bandwidth, the formula was applied:

20log (Vout/Vinput (ACsource)) (5.42)

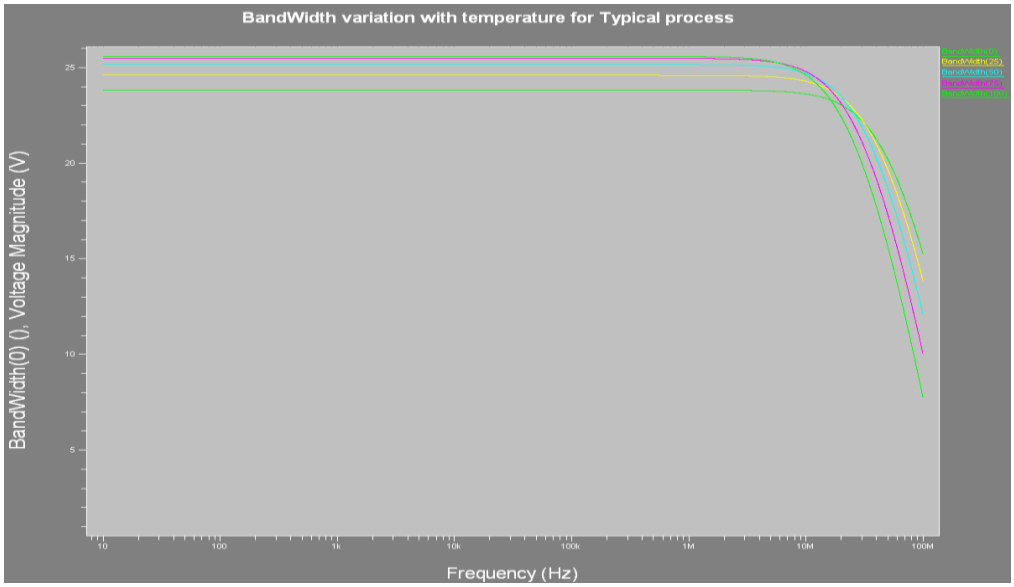

Fig. 5.13 Bandwidth simulation results.

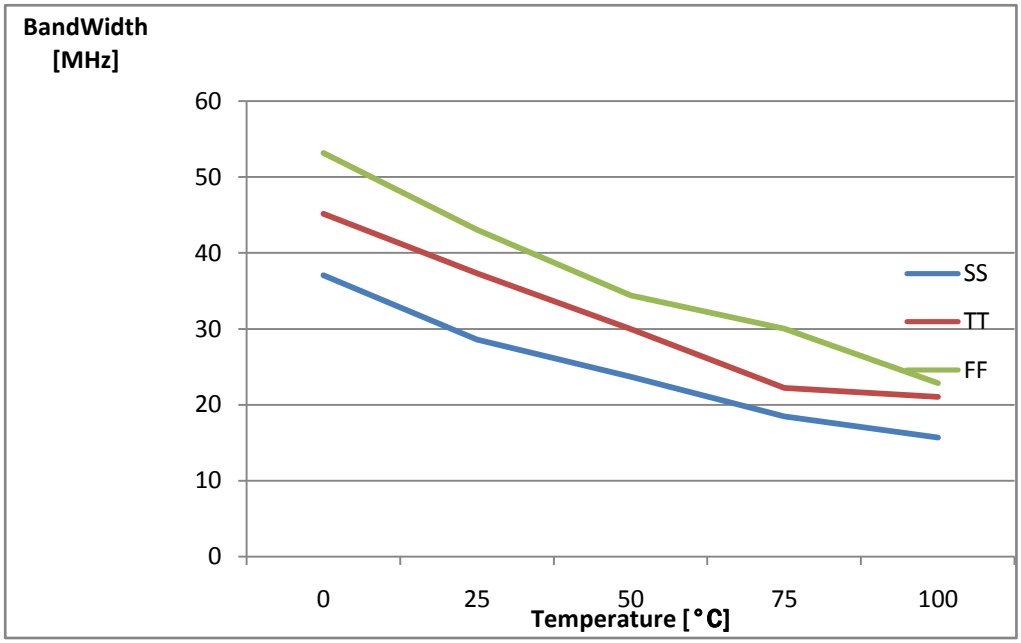

Fig. 5.14 Bandwidth simulation results function of temperature and process

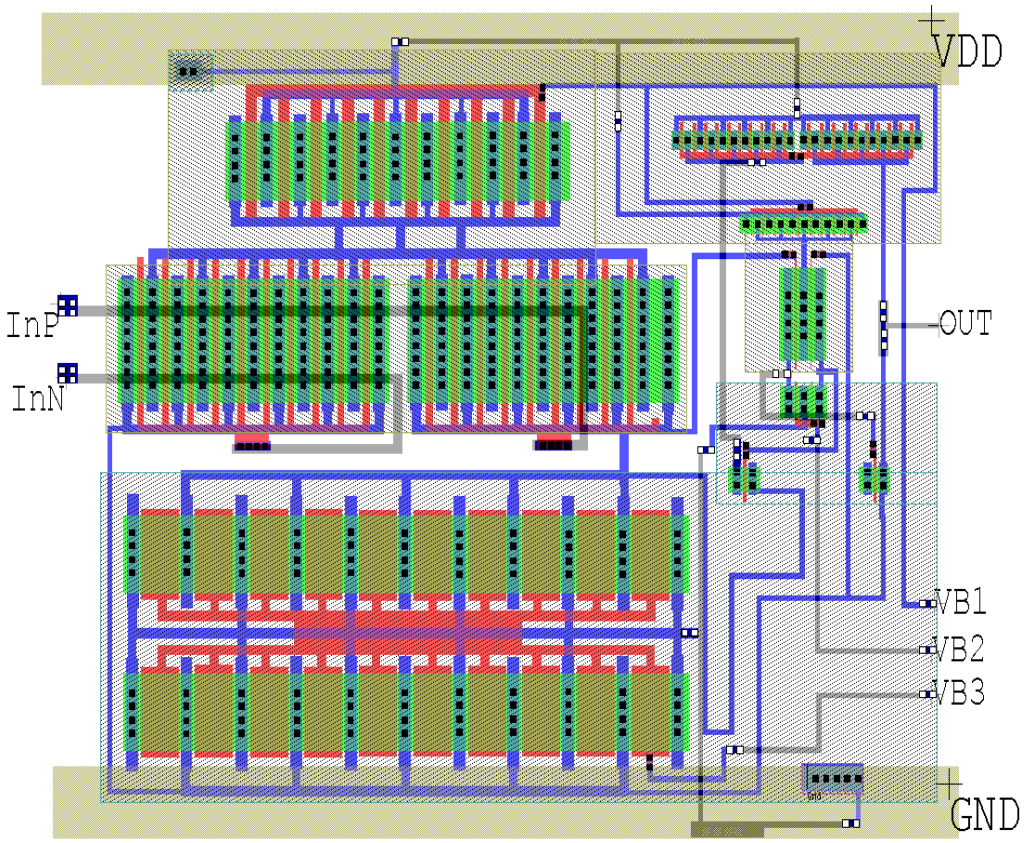

Fig. 5.15 3 levels of metallization CMOS GENERIC 0.25um OTA.

5.2 Keys design

As previous stated, at the beginning of the research, the author tried to use single transistors as keys for resetting the circuits but the results ware less than satisfactory, the transistors either remained open either close all the time. The decision was made for more complex circuitry. The decision was made for a high-speed fully differential current switch as seen in [159].

The effect of clock-feedthrough has been dramatically diminished by Swing-Reduced Drivers and neutralized with the help of dummy transistors. Using Swing-Reduced Drivers (SRD), requires less charges to be transferred to or from the gates of the switching transistors, the switching speed can be increased without significant output error. The SRDs also reduce the possible large current spikes on the outputs of the current switch. In [159] has been reported that the current switch is ideal for high-speed current mode signal processing. Anyhow, important problems in SI circuits are switch-induced errors, or the clock-feedthrough (CFT) effect, and, as demonstrated, it is impossible to realize high-speed switched-current circuits with acceptable accuracy without efficient clock-feedthrough cancellation. A commonly accepted technique for cancellation of the clock-feedthrough effect is to insert a

half-sized "dummy" MOSFET. This technique requires two clock phases, and its accuracy is mandatory dependent on the timing relationship between the clock phase edges, which is very hard and effort demanding to control. Some other papers reported replication techniques [160] or multi-path cancellation [161] , [162] which requires through current mirrors a cancellation current ripple. The current mirrors delay limits the current switches operation speed. SI systems based on a fully differential architecture have been presented in several papers [163] , [164]. In this kind of circuits, the current mirrors delay is no longer an issue. Anyhow, large common-mode output current spikes could be induced by a steep clock edge. A slower clock with a slower rise and fall times is necessary in this type of application. Another solution is to use some charge attenuation technique as reported in [165]. On the other hand, the speed is limited by the additional capacitors and the use of multiclock phases. The proposed high-speed current switch is composed by an NMOS differential pair. The possible common-mode output current spike has been reduced by reducing the voltage swing on the gates of the switching transistors. The Swing-ReducedDrivers (SRD) are used to reduce the voltage swing on the gates of the switching transistors. By reducing the voltage swing, the charges which are transferred to/from the gates are also reduced. This greatly reduces the transistors' switching transition times. The D type flip-flops (DFF) are used to synchronize the switching [159].

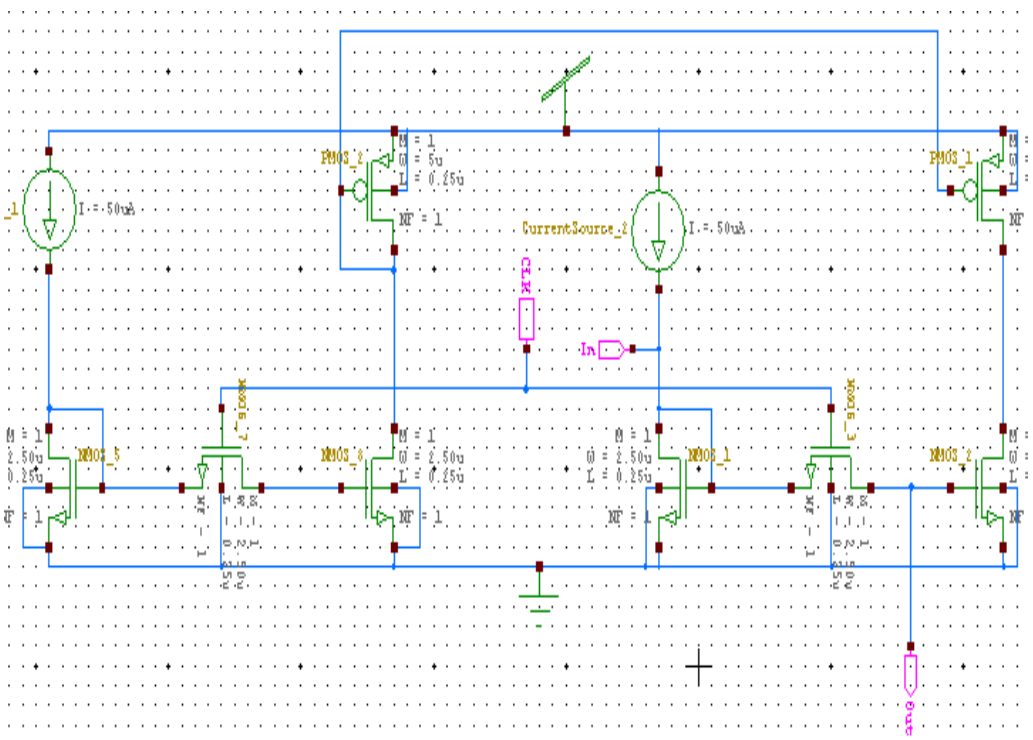

Fig. 5.16 Proposed design for keys circuits.

This circuit replaced well the old design with simple transistors. In next chapters the design of the keys will be integrated in the system and the simulations will demonstrate its viability.

6. DESIGNS OF ELECTROCHEMICAL SENSORS ARRAY

Why to use arrays instead of single sensors? Actually there are more reasons for that. The more sensors one uses in the same time, the chance of an error decreases. For example, a sensor can become inactive due to death of the sensing element. Being living organisms, one can not predict the exact behavior in all infield conditions. In case something happen with one cell, the chance that all cells are damaged is very small, in fact, if all conditions, algorithms and times are respected, the probability that all sensors in the matrix to be damaged is close to zero. In literature and in practice, more and more arrays of sensors are emerging. In this paragraph the author will present a few examples of existing arrays, created by scientists all over the world. There are a variety of sensors that can be integrated on one single chip. The classifications can be made after types of sensors, types of living cells, mammalian cells, bacteria, live tissue etc, after type of reactions that are monitored, type of signal that is measured or type of applications for what the array is designed for [166], [118].

In [167] Hang Chen reported in his PhD thesys a $GT0_2$ chemical sensor array. He managed to achieve an input current ranges from picoamps to microamps, with time scales ranging from milliseconds to seconds. This wide range of currents makes multiple scales of measurement a mandatory request, while the long time constants is allowing long integration times. Long integration times support and oversampling imply the use of a lower-order delta-sigma modulator. Oversampled delta-sigma data conversion cancel the need for anti-alias low-pass filters at the input, while decimation reduces current high-frequency noise along with the quantization shaped noise. Due to the fact that duty cycle effectively shunts the strength of the reference signal in the D/A feedback loop by the same factor, the gain of the input amplification is directly set by the digital control over the duty cycle of the shunting sequence. Generating the digital reference signal is more precise than analog scaling of the reference current, which is susceptible to mismatch errors. A gain factor G is achieved with precision by passing the D/A feedback for a single clock cycle and then by G−1 clock cycles of shunting the feedback. Thus the digital gain modulation over G clock cycles reduces the conversion rate by a factor G, it produces more precise results than increasing the delta-sigma oversampling ratio (OSR) with the same factor necessary to reduced noise. With fixed reference current but variable feedback digital gain G and also variable oversampling ratio OSR, the potentiostat is capable of ranging digitally over a wide range of currents, spanning 6 decades from 100fA to 500nA. The digitizing potentiostat is implemented as a first-order incremental ADC, a version of the first-order delta-sigma modulator with a counting decimator. The design uses a sampled-data switched capacitor.

The first-order incremental topology is desirable to be used for a simple and compact implementation, leading to significant savings in silicon area and power consumption. realization offers low-noise and low-power implementation [167].

Another integrated design for electrochemical potentiostat was reported in [168] and also in [169]. As one can see, in the last 5 years, scientific world showed an increase interest in integrating sensor array on the same chip with the signal conditioning system for reasons already presented in previous paragraphs.

Also, there is much attention given and greater interest in lab on a chip or biosensors array because of the great advantages this devices offers to scientist and have a major field of application all over the industry, defense field, medicine and so on [167]. The fabrication, problems that need to be overcome and algorithms are presented in [170].
There are 4 different architectures of sensors' matrix [126]. These types are judged on number of electrodes assigned for each sensor.

a) 3 electrodes for each individual cell,
b) an array of WE and only one CE and RE for all the array,
c) a matrix of arrays as in point b),
d) bipotentiostats

The first type of matrix of electrochemical cells is the most common one in which every cell has its own 3 electrodes, Counter, Working and Reference electrodes. Another architecture, as seen in [171] is with an array of Working electrodes and only one Counter and Reference electrode. In this case it is presented an 3X3 array of Working electrodes, this presenting the advantage of minimizing the area on chip of the created matrix and the complexity of the circuitry is diminished, too, but presents some drawbacks. The surface layer of the chip contains a reference electrode, an auxiliary electrode, and a 3x3 array of working electrodes fabricated on the readout chip using post-CMOS processing. A specific electrochemical cell within the array is selected by an on-chip current switch matrix. The potentiostat block establishes a potential between a selected working electrode and the reference electrode and measures the current flowing between the working and auxiliary electrodes. The circuitry supports both static voltage and cyclic voltammetry assays. The current readout block within the potentiostat converts the current to a voltage using a low-noise, power efficient switched capacitor circuit [172]. A third approach would be the combination of this 2 models, an array of arrays of working electrodes, in this way we would be able to have more than one species of bacteria, in each array of working electrodes we can have the same bacteria due to the fact that each specie react to a different voltage applied to the cell. In [171], one can see there are architecture involving any number of electrodes in electrochemical sensors. Our matrix of array of sensors uses the classical type, 3 electrodes for each individual cell.

6.1. Methods

We have used a complex multiplexer to measure one sensor at a time from a matrix of 64 cells, each cell can be used as 2 types of sensors, in this case we are using 128 actual sensors from a 64 cell matrix. Each cell will have 1 square millimeter on the final chip. We want to design low cost, disposable, single use cell matrix. Here we present a matrix of 3 electrode cells and we present the principle for the command circuit, as future work. The frequency is not very important here, we use a slow circuit because we wanted to avoid complexity and in this way the raising of the chip price. The frequency is low, in Hz-KHz range because the signals are varying very slow. A fast circuit is usually a complex and expensive one because we need to overcome a lot of noise on high frequencies etc.

The presence of toxicants induces a cascade of biological reactions in the genetically engineered bacteria, producing an increased concentration of the enzymatic bio-reporter alkaline phosphates. This enzyme catalyzes the reaction converting the substrate para-aminophenyl phosphate (pAPP) to the electro-active

species para-aminophenol (pAP). Therefore, by using an appropriate electrochemical transducing system, the generated electrochemical bio-signal can be detected. Fig. 1 presents chrono-amperometric results of the response of E. coli bacteria in the presence and the absence of the model toxicant NA. The response of the bacteria in the presence of NA showed an increasing electrochemical current after pAPP was added [143].

The reaction will be direct proportional with the concentration of the toxicants, the bigger will be the concentration of chemical toxic agents, even the stronger will be the signal emitted by the bacteria. Our signal conditioning system will transform the signals from bacteria into impulses, making the frequency of the obtained signal the main carrier of the information.

Another decision that we had to make was the number and style of potentiostats. Here we have to choose from a number of possibilities:

1. One potentiostat for each individual cell,
2. One potentiostat for each row or column in the matrix
3. Only one potentiostat for all the array of potentiostats
4. Somewhere in the middle

The first approach, one potentiostat for each individual cell in the matrix it is the simplest from the electronically point of view but it is inefficient from the cost point of view. Using a potentiostat for each cell is uneconomical tacking a lot of space on chip so increasing the cost of the system. The second approach is promising and presents some advantages, but also has drawbacks because of the command circuitry that are complicated and more circuitry mean more errors which need to be compensated, so increasing the chip area, increases the design cost, too. The third approach is the most radical approach because it uses only one potentiostatic device. Being the most radical it has the biggest problems because it is quite a challenge to create an ideal current multiplexer and also presents a lot of drawbacks from command circuit point of view. We decided to use the forth style, somewhere in the middle. Actually we decided to split the potentiostat in its component blocks. A regular potentiostat is made as seen in Fig. 5.1.

As one can see, the potentiostat is composed by two operational amplifiers, A1 and A2. The role of A1 is to keep the value of the voltage between Reference Electrode RE and Counter Electrode CE constant at a given value, while operational amplifier A2 has the role to measure current, independently, between Working Electrode WE and ground. We decided to split the design, using one amplifier A1 in Fig. 2 for each of the 64 cells and only one amplifier A1 for all array of cells. We decided to maintain potential Vcell constant for all the cells due to the fact that all electrochemical sensors in the matrix will contain the same bacteria so they will need the same constant voltage applied between RE and CE. In our opinion this approach is the most efficient from the electronic point of view giving the electrochemical and biology scientists in the same time some degrees of freedom that otherwise would be impossible to have. This is a compromise because the design still involves 65 operational amplifier but, anyhow, is better than 128 amplifiers, this in the case we would adopt the method with one potentiostat for each individual cell in the system. Each cell in the matrix of sensor will be approximately as seen in Fig. 3. Each cell in the matrix will take 1 square millimeter. The exact dimension and location on chip of the array of sensors will be dictated by the technology available and in agreement with the bio-chemists team. Also, the fabrication of the matrix of sensors will be made by the technical stuff from the electro-chemistry laboratory.

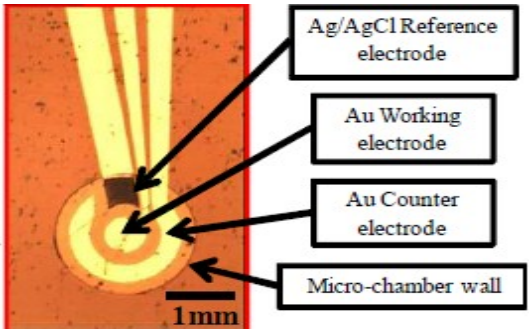

Fig. 6.1 Inside view of a single three electrode electrochemical micro-chamber.

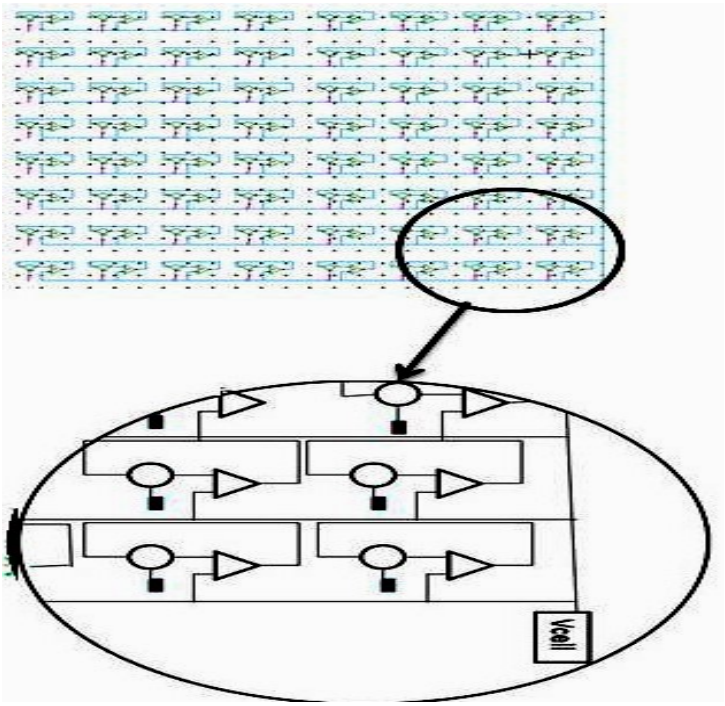

Fig. 6.2 Proposed array of sensors.

The main advantage of using arrays of sensors instead of single cells is accuracy of the measurements, even if more than one cells are inactive due to the death of bacteria, there are big chances that at least a few will react and attract attention and using living organisms one cannot predict its behavior with 100 percent accuracy and there always is the risk that bacteria in one cell will be death so will have no reaction to chemical agents, the toxicants so is better to use more than one cell and more than one reaction to obtain results with accuracy. Each cell in the matrix is designed as seen in previous paragraph. For its design we have had in mind our necessities, substances and bacteria that we have used and also the electro-chemical processes that will dictate the final behavior of our sensors.

Our focus in this paper is on electrochemical cells, presenting the link between signal conditioning system and the electrochemical sensors array as seen in Fig 2.

Both electrochemical and bioluminescent sensors are using the same type of bacteria and the same principle as seen in Fig. 2. There are several problems that one must overcome designing this kind of circuitry because of the variety of fields that are combining here, electronics, biology, electrochemistry, etc.

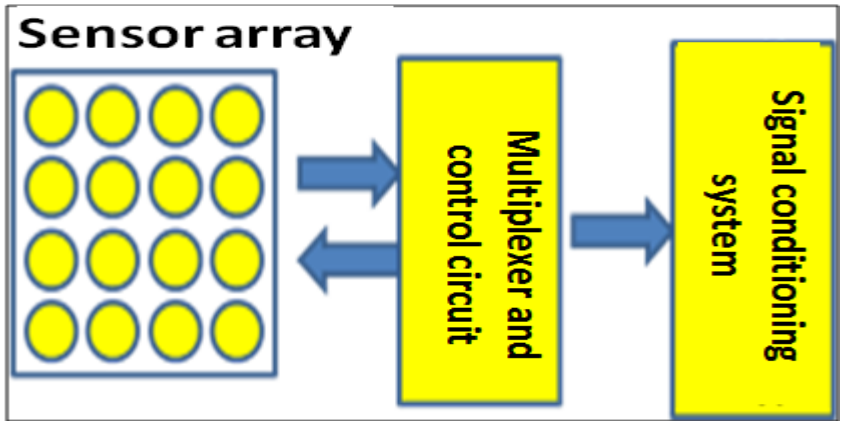

Fig. 6.3 Multiplexer and control circuit principle.

We decided to use sensor arrays for more than one reason. The main reason is that we are using live organisms, E-coli bacteria and being live organisms, you cannot predict with accuracy its behavior at any given moment and in any given condition that may appear on the field, so we improved the margin of error by using several sensors [1]. Another reason is that bacteria life on the shelf is 2-4 years, so when only a few bacteria remain alive on a cell, their response signal will become weaker or disappear so it is safer to use several sensors. Also, the duality between electrochemical and bioluminescent sensors encouraged us to implement this approach of the problem. There are many ways to design a sensor array [1]- [3], but we decided for the best approach from our point of view, splitting a classical potentiostat design in two parts.

This approach presents advantages because the control circuitry needed is quite simple and in the same time we managed to reduce area occupied on chip by the control and signal conditioning circuits.

We decided to design a new model for the control circuit using well known digital blocks for the main reason that these units are well researched and we can predict their behavior and limitations in almost all situations.

In Fig.6.5, the author presents a classical design for 8 to 1 multiplexer with enable. Even if the circuit is a classic one, the model has been designed so the errors caused by noise would not affect the functionality. Fig. 5 presents the model for Shift Register Selector.

The author used 8 simple 8 to 1 multiplexers that interact directly with the cells inside the sensor array. These 8 multiplexers will be controlled by one multiplexer with enable block and by a shift register. The author has modeled each 8 to 1 regular multiplexer so we obtain the minimum of complexity for the greatest accuracy. At the entrance of the circuit, the 8X8 sensors array will be kept at a

constant potential of 300 mV, while at the exit of the matrix, the multiplexers will read each of the 64 cells one at a time.

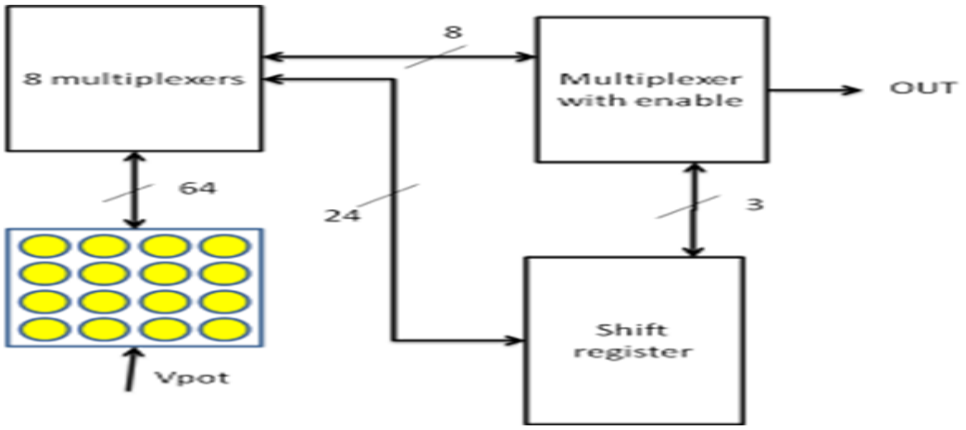

Fig. 6.4 Schematic model of the multiplexer circuit.

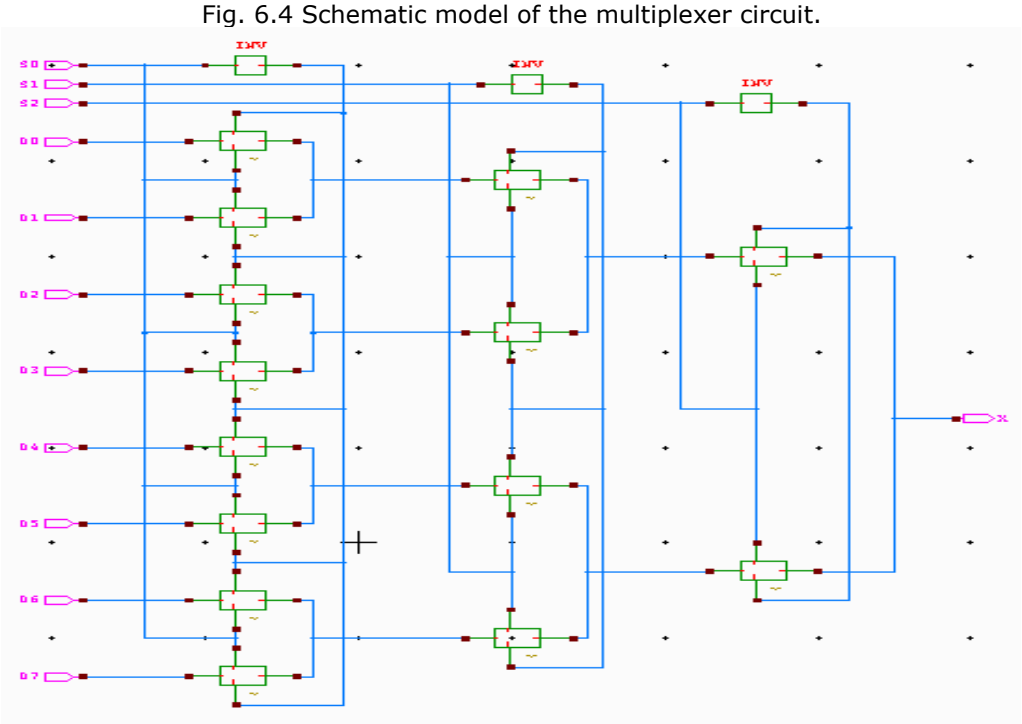

Fig. 6.5 81 MUX circuit

The 8 to 1 multiplexer enable circuit will dictate which of the 8 simple multiplexers will be active and what cell in the matrix will be read. After one of the 8 multiplexers has been selected, it will start to read the output currents from the cells in the matrix. The electronic equivalent circuit for electrochemical sensors was validated through experimental results, as seen in previous chapters. We have obtained signals that approximate very closely the behavior of a real life electrochemical sensor, both in transitory and in stable functionality.

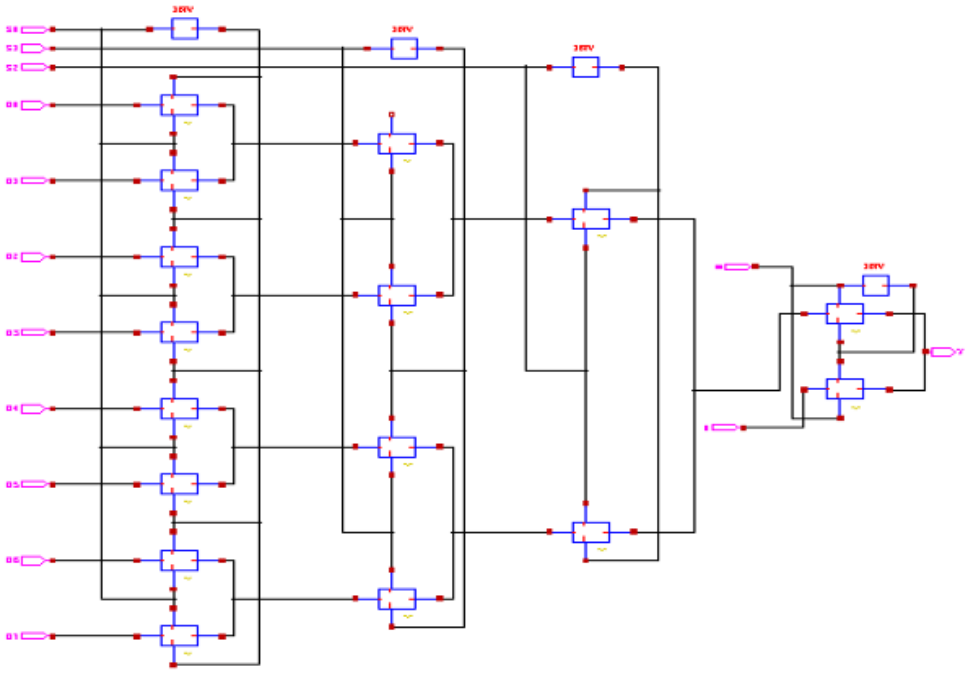

Fig. 6.6 Schematic design for 8 to 1 mux enable.

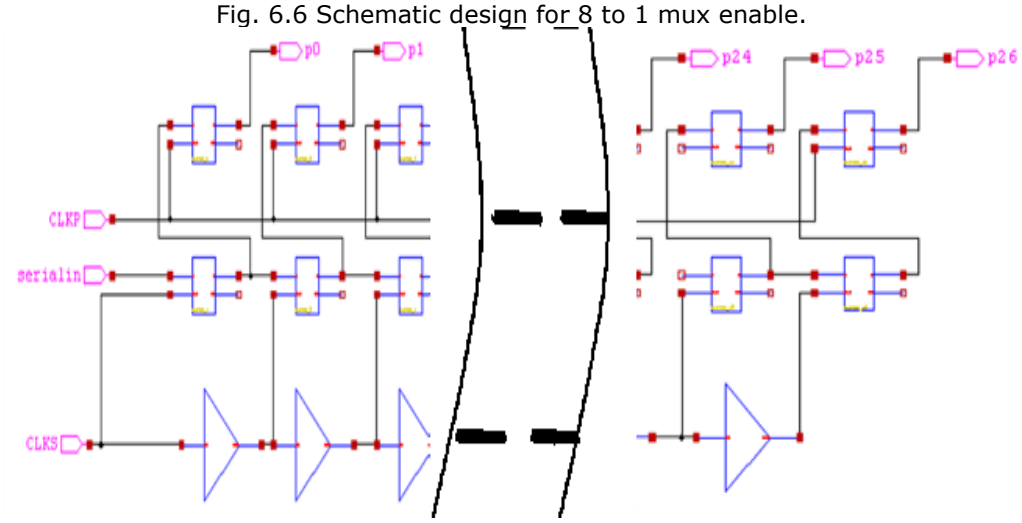

Fig. 6.7 Schematic design for Shift Register Selector.

CLKS is the clock that moves the information from the first flip-flop circuit to the last. The Shift Register consists of 26 groups, as seen in Fig. 5. CLKP is the clock that acts when all the flip-flops circuits are charged. When all the flip-flops circuits are charged, the dates will be transferred to each exit point from P0-P26. The buffers act as compensator to compensate the delay that is inserted by the flip-flops circuits. The command circuit, presented in this paper , has been designed to work with universal signal conditioning system presented in [3], as part of a

multidisciplinary project for toxic agents detection in water. As one can see, we tried to use classical designs, models that have been studied for a long time, so we will not encounter new situations or problems due to the fact that these circuits are widely used, so almost everything about their design and limitations are known. We have tried to create a circuit for a new application using common blocks and improving the behavior of the circuit by layout designs. All the simulations were made in Caspoc software.

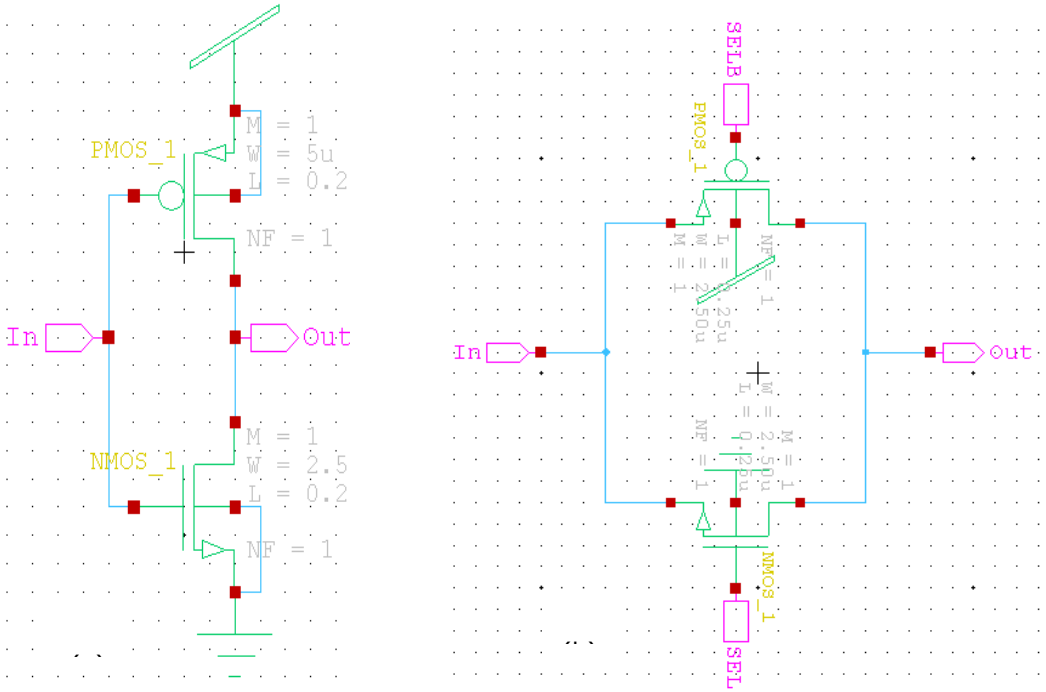

Fig. 6.8 (a)Inverter circuit and (b)Transmission Gate (TG)circuit.

As it is shown in Fig. 6.10, our OUT signal still presents some spikes that appear at commutation moments. Even if these spikes will not influence the functionality of our model, in the close future we are going to correct it by rescaling the transistors of the design. In Fig. 7, the noise analysis of the model is presented. As one can see, the results are in the satisfactory range, the shape of the curves are in good shape and the circuit work fine even in high frequencies, much higher than we are going to use it.

The output signal of the command circuit, OUT, will be furthermore analyzed and converted into impulses. At the end of all the conversions, we obtain a signal, whose frequency will be proportional with the concentration of toxic agents in the water. This frequency can be analized by a human operator or all the system can be integrated in a large network of sensors and the final result might be analized by a computer. The stability of the system and the linearity of the input output characteristic makes it suitable for this kind of applications. Furthure analisis of the issue need to be done.

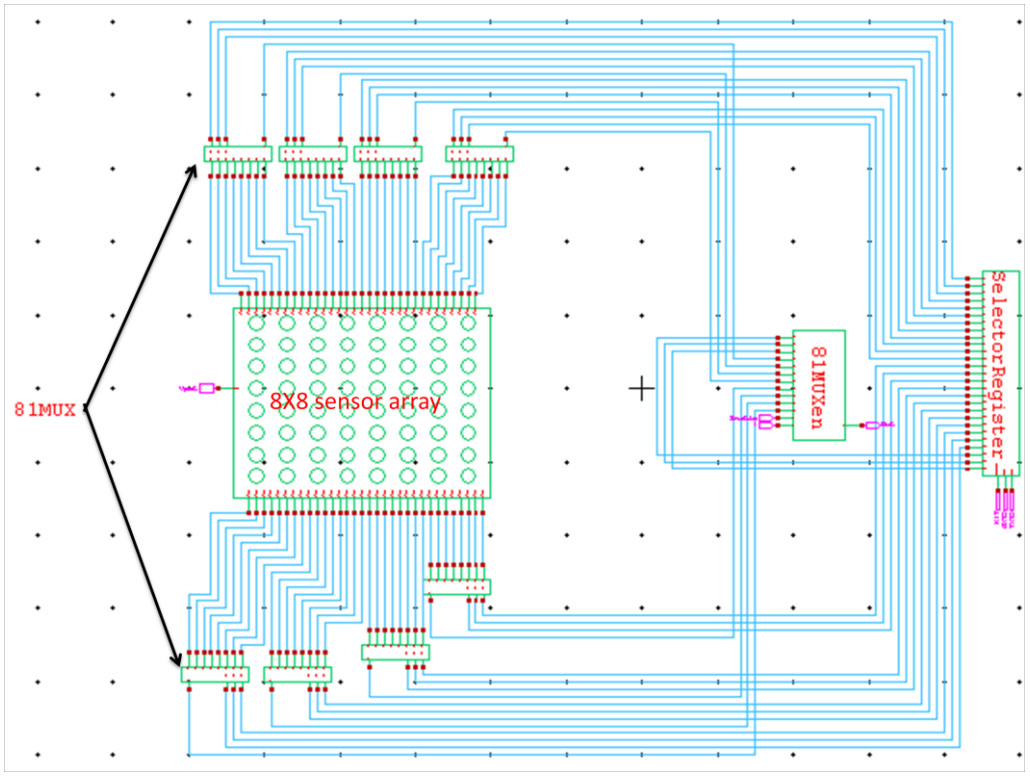

Fig. 6.9 Schematic design of proposed electrochemical cell array circuit with control part.

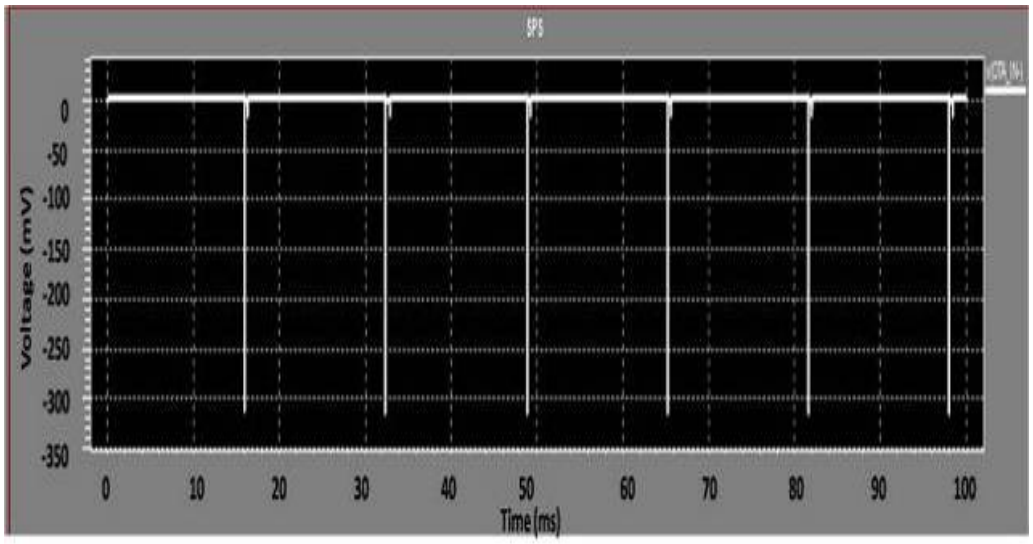

Fig. 6.10 Simulation results for output of command circuit of the sensor array.

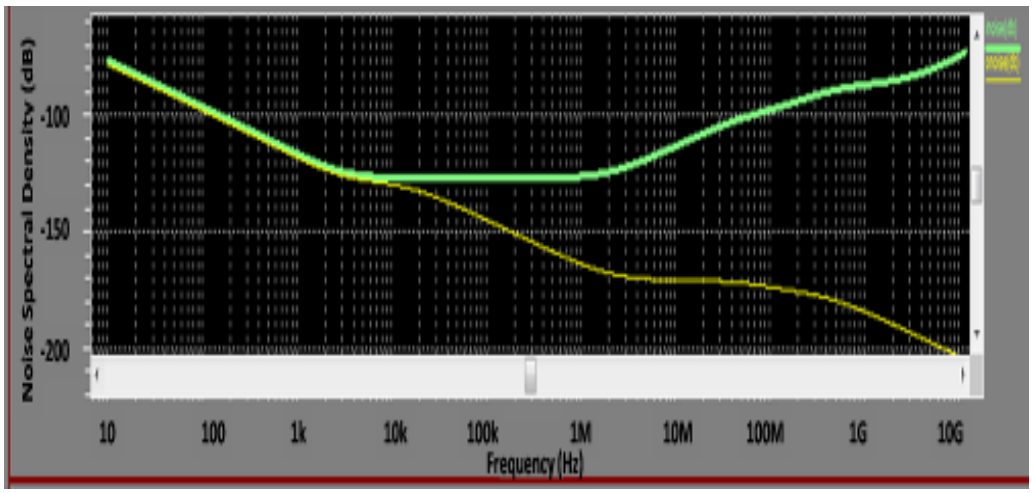

Fig.6.11 Noise spectral density (dB) for the command circuit.

A spectral density is a noise voltage or noise current per root hertz, i.e. V//Hz or A//Hz. Spectral densities are commonly used to specify noise parameters. The characteristic equations that identify noise sources are always integrated over frequency, indicating that spectral density is the natural form for expressing noise sources. To avoid confusion in the following analyses, spectral densities are identified, when used, by stating them as volts or amps per root hertz [174].

Our circuit, even if it is made combining quite simple and usual blocks, managed to satisfy our demand in accuracy and works well selecting cells in the array of sensors. All the simulations, at different temperatures and different technologies had proved that the control circuit is able to function in the desired range of accuracy but we need to rescale a few parts of the model, so we will be able to eliminate the spikes of the signal and to improve signal to noise ratio, maintaining in the same time simplicity of the circuit.

The main goal is to keep the complexity as low as we can, in the same time not affecting the accuracy of the circuitry. The frequency for this type of circuits is not so important because the rate of signals modification is very slow. Low complexity will translate into low energy consumption, we must keep in mind that this system will work in the field so low energy consume is imperative. Another advantage that low complexity circuitry is presenting is that the circuit will take a smaller area on chip, which make final price of the chip go down, furthermore, if the area occupied on chip by the command circuit and the signal conditioning circuit, on the same chip will remain more space to implement more cells of sensors so increasing the accuracy of the system.

7. WHOLE SENSORY SYSTEM SIMULATIONS AND RESULTS

In this chapter the author is presenting the functionality of its concept, sollutions for reducing the temperature effect over the circuit stability. The author is the first who investigated the temperature stability in system conditioning systems for electrochemical cells and found a high instability that needed to be compensated. Also, the author inserted a new block to compensate the temperature that affect the stability of the circuit mainly at small currents input.

All the simulations were made using CAD software and SPICE simulation tools. The author simulated the design using a 4X1 array of sensors due to limited power processing tools he have had at his disposal. This simulations prove the viability of the system. The whole sensory system without temperature compensation block is presented in Fig. 7.1.

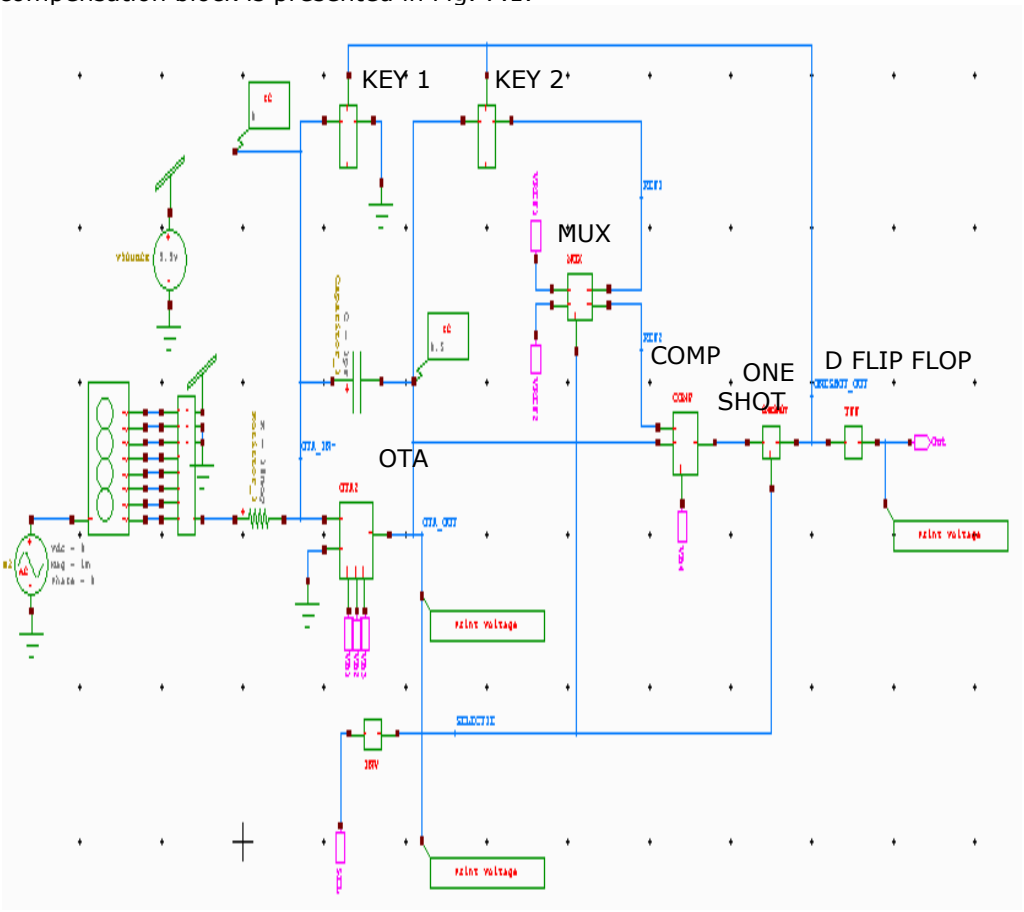

Fig. 7.1.Sensory system electronic design.

From left to right, the first block is an alternative voltage source to simulate the behaviour of electrochemical and bioluminescent sensors. Its only purpose is just for simulation.The next block is the 4X1 array of sensors wich is coupled to the multiplexer circuit. From this circuit the signal conditioning is beginning. Trough OTA, the signal will go to the comparator after the capacitor will be charge or discharged depending on which sensor is coupled at the time. The selection will be made through Selection Signal SELL from outside the circuit. The comparator COMP will trigger One Shot Circuit which will fire to reset the circuit and also provide the output impulse after it will pass trough D Flip Flop.

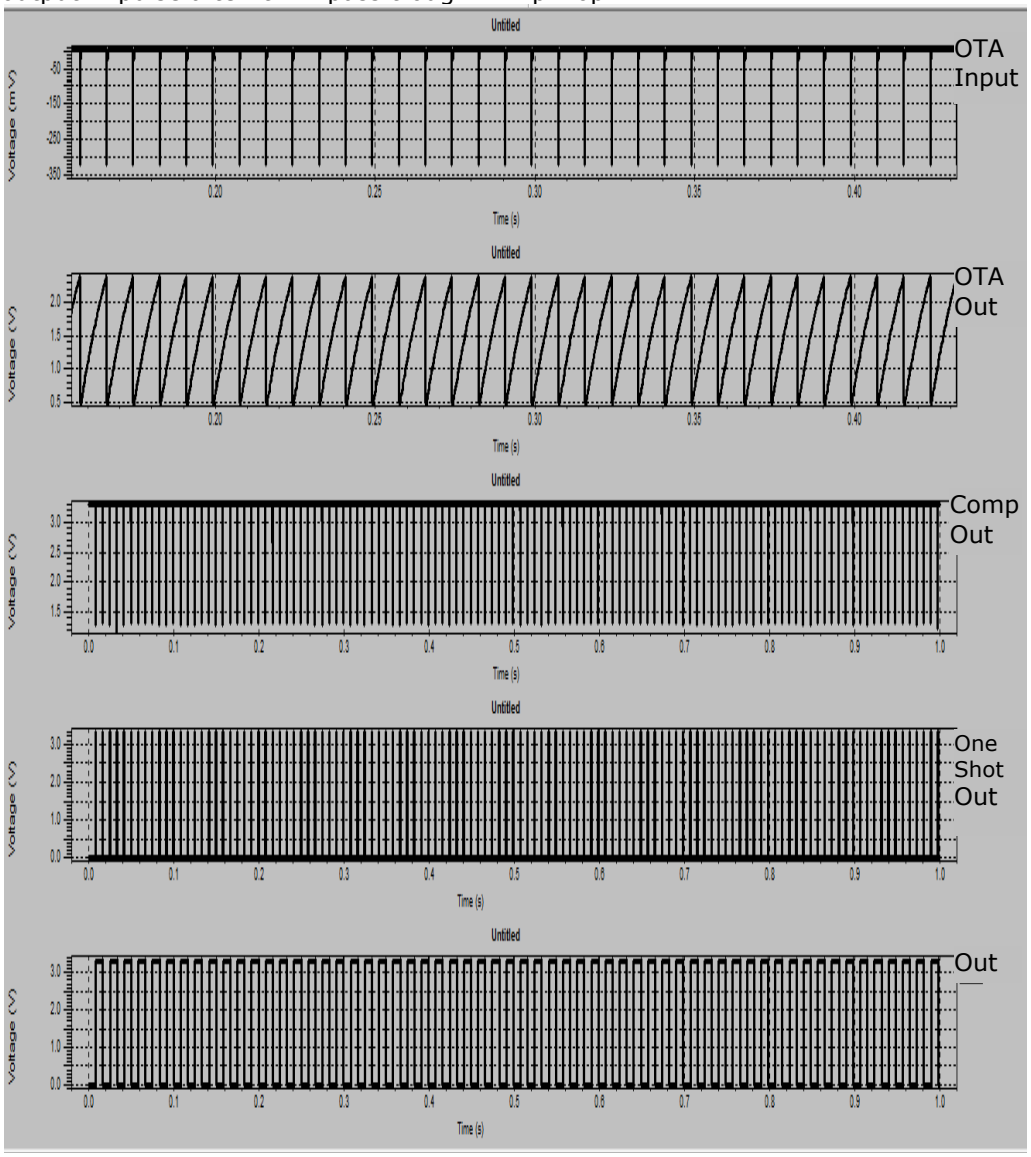

Fig. 7.2 Whole system simulation at 35°, TT process.

In Fig. 7.2 the signals generated inside the sensory system.From left to right in Fig. 7.1, Fig 7.2 from Up-Down the output of Multiplexer and Controll circuit, OTA, Comp, One Shot and the out signal are presented. Simulations ware made in this case for 35℃ in typical case.

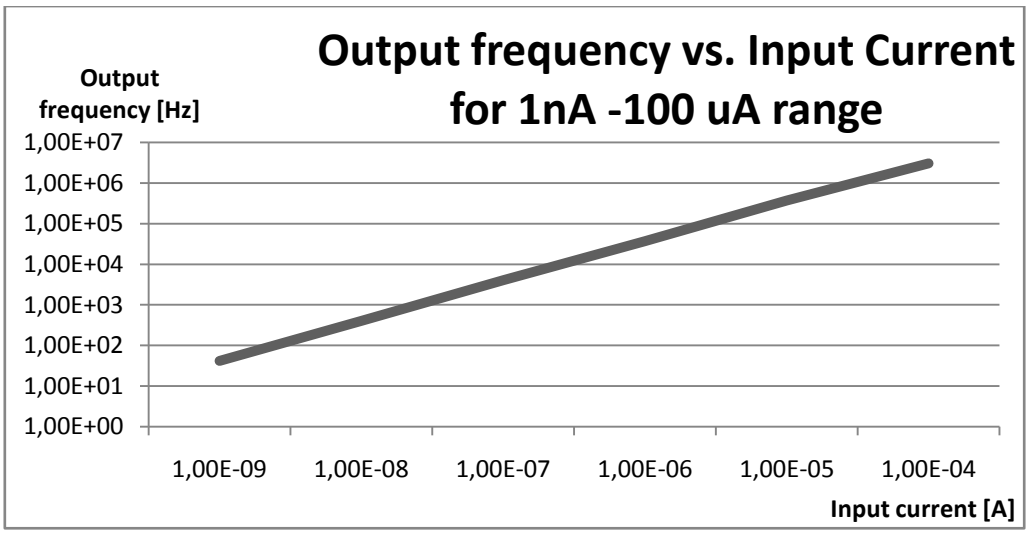

Fig. 7.3 Out/In transfer characteristic.

In Fig. 7.3 is presented the transfer characteristic for the senzorial system. For a 1nA up to 100 uA range at the input of the signal conditioning system, the aoutpus variation of frequency vary linearly between 4.17 Hz and 3.03 MHz. The SPICE simulations results can be seen at the end of the thesis, A.7-A.12.

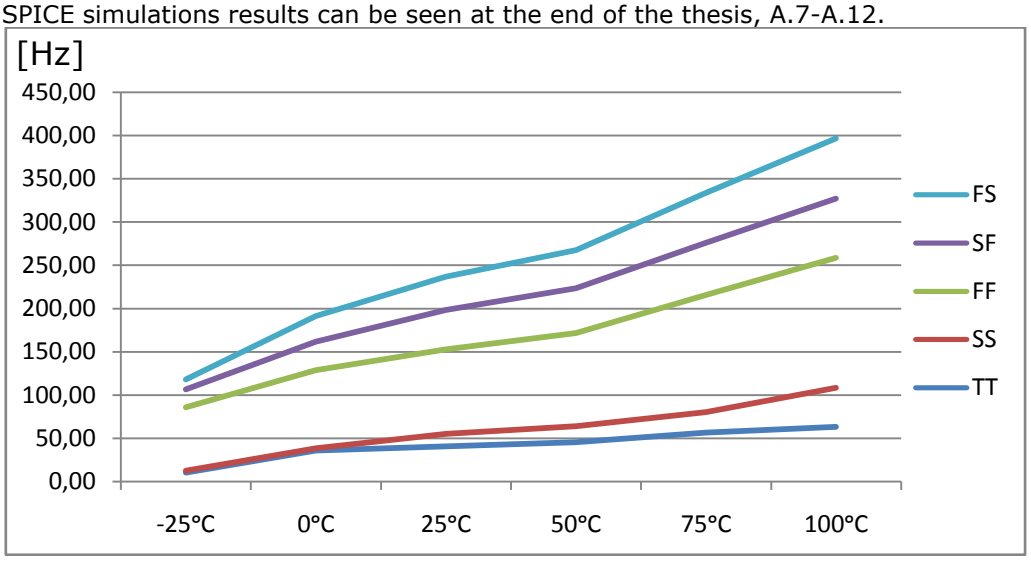

Fig. 7.4 Frequency variation as a function of temperature and technologic process without temperature compensation.

The main issue of this kind of circuits is temperature instability. In literature, no one addressed this problem. Papers reported with signal conditioning systems that transform currents into impulses promise great accuracy but do not say anything about temperatures. The author tested several designs and determined great instability, at a temperature variation of a few degrees the results present tremendous errors. For this reason, the author tested also its circuit. Also, in this case temperature vary as seen in Fig. 7.4, and for this, a temperature compensation circuit has been inserted. Thus the compensation is designed for the first quarter of the input currents range, smaller effects are also seen on higher currents.

7.1. Temperature compensation

Almost all circuits presented in literature promise to condition currents ranging from few pico amperes but there is no statement about temperature effects. It is true, those circuits are working fine dealing with pico amperes but only on exact temperatures, if temperature is varying a few degrees the errors will close to 100% or even bigger.

After the simulation results obtained for temperature and process simulation, the author decided that for small currents conversion, a compensation model is needed. First option for this issue was an external temperature to voltage converter or external temperature sensor. Even if there are now on the market good devices to perform this task, the goal of this research was to integrate as many parts as possible on the chip. Author so decided for an integrated solution, a circuit as simple as possible still able to perform well on our given conditions.

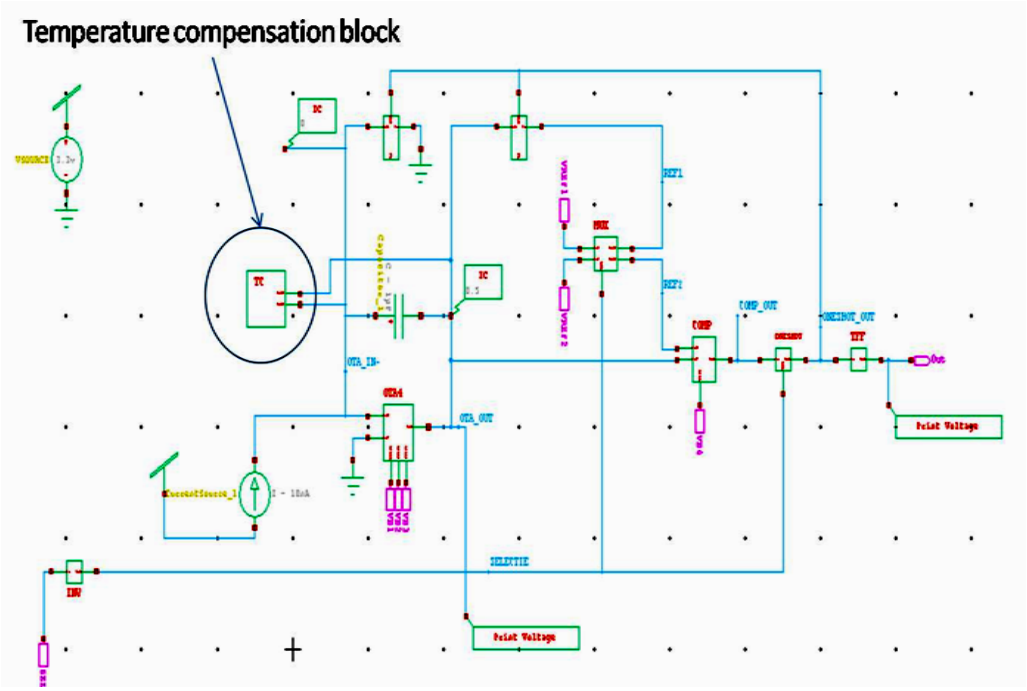

Fig. 7.5 Signal conditioning system with temperature compensation block.

The sensory system functionality is affected by the temperature variation mainly at smaller curents so for bioluminescent sensors case, due to the fact that this type of sensors have a lower curent range compared to electrochemical sensors. Thus, there are cases when electrochemical sensors provide smaller currents than usual so the compensation will work in both cases.

As a temperature sensor, the compensation block is using 3 diodes in series connection which can be easily implemented in the CMOS technology by using p-type diffusion in an N-Well and through them a constat current from a current source is flowing. It is well known that when a diode is in conduction area, the voltage on the diode -the forward voltage-FV is temperature dependent. This voltage has been used to control the capacitor battery realized by capacitor-coupled PMOS transistors, the drain coupled with the the source and the bulk. The controlling is made trough an repetor coupled operational amplifier, as seen in Fig. 7.6.

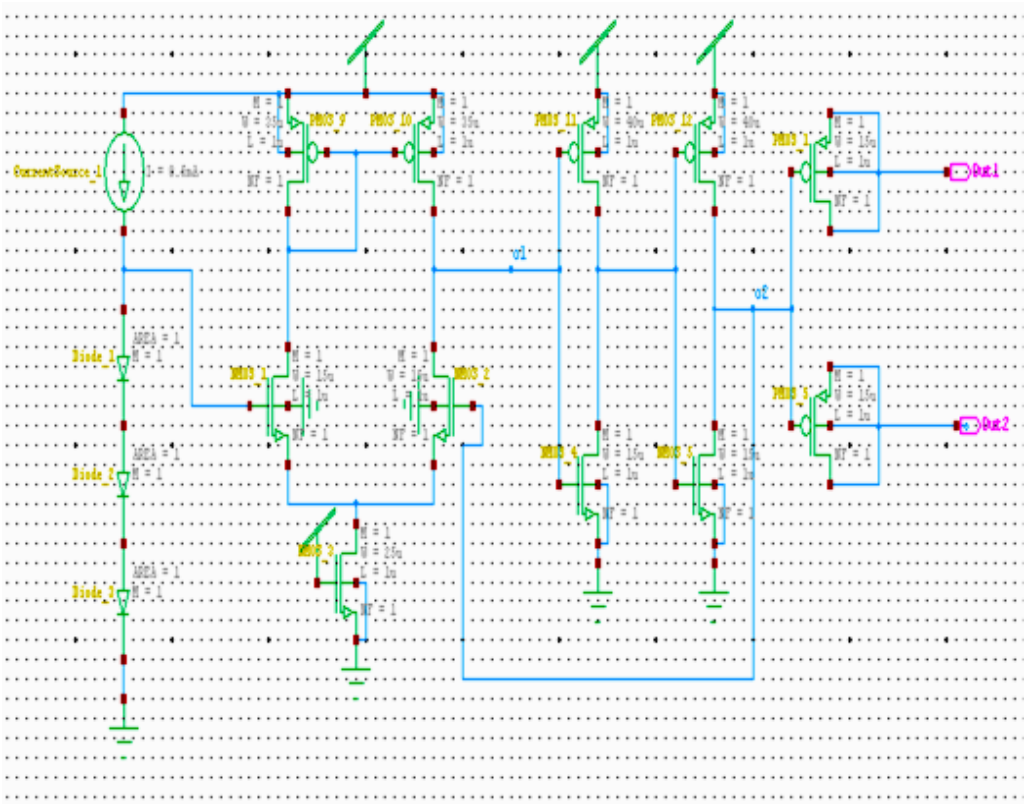

Fig. 7.6 Schematic of the temperature compensation network.

A temperature raising will provoke a decreasing of Vctrl voltage and, as a consequency, the input capacity is raising and so, a temperature decreasing will leed to an increase of the Vctrl voltage and so to a decreasing of the capacitance used for signal integration at the OTA entrance. The integration on chip of another block might be seen as a disadvantage due to the limitations imposed by chip area price but over all, even if it takes some space from the sensors area, the

advantages provided by the compensation made it a good decision. Also, an outside sensor would increase further more the final price of the design and also would require integrated circuits at the entrance of the circuit, ESD protection, compensation of errors and so on. The sensor integration, was, from author point of view the best choice for the temperature compensation issue.

Fig. 7.7 is presenting the Vctrl voltage variation with temperature variation.

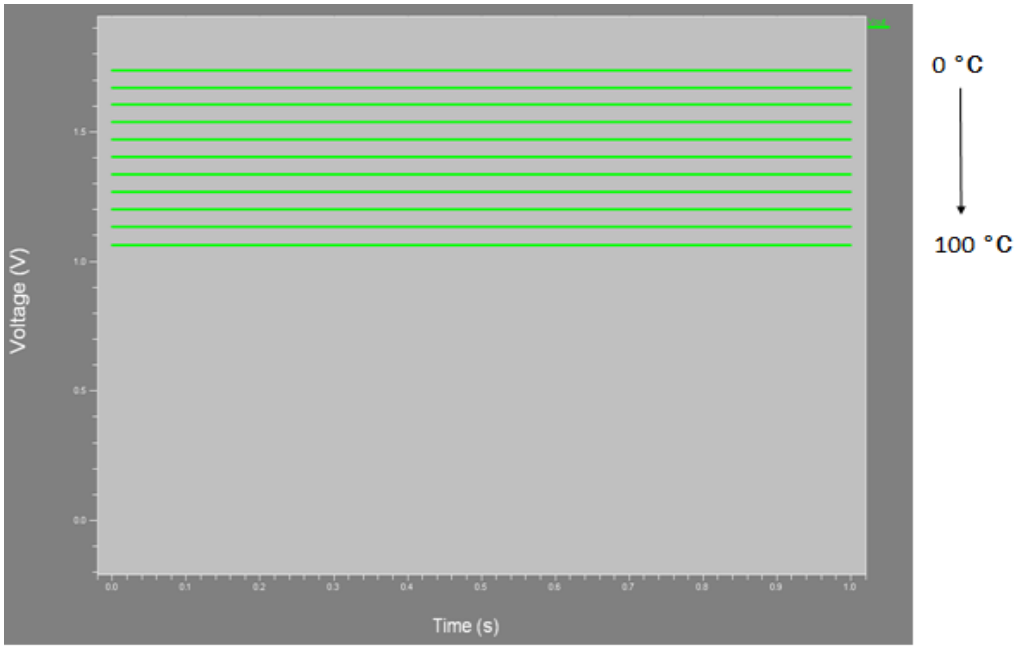

Fig. 7.7 Variation of the voltage control (Vctrl) with temperature.

As one can see, the Vctrl voltage has a good variation for temperature variation and the temperature effects are compensated as seen in Fig. 7.7.

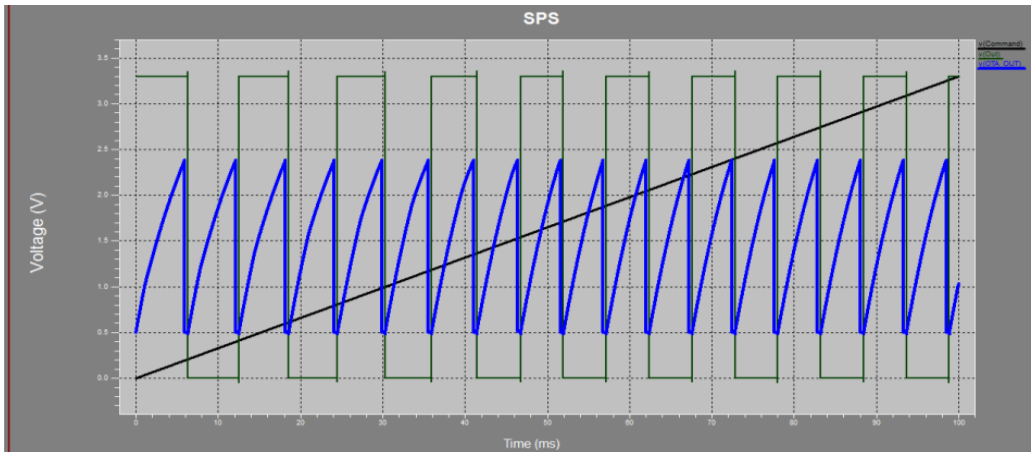

Fig. 7.8 Current compensation principle simulation.

In Fig. 7.8 the simulation to prove the concept is shown. At the entrance of the compensation part was applied a ramp signal similar to a temperature sensor given signal. When the voltage increase, the frequency of the signal is modified to compensate the temperature rising. In Fig. 7.9 and Fig. 7.10, due to the fact that the modification of the frequency is too little to be detected with naked eye, the author zoomed in some parts of the graphic obtained in Fig. 7.8.

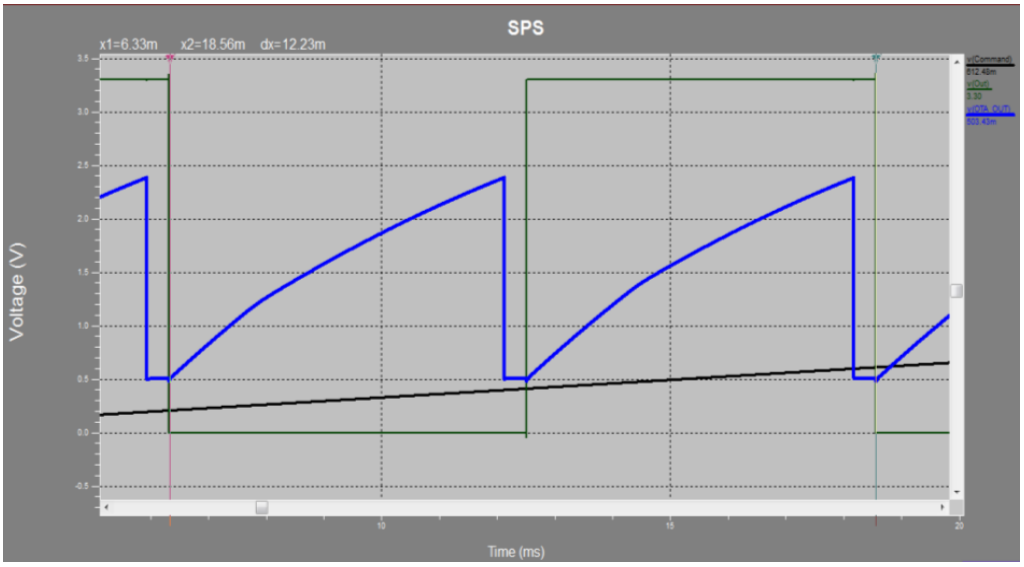

Fig. 7.9. First part of the signal presented in Fig. 7.8.

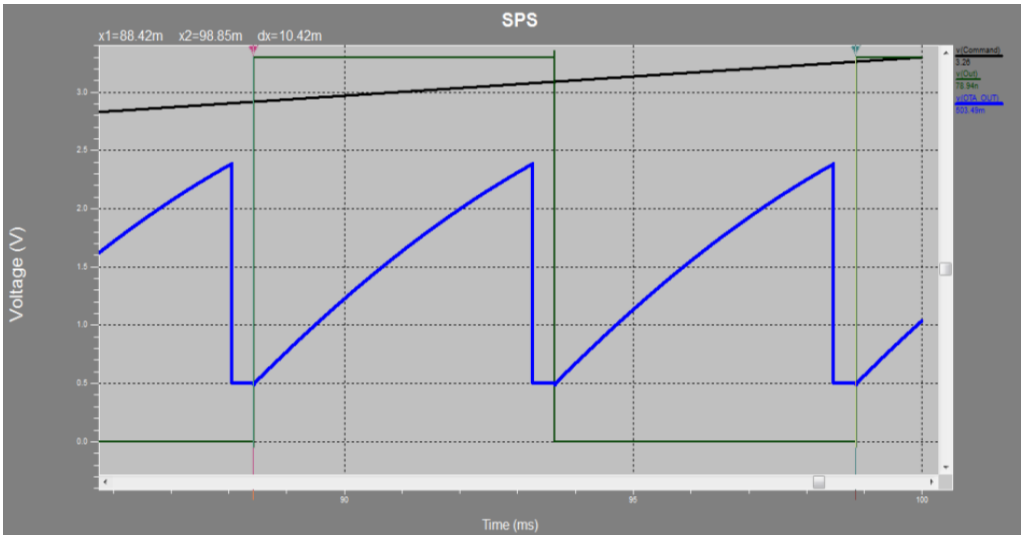

Fig. 7.10 Magnify part of the second half of simulation from Fig. 7.8.

Non linearity of the input-output characteristic is usually quite problematic.

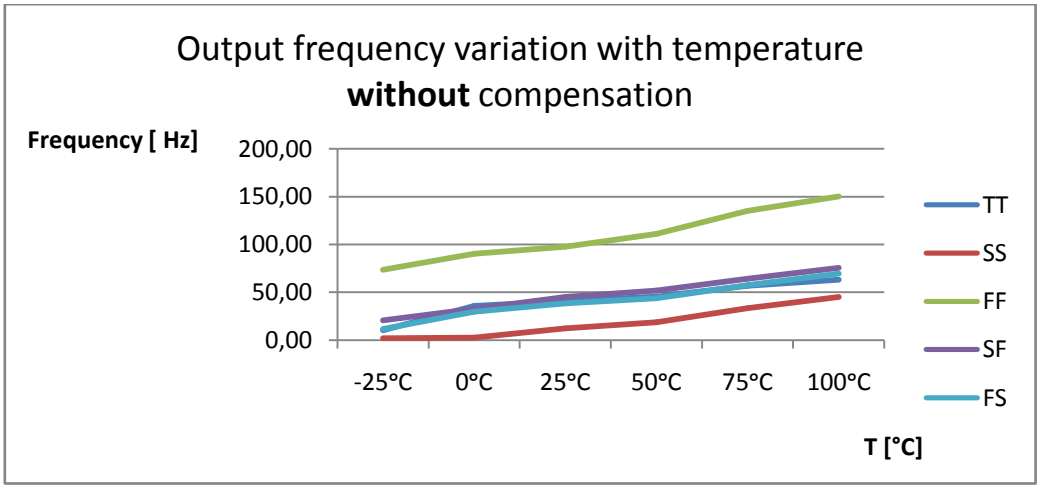

Fig 7.11 Output frequency variation with temperature without compensention.

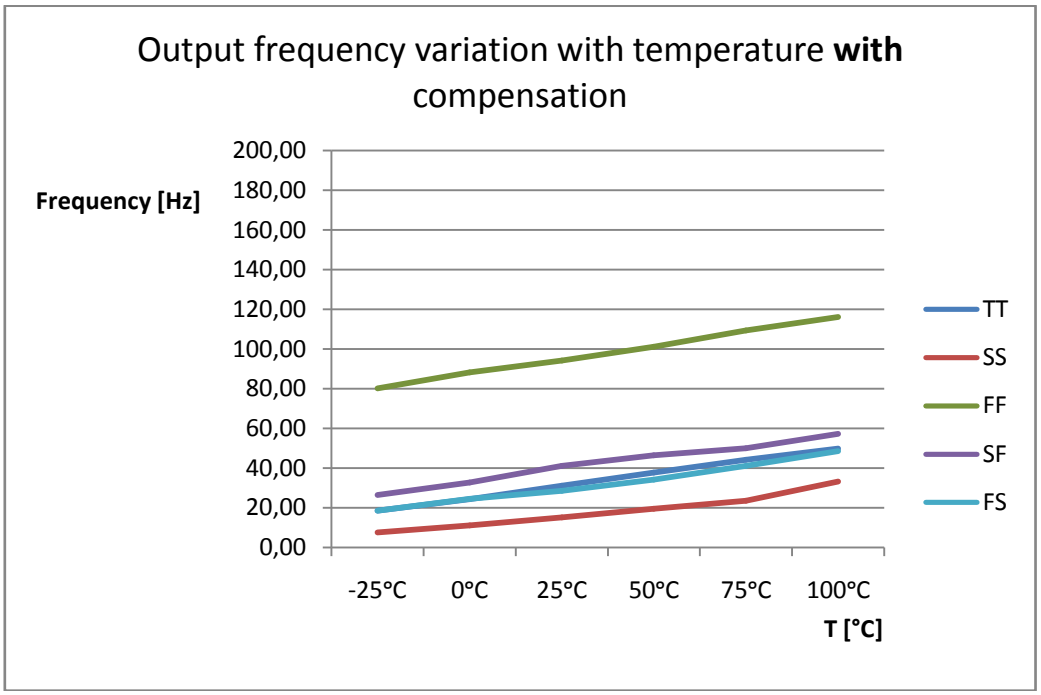

Fig 7.12 Output frequency variation with temperature with compensention.

As one can see, as stated before, the compensation is more obvious for smaller currents. The stability obtained is better for this sensory system comparing it to other designs present in literature. This is also a major theoretical and applicative contribution of the author.

8. CONCLUSIONS, PERSONAL CONTRIBUTIONS, FUTURE DIRECTIONS IN RESEARCH

In this chapter the author reports conclusions, its contributions and possible future directions in research.

8.1. Conclusions

In the last decade, bioterrorism and chemical terrorism became a real threat all over the world. Gouvernments are investing huge amounts of money to prevent this kind of events. New systems to prevent chemical war are emerging, more complicated and advanced systems, based on cutting edge technologies. The design presented in this thesis is dealing with this kind of circuits. Now, more than ever, research is being performed in biosensors technologies because of living tissues and bacteria characteristics which are more complex and stable than any detection method created by man. Furthermore, integrating more than one sensor or one cell on the same chip was tested and validated thus the attention of scientific world shifted from simple biosensors to lab on chip or micro total analyses systems uTAS.
„Universal Signal Conditioning System for electrochemical and bioluminescent sensor array" thesis, written and designed by the author wants to introduce new concepts and improvements regarding signal conditioning and electrochemical sensors area by proposing a new design able to work with electrochemical and bioluminescent sensor array. There is a huge interest in scientific communities shown towards various means of detection of several threats, from biological to chemical hazardous agents. The value of a system is given by the number of analysis it can perform and the number of threats it can detect. Single cells sensors started to be unable to satisfy the demands so that devices which can perform multiple analyses started to emerge. These devices are called whole cell biosesnors and they become the middle of the scientific world interest. The main advantage of this kind of systems is that they are tough, unsensible to errors and able to perform multiple analysis for different kinds of toxical agents. This kind of system can be a real tool to detect chemical hazardous materials in water, soil, air etc if and only if it is designed in close cooperation with chemistery and biology experts because its functionality and properties are highly dependent on the biological element and chemistry reactions which influence the processes from manufacturing to in field utilization. Due to the extense of the applicability of this design, the model represents a major interest in defence fields, water, soil and air monitoring and is subjected to further improvements.

The conception of the whole system has been made partially, the author made extended research on OTA circuitry, simplifying an existent design whithout any alteration of the original design qualities. Special attention has been given to keys, too. Usually, in this kind of circuits, keys are made of simple CMOS transistors but due to the fact that the model presented is more complex and able to work with several types of sensors, more complex circuitry was needed. The author of this

work modelled a circuit that he wanted to be implemented and tested in laboratories so in order to have good results, equivalent models for the simulation of various electrochemical and bioluminescent sensors was mandatory. Having this statement in mind, a new and original equivalent design for simulations for the entrance of the system, the electrochemical sensor was designed and validated through mathematical algorithms and experimental simulation. After designing the new equivalent model for the simulation of electrochemical cells, a comprehensive study on electrochemical sensor arrays was conducted. Having to chose between multiple concepts, from the number of electrodes to the number of potentiostats, the author implemented a model of electrochemical sensor array, also for simulation but with applicability in the manufactuing of the array. This concept tries to make possible the combination of any kind of amperometric sensors in a single monitoring system. Any kind of sensor which produces or consumes current can be integrated using this system that converts the electrochemical current into time, making the frequency the main carrier of information.

This concept is based on transforming any current into frequency, the higher the concentration of chemical agents, the higher the current that circulates into the electrolite. A higher current will be transformed into a smaller time to charge or discharge the capacitor so that the frequency will increase in the same way as the concentration of the chemical agents. Due to the different biological entities that can be integrated, from living tissues, bacteria to mammalian cells, the sensor must be recalibrated for the new bio entity but the design can remain. The design presented here was calibrated to work with E coli bacteria. The results obtained in equivalent electronic circuit for the electrochemical sensors were validated through experimental results conducted in Tel Aviv university laboratories under Prof. Yosy Shacham's supervision with Eng. Hadar Ben Yoav's collaboration. Another important step forward in the designing of this type of circuits is the implementation of temperature compensation circuits. No matter how precise and accurate a circuit is, if the errors produced by the temperature variation are bigger than a given value, that circuit becomes obsolete, in the field and even in the laboratory it is impossible to mantain a fixed temperature all the time. These temperature drifts are affecting mostly the small currents. Therefore, the author implemented a circuit that modifies the integration capacity of the operational amplifier thus modifying the time of integration and the frequency of the signal.

The circuit reported represents a novelty because its capacity to work with any kind of amperometric sensor, regardless the direction of the current flow and the large excursion of currents accepted at the entrance of the circuit. All the research has been carried out during a three- year period and was based on a comprehensive study of materials available in literature in all fields involved in this multidisciplinary thesis ranging from biology, electrochemistry, chemistry to electronics. The circuit can also be implemented with different types of sensors than electrochemical or bioluminescent and can be extended to voltametric sensors with small moddifications in the design. The author is determined to continue this research by extending the range of currents that the signal congitioning circuit can accept at its entrance and to enlarge the area of sensors, others than the ones used here.

8.2. Personal contributions

Here the author presents a short review the personal contributions that he consider he brough to science in his research. From all contributions, other then bibliographic research, 5 have mainly theoretical purpose and 5 have mainly aplicative purpose so the contributions will be devided in theoretical, applicative and bibliographic research.

Theoretical contributions:

The author designed a new equivalent electronic model for electrochemical cells. During his research, author found equivalent models from the simplest to the more complex moddels but no one was quite suitable for its purpose. In general, there are designs based entirelly on mathematical moddels and designs that are based mainly on experimental results. The schematic one must chose depends entirely on the purpose the system to be simulated was created for. Based on mathematical and phisics algorithms, author has detemined an original model that was simulated and validated trough experimental results. The experimental results ware obtained using an electrochemical sensor as seen in Fig. 3.1 using E coli as a bio element.

The author has proposed a new universal signal conditioning system for electrochemical and bioluminescent sensor arrays. This circuit is based on converting the signal provided by the sensors, electrochemical current in this case, into impulses, making the frequency the main carrier of information. This principle is presented in several papers in literature. The author of this thesis improved the principle design by replacing the existing simple transistor key with 2 more complex fast currents switches. Also, due to the large range of output signals provided by these two types of sensors and the dirrection of the current that vary according to the type of sensor, the circuit was modified and new bloks ware inserted. The main goal of this research was to maintain to minimum the complexity and number of electronic parts integrated on chip, thus keeping as large area as possible on the chip for the sensor array. The author used classic parts such as multiplexers, inverters, transmision gates and so on to implement an original design that can be called universal signal conditioning system for amperometric sensors. Decision for classical and largelly accepted circuits ware chosen because their behaviour is well known and easy to predict in allmost any given conditions. Also the author proposed a modified Folded Cascode OTA able to interact with both types of sensors.

The author is the first in known literature to investigate the temperature stability for the signal conditioning circuit for electrochemical sensors. After detecting some instability problems, mainly at smaller currents, the author decided to integrate also a temperature compensation block. The method that the author of this research has decided to use is a simple and very effective one. The mothod is based on modification of the integrating capacitor value accordingly to the temperature variations. The circuit proposed for this was moddeled having in mind as a priority the simplicity and the reduced number of tranzistors that the author wanted to integrate, maintaining in the same time the functionality of the circuit.

The author proposed a new moddel for simulation of a 8X8 sensor array. This moddel was selected after a comprehensive study of the possibilities that one have in developing an electrochemical sensor array. The research has focussed on electrochemical sensor thus the cells in the matrix will be able to perform both as

electrochemical and bioluminescent sensors. Having to chose between multy WE cells, regular 3 electrode cells and number of potentiostats per sensor array, due to the necessity to combine the 2 types of sensors and the restrictions imposed by this decision, the author moddeled a 8X8 array composed by classical 3 electrode sensors. The decision was made for splitting a classical potentiostat in 2 parts, each cell having its own operational amplifier for keeping the internal potential at a constant value and only one operational amplifier to perform as the potentiostatic device.

Applicative contributions will be presented next.

The author has modelled a folded cascode operational transductance amplifier. The design was inpired by the OTA reported in [154] but represents a simplified version based on mathematical algorithm and requests allready presented from [158]. The simplified moddel is keeping the characteristics of the original design, having in the same time lower complexity and fiewer components, reducing in this way overall price of the system. The proposed OTA is more complicated than regular OTAs but simpler than the model that inspired the author. This design represents a compromise between tomplexity and number of components but meintaining the qualities of the original moddel unalterated.

The equivalent model for simulation for an electrochemical cell was validated trough experimental measurements and as seen in previous chapters, the moddel emulate closely the behaviour of the real cell. With Prof. Yosi Shacham support and his team colaboration, experiments ware made with different number of bacteria imobilized on chip. The number varied between tens of thousands to hundreds and even less bacteria in solution. Also the concentration of the toxicants in the analyte has been varied. The results ware compared with the SPICE simulations and the mathematical results and the original design was implemented in a simulation array to determine the behaviour of the sensory system.

The author has tested and quantified the importance of the temperature compensation circuit. The tests ware made in SPICE programs at different temperatures and different technology corners. The temperature compensation schematic has proved its value especially at small currents. Also, due to its simple design and clear principle of functionality, one can predict its behaviour at every temperature in the range the circuit was designed for. The principle used in this compensation method makes it suitable for other designs that might also be affected by the temperature variations.

After determining the importance of the compensation blocks, the author tested the full sensory system. The tests ware made on full range temperatures, from minus 25 C to plus 100C, even if the practical range of temperatures where the biosensors can be used is between 10° and 70° C. The system behaved well under given conditions. Also the author tested the system in all technology corners and even if the behaviour was a little alltered from FF to SS case, over all functionality was proved.

The author has also elaborated a multiplexing and controll model circuit for handeling the sensor array. For this, simple and well known blocks have been used so their behaviour and limitations could be easily predicted.

The author has also conducted bibliographic research in several fields of interest in his research:

Bibliographic research in:

The author conducted a comprehensive introduction in biosensors technology, a short classification of biosensors acordingly to their principle of functionality and signal measured.

The author focussed his research on electrochemical sensors fabrication and functionality, trying to present as well as the research allowed him all the aspects from fabrication, deposition, types of anzyme used and so on.

Several qualities of signal conditioning systems for electrochemical sensors ware presented. Also there are several principles to control and quantify signals from 3 electrode cells that have been shortly presented.

Several models of equivalent 3 electrode cells for simulation have been reported. Those models are ranging from the simplest that emulate only major components of a sensor to more complex that emulate the behaviour with the big majority of parasitic effects in an electrochemical cell. The design one must chose must be acordingly to the application the sensor was designed for.

During 3 years period of research, author has published or send for publication 13 papers on national and international manifestations.

8.3. Future directions in research

The multitude of genetic information contained in bacteria and living tissue make them perfect detection materials for biosensing applications. The wide variety of amperometric and voltametric sensors make impossible for now existence of an universal signal conditioning sistem for sensors having as sensor heads living material.

Having this statements in mind, author is proposing a few directions in future research:

Improving furthure more the temperature stability with more complex circuitry to compensate larger variations.

Redesigning the system so it will be able to work with a learger diversity of sensors, voltametric sensors included.

Enlarging the excursion of currents that can be accepted at the entrance of the signal conditioning circuit.

8.4. Publications List

Publication list (conferences):

1. D Cristea, Tiponut V, Tendencies on Signal Conditioning Circuits, Lucrarile sesiunii de comunicari stiintifice "DOCTOR Etc 2009", ISSN 2066-883X, Editura "Politehnica", Timisoara, Sept. 2009, pp.13-16.
2. M. E. Basch, D. G. Cristea, V. Tiponut, T. Slavici, Elaborated Motion Detector based on Hassenstein-Reichardt correlator Model, LATEST TRENDS on SYSTEMS, WSEAS, ISSN: 1792-4235, ISBN: 978-960-474-199-1, Corfu Island, Greece, vol. 1, 22-24 Iulie 2010, pp. 192-195.

3. Z. Haraszy, D. G. Cristea, V. Tiponut, T. Slavici, Improved Head Related Transfer Function Generation and Testing for Acoustic Virtual Reality Development, LATEST TRENDS on SYSTEMS, WSEAS, ISSN: 1792-4235, ISBN: 978-960-474-199-1, Corfu Island, Greece, vol. 2, 22-24 Iulie 2010, pp.411-416.
4. D. Cristea, Y. Shacham-Diamand, V. Tiponut, H. Ben-Yoav, M. Basch, Z. Haraszy. VLSI Universal Signal Conditioning Circuit for Electrochemical and Bioluminescent Sensors, 26th IEEE Convention of Electrical and Electronics Engineers in Israel, ISBN: 978-1-4244-8682-3, 2010, pp. 249-252.
5. D. G. Cristea, M. E. Basch, Z. Haraszy, N. Fishelson, V. Tiponut, A new Electronic Equivalent Circuit for Electrochemical Cells, ICOMOS conference
6. D. G. Cristea, M. E. Basch, Z. Haraszy, V. Tiponut A new model for electrochemical sensors array, SIITME 2011- in press
7. M. E. Basch, D. G. Cristea, R. I. Lorincz, V. Tiponut, A Bio-inspired Obstacle Avoidance System Concept for Visually Impaired People, Recent Researches in Circuits, Systems and Signal Processing, WSEAS, ISBN: 978-1-61804-017-6; Corfu Island, Greece, 14-16 July, 2011, pp.288-291.
8. R. I. Lorincz, M. E. Basch, D. G. Cristea, V. Tiponut, Hardware Implementation of Field-Weakening BLDC Motor Control, Recent Researches in Circuits, Systems and Signal Processing, WSEAS, ISBN: 978-1-61804-017-6; Corfu Island, Greece, 14-16 July, 2011, pp.208-213
9. Z. Haraszy, D. G. Cristea, S. Micut, V. Tiponut, Efficient Algorithm for Extracting Essential Head Related Impulse Response Data for Acoustic Virtual Reality Development, 14th WSEAS International Conference on Systems, Corfu Island, Greece, 2011.
10. D Cristea, M-E Basch, Z Haraszy, R I Lõrincz, V Tiponut, A New Model For Designing Electrochemical Sensors Array, 2011 IEEE 17th International Simposium for Design and Technology in Electronic Packaging, Timisoara, Romania, October 2011.

Original papers in professional journals:

1. Papazian Petru, David Cristea, IEEE 1451.2 Compliant Smart Power Supply, at AECE-Advances in Electrical and Computer Engineering Journal, to be published.
2. D. G. Cristea, M. E. Basch, A New Control Circuit for a Sensor Array, sent at Romjist journal, waiting for approval.
3. M. E. Basch, D. G. Cristea, R. I. Lorincz, V. Tiponut, A Bio-inspired Obstacle Avoidance System Concept for Visually Impaired People-extended version, WSEAS journal, in press
4. D. G. Cristea, M. E. Basch, H. Ben-Yoav, V. Tiponut, Y. Shacham- Diamand, Universal Signal Conditioning System for Amperometric Sensors, accepted at AECE journal, to be published.

REFERENCES

[1] F. R. Blattner, G. Plunkett III, C. A. Bloch, N. T. Perna, V. Burland, M. Riley, J. Collado-Vides, J. D. Glasner, C. K. Rode, G. F. Mayhew, J. Gregor, N. W. Davis, H. A. Kirkpatrick, M. A. Goeden, D. J. Rose, B. Mau, Ying Shao, The Complete Genome Sequence of Escherichia coli K-12, Science 5 September 1997, pp. 1453-1462, DOI 10.1126/science. 277.5331.1453]

[2] http://microbewiki.kenyon.edu/index.php/Escherichia , accesed at 14.09.2011.

[3] http://microbewiki.com , accessed at 14.09.2011.

[4] M. E. Basch, D. G. Cristea, V. Tiponut, T. Slavici, Elaborated Motion Detector based on Hassenstein-Reichardt correlator Model, LATEST TRENDS on SYSTEMS, WSEAS, ISSN: 1792-4235, ISBN: 978-960-474-199-1, Corfu Island, Greece, vol. 1, 22-24 July 2010, pp. 192-195.

[5] Z. Haraszy, D. G. Cristea, V. Tiponut, T. Slavici, Improved Head Related Transfer Function Generation and Testing for Acoustic Virtual Reality Development, LATEST TRENDS on SYSTEMS, WSEAS, ISSN: 1792-4235, ISBN: 978-960-474-199-1, Corfu Island, Greece, vol. 2, 22-24 July 2010, pp. 411-416.

[6] M. E. Basch, D. G. Cristea, R. I. Lorincz, V. Tiponut, Bio-inspired Obstacle Avoidance System Concept for Visually Impaired People, accepted to 14th WSEAS International Conference on Systems, Corfu Island, Greece, 2011.

[7] Z. Haraszy, D. G. Cristea, S. Micut, V. Tiponut, Efficient Algorithm for Extracting Essential Head Related Impulse Response Data for Acoustic Virtual Reality Development, 14th WSEAS International Conference on Systems, Corfu Island, Greece, 2011.

[8] Extended version mihai

[9] R. I. Lorincz, M. E. Basch, D. G. Cristea, V. Tiponut, Hardware Implementation of Field-Weakening BLDC Motor Control, 14th WSEAS International Conference on Systems, Corfu Island, Greece, 2011.

[10] P. Papazian, D. G. Cristea, IEEE 1451.2 Compliant Smart Power Supply, accepted as AECE journal.

[11] A. Hulanicki, S. Geab, F. Ingman, Chemical Sensors Definitions And Classification, Pure&App/. Chern., vol. 63, n. 9, 1991, pp. 1247-1250.

[12] S. P. Mohanty, Biosensors : A Survey Report, 2001.

[13] S. P. Mohanty, E. Kougianos, Biosensors: A Tutorial Review, Potentials, IEEE, vol. 25, n. 2 , ISSN: 0278-6648, 2006, pp. 35-40.

[14] H. Javed, K.M. Niazi, Introduction course, Biosensors.

[15] D. Ramiz, PhD Thesis, 2010, Tel Aviv University, Israel.

[16] M. L. Simpson, G. S. Sayler, J. T. Fleming, B. Applegate, Whole-cell biocomputing, TRENDS in Biotechnology, vol. 19, n. 8, August 2001.

[17] B. Polyak, S. Geresh, R. S. Marks, Synthesis and characterization of a biotin-alginate conjugate and its application in a biosensor construction". Biomacromolecules, n. 5, 2004, pp. 389-396.

[18] R. Pedahzur, B. Polyak, R. S. Marksand, S. Belkin, Water toxicity detection by a panel of stress responsive luminescent bacteria. Journal of Applied Toxicology, n. 24, 2004, pp. 343-348.

[19] J. R. Premkumar, Ovadia Lev, R. S. Marks, B. Polyak, R. Rosen, S. Belkin, Antibody-based immobilization of bioluminescent bacterial sensor cells, Elsevier, Talanta 55, 2001, pp. 1029-1038.
[20] S. Andreescu, O. A. Sadik, Trends & Challenges in Biochemical Sensors for Clinical and Environmental Monitoring, Pure and Applied Chemistry, v. 76, n. 4, 2004, pp. 861-878.
[21] A. J. Baeumner, Biosensors for Environmental Pollutants and Food Contaminants, Analytical and Bioanalytical Chemistry, v. 377, n. 3, 2003, pp. 434-445 (invited review).
[22] B. O. Jansson, Encyclopedia of Global Environmental Change. v. 4, Wiley & Sons, LTD. Chichester, 2002, pp. 517-521.
[23] J. Hastings, Q. Gibson, J. Friedland, J. Spudich, Molecular Mechanisms in Bacterial Bioluminescence: On Energy Storage Intermediates and the Role of Aldehyde in the Reaction, Bioluminescence in Progress, F. Johnson and Y. Haneda, Princeton Univ Press, Princeton NJ USA, 151, 1966.
[24] J. Hastings, W. Riley, J. Massa, The Purification, Properties, and Chemiluminescence Quantum Yield of Bacterial Luciferase , J Biol Chem 240, 1473, 1965.
[25] J. Hastings, J. Spudich, G. Malnic, The Influence of Aldehyde Chain Length upon the Relative Quantum Yield of the Bioluminescent Reaction of Achromobacter fischeri , J Biol Chem 238, 3100, 1963.
[26] O. Shimomura, F. Johnson, T. Masugi, Cypridina Bioluminescence: Light-Emitting Oxyluciferin-Luciferase Complex, Science 164, 1299, 1969.
[27] S. Tu, C. Waters, J. Hastings, Photoexcited Bacterial Bioluminescence. Identity and Properties of the Photoexcitable Luciferase , Biochem 14, 1970, 1975.
[28] P. Rozen, F. Lubin, N. Papo, J. Knaani, H. Farbstein, M. Farbstein, G. Zajicek, Calcium supplements interact significantly with long-term diet while suppressing rectal epithelial proliferation of adenoma patients. Cancer, 91, 2001, pp. 833-840.
[29] M. B. Gu, P. S. Dhurjati, T. K. Van Dyk, R. A. LaRossa, A Miniature Bioreactor for Sensing Toxicity Using Recombinant Bioluminescent Escherichia coli Cells, , Biotechnology Progress vol. 12, n. 3, 1996, pp. 393-397.
[30] K. S. Cho, H. W. Ryu, N. Y. Lee, Biological deodorization of hydrogen sulfide using porous lava as a carrier of Thiobacillus thiooxidans. Journal of Bioscience and Bioengineering, vol. 90, n. 1, 2000, pp. 25-31.
[31] H. Funabashi, M. Fujioka, M. Kohchi, Y. Tateishi, N. Matsuoka, Collaborative work to evaluate toxicity on male reproductive organs by repeated dose studies in rats. Effects of 2- and 4-week administration of theobromine on the testis. J. Toxicol. Sci., 25, 2000, pp. 211-221.
[32] R. Turpeinen, Academic dissertation in environmental ecology, Faculty of Science of the University of Helsinki, for public criticism in Auditorium, Neopoli, Lahti.
[33] S. Belkin, A panel of stress-responsive luminous bacteria for monitoring wastewater toxicity. Methods Mol Biol 102, 1998.
[34] E. D. Rosen, P. Sarraf, A. E. Troy, G. Bradwin, K. Moore, D. S. Milstone, B. M. Spiegelman, R. M. Mortensen, PPAR_ is required for the differentiation of adipose tissue in vivo and in vitro.Mol. Cell 4, 1999, pp. 611-617.
[35] C. Lu, W.E. Bentley, G. Rao, Comparisons of oxidative stress response genes in aerobic Escherichia coli fermentations. Biotechnol Bioeng 83 (7), 2003, pp. 864-870.

[36] S. Kalir, J. McClure, K. Pabbaraju, C. Southward, M. Ronen, S. Leibler, M. G. Surette , U. Alon, 2001. Ordering genes in a flagella pathway by analysis of expression kinetics from living bacteria. Science 292 (5524), pp. 2080-2083.

[37] J. Sabina, N. Dover, L. J. Templeton, D.R. Smulski, D. Soll, R. A. LaRossa, Interfering with different steps of protein synthesis explored by transcriptional profiling of Escherichia coli K-12. J Bacteriol 185 (20), 2003, pp. 6158-6170.

[38] J. Rine, J. Phillips, S. Scherer, P. Cundiff, K. DeBord, D. Gilliland, S. Hickman, A. Jarvis, L. Tong, et al., Comprehensive evaluation of isoprenoid biosynthesis regulation in Saccharomyces cerevisiae utilizing the Genome Reporter MatrixTM. J Lipid Res 40 (5), 1999, pp. 850-860.

[39] R. K. Gupta, S. S. Patterson, S. Ripp, M. L. Simpson , G. S. Sayler, Expression of the Photorhabdus luminescens lux genes (luxA, B, C, D, and E) in Saccharomyces cerevisiae. Fems Yeast Res 4 (3), 2003, pp. 305-313.

[40] K. Hakkila, M. Maksimow, M. Karp, M. Virta, Reporter genes lucFF, luxCDABE, gfp, and dsred have different characteristics in whole-cell bacterial sensors. Anal Biochem 301 (2), 2002, pp. 235-242.

[41] A. J. Forsberg, G. D. Pavitt, C. F. Higgins, Use of transcriptional fusions to monitor gene-expression-A cautionary tale. J Bacteriol 176 (7), 1994, pp. 2128-2132.

[42] M. P. DeLisa, J. C. Li, G. Rao, W. A. Weigand, W. E. Bentley, Monitoring GFP-operon fusion protein expression during high cell density cultivation of Escherichia coli using an on-line optical sensor. Biotechnol Bioeng 65 (1), 1999, pp. 54-64.

[43] M. B. Gu, P. S. Dhurjati, T. K. VanDyk, R. A. LaRossa, A miniature bioreactor for sensing toxicity using recombinant bioluminescent Escherichia coli cells. Biotechnol Prog 12 (3), 1996, pp. 393-397.

[44] A. Zanzotto, N. Szita, P. Boccazzi, P. Lessard, A.J. Sinskey, K. F. Jensen, A membrane-aerated microbioreactor for high-throughput bioprocessing. Biotechnol Bioeng 87 (2), 2004, pp. 243-254.

[45] A. Zanzotto, P. Boccazzi, N. Gorret, K. T. Van Dyk, A. J. Sinskey, K. F. Jensen, In Situ Measurement of Bioluminescence and Fluorescence in an Integrated Microbioreactor, Wiley InterScience www.interscience.wiley.com). 2005, DOI 10.1002/bit.20708

[46] D. Ramiz, PhD Thesis, 2010, Tel Aviv University, Israel.

[47] R. A. Yotter, D. M. Wilson, Sensor Technologies for Monitoring Metabolic Activity in Single Cells-Part II: Nonoptical Methods and Applications, IEEE Sensors Journal, vol. 4, n. 4, August 2004.

[48] E. Thrush, O. Levia, K. Wanga, J. S. Harris Jr., S. J. Smith, High throughput integration of optoelectronics devices for biochip fluorescent detection, Proceedings of SPIE 4982, 162, 2003.

[49] C. Yi, Q. Zhang, C. W. Li, J. Yang, J. Zhao, M. Yang, Optical and electrochemical detection techniques for cell-based microfluidic systems, Anal Bioanal Chem (2006) 384, pp. 1259-1268.

[50] J. Chou, Hazardous Gas Monitors: A Practical Guide to Selection, Operation, and Applications , McGraw-Hill Professional, 1st edition, (October 30, 1999).

[51] A. Q. Contractor, T. N. Sureshkumar, R. Narayanan, S. Sukeerthi, R. Lal, R. S. Srinivas, Conducting polymer-based biosensors. Electrochim. Acta 39, 1994, pp. 1321-1324.

[52] D. S. Papastathopoulos, , G. A. Rechnitz, Enzymatic cholesterol determination using ion selective membrane electrodes. Anal. Chem. 47, 1975, pp. 1792-1796.
[53] M. Mascini, Potentiometry: enzyme electrodes. Encyclopedia of analytical Science, 1995, pp. 4112-4118.
[54] A. Senillou, A. Jaffrezic-Renault, C. Martelet, S. Cosnier, A miniaturized urea sensor based on the integration of both ammonium based urea enzyme field effect transistor and a reference field effect transistor in a single chip. Talanta 50, 1999, pp. 219-226.
[55] R. Koncki, A. Radomska, S. Glab, Potentiometric determination of dialysate urea nitrogen, Talanta 52, 2000, pp. 13-17.
[56] A. Lindgren, T. Ruzgas, L. Gorton, E. Csoregi, G. B. Ardila, I. Y. Sakharov, I. G. Gazaryan, Biosensors based on novel peroxidases with improved properties in direct and mediated electron transfer. Biosens. Bioelectron. 15, 2000, pp. 491-497.
[57] G. Davis, Electrochemical techniques for the development of amperometric biosensors, Biosensor 1, 1985, pp. 161-178.
[58] S. J. Updike, G. P. Hicks, The enzyme electrode. Nature 214, 1967, pp. 986-988.
[59] G. G. Guilbault, G. J. Lubrano, An enzyme electrode for the amperometric determination of glucose. Anal. Chim. Acta 64, 1973, pp. 439-455.
[60] A. E. G. Cass, G. Davis, G. D. Francis, H. A. O. Hill, W. J. Aston, I. J. Higgins, E. V. Plotkin, L. D. L. Scott, A. P. F. Turner, Ferrocene-mediated enzyme electrode for amperometric determination of glucose. Anal. Chem. 56, 1984, pp. 667-671.
[61] A. Chaubey, B. D. Malhotra, Review Mediated biosensors, Elsevier, Biosensors & Bioelectronics 17, 2002, pp. 441-456.
[62] H. Ben-Yoav, S. Melamed, A. Freeman, Y. Shacham-Diamand, S. Belkin, Whole-cell biochips for bio-sensing: integration of live cells and inanimate surfaces, Critical Reviews in Biotechnology, 2010, 1-17, 2011 Informa Healthcare USA, Inc. ISSN 0738-8551 print/ISSN 1549-7801 online, DOI 10.3109/07388551.2010.532767.
[63] J. W. Costerton, P. S. Stewart, E. P. Greenberg, Science 284, 1999, pp. 1318.
[64] A. Bressel, J. W. Schultze, W. Khan, G. M. Wolfaardt, H. P. Rohns, R. Irmscher, M. J. Schöning, Electrochim. Acta 48, 2003, pp. 3363.
[65] J. Gamby, A. Pailleret, C. B. Clodic, C. M. Pradier, B. Tribollet, Electrochim.Acta 54, 2008, pp. 66.
[66] W. Wang, X. Zhang, J. Wang, Mater.Corros.60, 2009, pp. 957.
[67] X. Muñoz-Berbel, F. J. Muñoz, N. Vigués, J. Mas, Sens.ActuatorsB:Chem. 118, 2006, pp. 129.
[68] E. Marsili, J. B. Rollefson, D. B. Baron, R. M. Hozalski, D. R. Bond, Appl.Environ. Microbiol. 74, 2008, pp. 7329.
[69] X. Muñoz-Berbel, N. Vigués, A. T. A. Jenkiñs, J. Mas, F. J. Muñoz, Biosens.Bioelectron. 23, 2008, pp. 1540.
[70] X. Muñoz-Berbel, N. Vigués, J. Mas, A. T. A. Jenkiñs, F. J. Muñoz, Electrochem. Commun. 9, 2007, pp. 2654.
[71] S. Bayoudh, A. Othmane, L. Ponsonnet, H. BenOuada, ColloidsSurf.A:Physicochem. Eng.Asp.318, 2008, pp. 291.
[72] R. Gómez-Sjöberg, D. T. Morisette, R. Bashir, Microelectromech.Syst.14, 2005, pp. 829.

[73] M. J. Hernández-Gayosso, G. Zavala-Olivares, N. Ruiz-Ordaz, R. García-Esquivel, J. L. Mora-Mendoza, Mater.Corros.55, 2004, pp. 676.
[74] R. P. C. Neto, C. A. C. Sequeira, KeyEng.Mater.230-232, 2002, pp. 432.
[75] R. P. Ramasamy, Z. Ren, M. M. Mench, J. M. Regan, Biotechnol.Bioeng.101, 2008, pp. 101.
[76] H. Ben-Yoav, et al., An electrochemical impedance model for integrated bacterial biofilms, Electrochim. Acta (2011), DOI 10.1016/j.electacta.2010.12.025.
[77] M. F. Cardosi, A. P. F. Turner, The realization of electron transfer from biological molecules to electrodes. In: Turner, A.P.F., Karube, I., Wilson, G.S. (Eds.), Biosensors: Fundamentals and Applications. Oxford University Press, London and New York, 1987, pp. 257-275.
[78] P. D. Hale, T. Inagaki, H. I. Karan, Y. Okamoto, T. A. Skotheim, A new class of amperometric biosensor incorporating a polymeric electron transfer mediator. J. Am. Chem. Soc. 111, 1989, pp. 3482-3484.
[79] P. D. Hale, H. S. Lee, Y. Okamoto, Electrical communication between glucose oxidase and novel ferrocene-containing siloxaneethylene oxide copolymers: biosensor applications. Anal. Lett. 26, 1993, pp. 1-16.
[80] E. A. H. Hall, Overview of Biosensors. In: P.G. Edelman, J. Wang (Eds.), Biosensors and Chemical sensors, optimizing performance through polymeric materials, ACS Symposium series, 487, 1992, pp. 1-5.
[81] J. F. Kennedy, S. A. Barker, A. Rosevear, Preparation of water insoluble trans-2, 3-cyclic carbonate derivative of macroporous cellulose and its use as a matrix for enzyme immobiliztion. J. Chem. Soc. Perkin Trans I, 1973, pp. 2293-2299.
[82] J. Moiroux, P. J. Elving, Effects of adsorption, electrode material and operational variables on the oxidation of dihydronicotinamide adenine dinucleotide at carbon electrode. Anal. Chem. 50, 1978, pp. 1056-1062.
[83] D. B. Swartz, G. S. Wilson, Small volume coulometric redoxostat. Anal. Biochem. 40, 1971, pp. 329-400.
[84] M. Ito, T. Kuwana, Spectroelectrochemical study of indirect reduction of triphosphopyridine nucleotide. J. Electroanal. Chem.32, 1971, pp. 415-425.
[85] W. J. Albery, J. H. Craston, In: Turner, A.P.F., Karube, I., Wilson, G.S. (Eds.), Biosensors: Fundamentals and Applications. Oxford University Press, Oxford, 1987, pp. 180.
[86] N. K. Cenas, J. J. Kulys, Biocatalytic oxidation of glucose on conductive charge transfer complexes. J. Electroanal. Chem. 128, 1981, pp. 103-113.
[87] H. Huck, H. L. Schmidt, Chloranil alskatalysator zur elektrochemischen oxidation von NADH zu NAD+. Angewandt. Chemie. 93, 1981, pp. 421-422.
[88] H. Jaegfeldt, T. Wuwana, G. Johansson, Electrochemical stability of catechols with pyrene side chain in strongly adsorbed on graphite electrodes for catalytic oxidation of dihydronicotinamide adenine dinucleotide. J. Am. Chem. Soc. 105, 1983, pp. 1805-1814.
[89] B. Persson, H. L. Lan, L. Gorton, V. Okamoto, P. D. Hale, L. I. Boguslavsky, T. Skotheim, Amperometric biosensor based on electrocatalytic regeneration of NAD+ at redox polymer modified electrodes. Biosens. Bioelectron. 8, 1993, pp.81-88.
[90] E. Lorenzo, F. Pariente, L. Hernandez, F. Tobalina, M. Darder, Q. Wu, M. Maskus, H. D. Abruna, Analytical starategies for amperometric biosensors based on chemically modified electrodes. Biosens. Bioelectron. 13, 1998, pp. 319-332.

[91] M. D. Disney, P. H. Seeberger, The use of carbohydrate microarrays to study carbohydrate-cell interactions and to detect pathogens.Chem Biol, 11, 2004, pp. 1701-1707.
[92] R. Muller, S. Ruhl, K. A. Hiller, G. Schmalz, H. Schweikl, Adhesion of eukaryotic cells and Saphylococcus aureus to silicon model surfaces. J Biomed Mater Res A, 84, 2007, pp. 817-827.
[93] D. O. Fesenko, T. V. Nasedkina, A. D. Mirzabekov, A bacterial microchip: The principle of operation as exemplified by detection of antibiotics. Dokl Biochem Biophys, 381, 2001, pp. 427-429.
[94] J. C. Zguris, L J Itle, W. G. Koh, M. V. Pishko, A novel single-step fabrication technique to create heterogeneous poly (ethylene glycol) hydrogel microstructures containing multiple phenotypes of mammalian cells. Langmuir, 21, 2005, pp. 4168-4174.
[95] S. Venkatasubbarao, Microarrays - status and prospects. Trends Biotechnol, 22, 2004, pp. 630-637.
[96] H. Huang, E. Pierstorff, E. Osawa, D. Ho, Protein-mediated assembly of nanodiamond hydrogels into a biocompatible and biofunctional multilayer nanofilm. ACS nano, 2, 2008, pp. 203-212.
[97] B. Kasemo, Biological surface science. Curr Opin Solid State Mater Sci, 3, 1998, 451-459.
[98] B. Kasemo, J. Gold, Implant surfaces and interface processes.Adv Dent Res, 13, 1999, pp. 8-20.
[99] J. S. Dickson, M. Koohmaraie, Cell surface charge characteristics and their relationship to bacterial attachment to meat surfaces.Appl Environ Microbiol, 55, 1989, pp. 832-836.
[100] T. Cao, H. Tang, X. Liang, A. Wang, G. W. Auner, S.O. Salley, K. Y. Ng, Nanoscale investigation on adhesion of E. coli to surface modified silicone using atomic force microscopy. Biotechnol Bioeng, 94, 2006, pp. 167-176.
[101] R. O. Hynes, Integrins: Bidirectional, allosteric signaling machines. Cell, 110, 2002, pp. 673-687.
[102] B. Geiger, A. Bershadsky, R. Pankov, K. M. Yamada, Transmembrane crosstalk between the extracellular matrix and the cytoskeleton. Nat Rev Mol Cell Biol, 2, 2001, pp. 793-805.
[103] D. E. Discher, P. Janmey, Y. l. Wang, Tissue cells feel and respond to the stiffness of their substrate. Science, 310, 2005, pp. 1139-1143.
[104] L. Raj, Biomaterials: Protein-surface interactions. In: Bowlin GL, Wnek G, eds. Encyclopedia of Biomaterials and Biomedical Engineering. New York: Taylor & Francis, 1-15, 2005.
[105] P. Colpo, A. Ruiz, L. Ceriotti, F. Rossi, Surface functionalization for protein and cell patterning. Adv Biochem Engin/Biotechnol, 117, 2010, pp. 109-130.
[106] Z. Yang, S. Sasaki, I. Karube, H. Suzuki, Fabrication of oxygen electrode arrays and their incorporation into sensors for measuring biochemical oxygen demand. Anal Chim Acta, 357, 1997, pp. 41-49.
[107] M. A. Lan, C. A. Gersbach, K. E. Michael, B. G. Keselowsky, A. J. Garcia, Myoblast proliferation and differentiation on fibronectincoated self assembled monolayers presenting different surface chemistries. Biomaterials, 26, 2005, pp. 4523-4531.
[108] W. S. Yeo, M. Mrksich, Electroactive self-assembled monolayers that permit orthogonal control over the adhesion of cells to patterned substrates. Langmuir, 22, 2006, pp. 10816-10820.

[109] M. Ito, T. Kuwana, Spectroelectrochemical study of indirect reduction of triphosphopyridine nucleotide. J. Electroanal. Chem.32, 1971, pp. 415-425.
[110] J. Fukuda, A. Khademhosseini, J. Yeh, G. Eng, J. Cheng, O. C. Farokhzad, R. Langer, Micropatterned cell co-cultures using layer-bylayer deposition of extracellular matrix components. Biomaterials, 27, 2006, pp. 1479-1486.
[111] S. Rozhok, Z. Fan, D. Nyamjav, C. Liu, C. A. Mirkin, R. C. Holz, Attachment of motile bacterial cells to prealigned holed microarrays. Langmuir, 22, 2006, pp. 11251-11254.
[112] N. P. Westcott, M. N. Yousaf, Synergistic microfluidic and electrochemical strategy to activate and pattern surfaces selectively with ligands and cells. Langmuir, 24, 2008, pp. 2261-2265.
[113] D. W. Branch, J. M. Corey, J. A. Weyhenmeyer, G. J. Brewer, B. C. Wheeler, Microstamp patterns of biomolecules for high-resolution neuronal networks. Med Biol Eng Comput, 36, 1998, pp. 135-141.
[114] J. Choi, W. Lee, D. Lee, C. Park, J. Kim, Y. Jang, Y. Kim, Electrochemical detection of pathogen infection using cell chip. Environ Monit Assess, 129, 2007, pp. 37-42.
[115] D. A. Heller, V. Garga, K. J. Kelleher, T. C. Lee, S. Mahbubani, L. A. Sigworth, T. R. Lee, M. A. Rea, Patterned networks of mouse hippocampal neurons on peptide-coated gold surfaces. Biomaterials, 26, 2005, pp. 883-889.
[116] H. Ben-Yoav, S. Melamed, A. Freeman, Y. Shacham-Diamand, S. Belkin, Whole-cell biochips for bio-sensing: integration of live cells and inanimate surfaces, Critical Reviews in Biotechnology, 2010, 1-17, 2011 Informa Healthcare USA, Inc., ISSN 0738-8551 print/ISSN 1549-7801 online.
[117] http://www.enotes.com/topic/Randles_circuit , accesed at 20.09.11.
[118] H. Ben-Yoav, A. Biran, R. Pedahzur, S. Belkin, S. Buchinger, G. Reifferscheid, Y. Shacham-Diamand, A whole cell electrochemical biosensor for water genotoxicity bio-detection, Electrochimica. Acta, 2009, electacta.2009.
[119] V. Horvat-Radoševic, K. Kvastek, hree-electrode cell set-up electrical equivalent circuit applied to impedance analysis of thin polyaniline film modified electrodes, Journal of Electroanalytical Chemistry 631, 2009, pp. 10-21.
[120] N. A. Sekushin, Universal Equivalent Circuit of Electrochemical Cell, ISSN 1023-1935, Russian Journal of Electrochemistry, 2009, vol. 45, n. 3, Pleiades Publishing, Ltd. 2009, pp. 350-355.
[121] A. Amirudin, D. Thierry, Application of electrochemical impedance spectroscopy to study the degradation of polymer-coated metals, Progress in Organic Coatings 26, 1995, pp. 1-28.
[122] J. M. McIntyre, H. Q. Pham, Electrochemical impedance spectroscopy; a tool for organic coatings optimizations, Progress in Organic Coatings 27, 1996, pp. 201-207.
[123] R. Gomez, R. Bashir, A. Sarikaya, M. R. Ladish, J. Sturgis, J. P. Robinson, T. Geng, A. K. Bhunia, H. L. Apple, S. Wereley, Microfluidic Biochip for Impedance Spectoscropy of Biological Species, Biomedical Microdevices 3:3, 201-209, 2001.
[124] A. Hassibi, T. H. Lee, A Programmable 0.18-?m CMOS Electrochemical Sensor Microarray for Biomolecular Detection, IEEE Sensors Journal, vol. 6, n. 6, December 2006.
[125] N.Fishelson, A.Inberg, N.Croitoru, Y.Shcham-Diamand, Microelectronic Engineering (on publishing, reference number MME 8037, 2011).

[126] D. G. Cristea, M. E. Basch, Z. Haraszy, R. I. Lorincz, V. Tiponut, A new model for dessigning electrochemical sensors array, accepted at SIITME 2011 Timisoara.
[127] D. G. Cristea, M. E. Basch, Z. Haraszy, N. Fishelson, V. Tiponut, A New Electronic Equivalent Circuit for Electrochemical Cells, 2nd International Conference on Modelling and Simulations, ICOMOS 2011, ISSN: 2038-3975, 11-25 July 2011.
[128] J. Chou, Hazardous Gas Monitors: A Practical Guide to Selection, Operation, and Applications , McGraw-Hill Professional, 1st edition, (October 30, 1999).
[129] http://www.customsensorsolutions.com , accesed at 20.09.11.
[130] http://www.angelfire.com/pe2/joserojas/pdfs/potencio.pdf -Potentiostats-Introduction , accesed at 20.09.11.
[131] W.S. Wang, W. T. Kuo, H. Y. Huang, C. H. Luo, Wide Dynamic Range CMOS Potentiostat for Amperometric Chemical Sensor, Sensors 2010, 10, 1782-1797, DOI 10.3390 /s100301782.
[132] L. Busoni, M. Carla, L. Lanzi, A comparison between potentiostatic circuits with grounded workor auxiliary electrode. Rev. Scient. Instrum. 2002, 73, pp. 1921-1923.
[133] W. Y. Chung, A. C. Paglinawan, Y. H. Wang, T. T. Kuo, A 600 μm read-out circuit with potentiostat for amperometric chemical sensors and glucose meter applications. In Proceedings of IEEE Conference on Electron Devices and Solid-State Circuits, Tainan, Taiwan, December 20-22, 2007, pp. 1087-1090.
[134] Z. Jichun, N. Trombly, A. Mason, A low noise readout circuit for integrated electrochemical biosensor arrays. In Processing of IEEE Sensors, Vienna, Austria, October 24-27, 2004, pp. 36-39.
[135] K. Iniewski, VLSI Circuits for Biomedical Applications, 1st ed., Artech House, Boston, MA, USA, 2008, pp. 272-275.
[136] R. Genov, M. Stanacevic, M. Naware, G. Cauwenberghs, N. V. Thakor, 16-channel integrated potentiostat for distributed neurochemical sensing. IEEE Trans. Circ. Syst. I: Regular Papers 53, 2006, pp. 2371-2376.
[137] S. Ayers, K. D. Gillis, M. Lindau, B.A. Minch, Design of a CMOS potentiostat circuit forelectrochemical detector arrays. IEEE Trans. Circ. Syst. I: Regular Papers 54, 2007, pp. 736-744.
[138] S. M. R. Hasan, Stability analysis and novel compensation of a CMOS current-feedbackpotentiostat circuit for electrochemical sensors. IEEE Sens. J. 7, 2007, pp. 814-824.
[139] H. S. Narula, J. G. Harris, A time-based VLSI potentiostat for ion current measurements. IEEE Sens. J. , 6, 2006, pp. 239-247.
[140] R. F. B. Turner, D. J. Harrison, H.P. Baltes, A CMOS potentiostat for amperometric chemicalsensors. IEEE J. Solid-State Circuits 22, 1987, pp. 473-478.
[141] H. S. Narula, J. G. Harris, Integrated VLSI potentiostat for cyclic voltammetry in electrolyticreactions. In Proceedings of IEEE Computer Society Annual Symposium on VLSI, Lafayette, LA, USA, February 19-20, 2004, pp. 268-270.
[142] M. M. Ahmadi, G. A. Jullien, A very low power CMOS potentiostat for bioimplantable applications. In Proceedings of Fifth International Workshop on System-on-Chip for Real-Time Applications, Banff, Alberta, Canada, July 20-24, 2004, pp. 184-189.

[143] G. Schouten, J. G. F. Doornekamp, Potentiostat to use in electro-chemical experiments, 1953, Appl. sci. Res., Sec.B vol. 3.
[144] M. H. Nazari, R. Genov, A Fully Differential CMOS Potentiostat. In: 2009 IEEE International Symposium on Circuits and Systems. IEEE , ISBN 978-1-4244-3827-3, 2009 pp. 2177-2180.
[145] H. S. Narula, J. G. Harris, VLSI potentiostat for amperometric measurements for electrolytic reactions, Circuits and Systems, 2004. ISCAS '04. Proceedings of the 2004 International Symposium on, May 2004, pp. I - 457-60 vol. 1, ISBN: 0-7803-8251-X.
[146] M. Kimura, H. Fukushima, Y. Sagawa, K. Setsu, H. Hara, S. Inoue, An Integrated Potentiostat With an Electrochemical Cell Using Thin-Film Transistors, IEEE Transactions On Electron Devices, vol. 56, n. 9, September 2009.
[147] S. Y. C. Catunda, J. F. Naviner, G. S. Deep, R. C. S. Freire, Designing a Programmable Analog Signal Conditioning Circuit Without Loss of Measurement Range, IEEE Transactions On Instrumentation And Measurement, vol. 52, n. 5, October 2003.
[148] V. Ferrari, C. Ghidini, D. Marioli, A. Taroni, Oscillator-Based Signal Conditioning with Improved Linearity for Resistive Sensors, IEEE Transactions On Instrumentation And Measurement, vol. 47, n. 1, February 1998.
[149] B. George, V. J. Kumar, Switched Capacitor Signal Conditioning for Push-Pull Type Capacitive Sensors, IMTC 2005 - Instrumentation and Measurement Technology Conference Ottawa, Canada, 17-19 May 2005.
[150] D. R. Belfort, S. Y. C. Catundal, F. R. de Sousa, Progra-mmable Analog Signal Conditioning Circuit for Integrated Systems, I2MTC 2008 - IEEE International Instrumentation and Measurement Technology Conference Victoria, Vancouver Island, Canada, May 12-15, 2008.
[151] J. Zhang, A. Mason, Characterization of a Configurable Sensor Signal Conditioning Circuit for Multi-Sensor Microsystems, 2004 IEEE.
[152] N. M. Mohan, V. J. Kumar, Novel Signal Conditioning Circuit for Push-pull Type Capacitive Transducers, IMTC 2005 - Instrumentation and Measurement Technology Conference Ottawa, Canada, 17-19 May 2005.
[153] X. Zou, X. Xu, L. Yao, Y. Lian, A 1-V 450-nW Fully Integrated Programmable Biomedical Sensor Interface Chip, IEEE Journal Of Solid-State Circuits, vol. 44, n. 4, April 2009.
[154] S. K. Islam, R. Vijayaraghavan, M. Zhang, S. Ripp, S. D. Caylor, B. Weathers, S. Moser, S. Terry, B. J. Blalock, G. S. Sayler, Integrated Circuit Biosensors Using Living Whole-Cell Bioreporters, IEEE Transactions on Circuits and Systems - I: Regular Papers, vol. 54, n. 1, Jan. 2007.
[155] H. S. Narula , J. G. Harris, VLSI potentiostat for amperometric measurements for electrolytic reactions, 2004. ISCAS '04, Proceedings of the International Symposium on Circuits and Systems, vol. 1, pp: I - 457-60, 23-26 May 2004.
[156] D.G. Cristea, V. Tiponut, Tendencies on Signal Conditioning Circuits, Lucrarile sesiunii de comunicari stiintifice "DOCTOR Etc 2009", ISSN 2066-883X, Editura "Politehnica", Timisoara, Sept. 2009, pp.13-16.
[157] D. G. Cristea, Y. Shacham-Diamand, V. Tiponut, H. Ben-Yoav, M. E. Basch, Z. Haraszy, VLSI Universal Signal Conditioning Circuit for Electrochemical and Bioluminescent Sensors, 26th IEEE Convention of Electrical and Electronics Engineers in Israel, ISBN: 978-1-4244-8682-3, 2010, pp. 249-252.

[158] P. R. Gray, P. J. Hurst, S. H. Lewls, R. G. Meyer, Analysis And Design of Analog Integrated Circuits, Fourth Edition, John Wlley & Sons, Inc., 2001.
[159] L. Luh, J. Choma Jr., J. Draper, A High-Speed Fully Differential Current Switch, IEEE Transactions on Circuits and Systems, April 2000.
[160] H. C. Yang, T. S. Fiez, D. J. Allstot, Currentfeedthrough effects and cancellation techniques in switched-current circuits, in Proc. IEEE Int. Symp.Circuits Syst., May 1990, pp. 3168-3188.
[161] B. Jonsson, N. Tan, Clock-feedthrough compensated first-generation SI circuits and systems, in Analog Integrated Circuits and Signal Processing, vol.12, issue 3, May, 1997, pp. 201 - 210.
[162] H. Cha, S. Ogawa, K. Watanabe, A clockfeedthrough compensated switched-current memory cell, " in IEICE Trans. Fundamentals, vol. E80-A, n. 6, Jun, 1997, pp. 1069-1072.
[163] C. Wu, C. Chen, J. Cho, A cmos transistor only 8-b 4.5-Ms/s pipelined analog-to-digital converter using fully-differential current-mode circuit techniques, IEEE J. Solid-State Ckt, vol. 30, n. 5, May, 1995, pp. 522-532.
[164] M. Bracey, W. Redman-White, J. Richardson, J. B. Hughes, A full Nyquist 15MS/s 8-b differential switched-currentA/Dconverter, IEEE J. Solid-State Ckt., vol. 31, n. 7, Jul, 1996, pp. 945-951.
[165] D. Vallancourt, Y. P. Tsividis, S. J. Daubert, Current-copier cells, Electron. Lett., vol. 24, n. 25, Dec, 1988, pp. 1560-1562.
[166] É. Lojou, P. Bianco, Application of the electrochemical concepts and techniques to amperometric biosensor devices, J Electroceram (2006) 16: 79-91 DOI 10.1007/s10832-006-2365-9
[167] H. Chen, Modulation Effects On Organic Electronics, PhD Thesis, School of Chemistry and Biochemistry, Georgia Institute of Technology, December 2005.
[168] M. Stanaçeviç, K. Murari, A. Rege, G. Cauwenberghs, N. V. Thakor, VLSI Potentiostat Array With Oversampling Gain Modulation for Wide-Range Neurotransmitter Sensing, IEEE Transactions On Biomedical Circuits And Systems, vol. 1, n. 1, March 2007.
[169] E. Sagi, N. Hever, R. Rosen, A. J. Bartolome, J. R. Premkumar, R. Ulber, O. Lev, T. Scheper, S. Belkin, Fluorescence and bioluminescence reporter functions in genetically modified bacterial sensor strains, Sensors and Actuators B 90, 2003, pp. 2-8.
[170] A. Hierlemann, The 13th International Conference on Solid-State Sensors. Actuators and Microsystems, Seoul, Korea, June 5-9, 2005.
[171] Y. Iwasaki, M. Morita, Electrochemical Measurements with Interdigitated Array Microelectrodes, Current Separations 14:1, 1995.
[172] J. Zhang, Y. Huang, N. Trombly, C. Yang, A. Mason, Electrochemical Array Microsystem with Integrated Potentiostat, IEEE. 0-7803-9056-3/05 2005.
[173] M. Song, Y. Lee, W. Kim, A clock feedthrough reduction circuit for switched-current systems, " in IEEE J. Solid-State Circuits, vol. SC-28, Feb, 1993, pp. 133- 137.
[174] Texas Instruments, Noise Analysis in Operational Amplifier Circuits, Application Report, 1998 Digital Signal Processing Solutions.

APPENDIX

A.1. Experimental results (first quarter)

Current results in absence of toxins				Current results in presence of toxins			
2, 05E-02	1, 45E-01	9, 44E-02	6, 56E-02	2, 04E-02	7, 10E-01	6, 76E-01	6, 70E-01
1, 89E-01	1, 50E-01	9, 43E-02	8, 19E-02	2, 05E-01	7, 03E-01	6, 85E-01	6, 72E-01
2, 29E-01	1, 43E-01	9, 46E-02	7, 80E-02	7, 74E-01	7, 09E-01	6, 73E-01	6, 62E-01
2, 20E-01	1, 41E-01	9, 93E-02	7, 51E-02	7, 59E-01	7, 06E-01	6, 70E-01	6, 62E-01
2, 18E-01	1, 37E-01	9, 17E-02	7, 23E-02	7, 68E-01	7, 17E-01	6, 80E-01	6, 58E-01
2, 11E-01	1, 42E-01	9, 40E-02	7, 93E-02	7, 54E-01	6, 99E-01	6, 75E-01	6, 69E-01
2, 05E-01	1, 38E-01	8, 80E-02	7, 67E-02	7, 52E-01	6, 94E-01	6, 71E-01	6, 69E-01
2, 12E-01	1, 37E-01	8, 98E-02	7, 06E-02	7, 49E-01	7, 05E-01	6, 70E-01	6, 66E-01
2, 01E-01	1, 35E-01	9, 06E-02	8, 62E-02	7, 43E-01	7, 08E-01	6, 75E-01	6, 65E-01
1, 97E-01	1, 41E-01	9, 12E-02	7, 62E-02	7, 41E-01	7, 00E-01	6, 84E-01	6, 69E-01
1, 95E-01	1, 32E-01	9, 66E-02	7, 97E-02	7, 43E-01	7, 01E-01	6, 73E-01	6, 50E-01
1, 90E-01	1, 36E-01	8, 86E-02	7, 78E-02	7, 33E-01	6, 98E-01	6, 70E-01	6, 61E-01
1, 92E-01	1, 32E-01	1, 00E-01	8, 36E-02	7, 38E-01	7, 01E-01	6, 69E-01	6, 57E-01
1, 81E-01	1, 42E-01	9, 09E-02	7, 97E-02	7, 35E-01	6, 87E-01	6, 67E-01	6, 63E-01
1, 87E-01	1, 36E-01	9, 43E-02	7, 67E-02	7, 37E-01	6, 95E-01	6, 70E-01	6, 58E-01
1, 76E-01	1, 38E-01	8, 58E-02	8, 13E-02	7, 22E-01	6, 85E-01	6, 74E-01	6, 56E-01
1, 81E-01	1, 33E-01	9, 34E-02	7, 96E-02	7, 31E-01	7, 03E-01	6, 73E-01	6, 63E-01
1, 80E-01	1, 36E-01	9, 11E-02	7, 76E-02	7, 36E-01	6, 92E-01	6, 68E-01	6, 54E-01
1, 76E-01	1, 32E-01	9, 06E-02	7, 60E-02	7, 39E-01	6, 95E-01	6, 64E-01	6, 68E-01
1, 68E-01	1, 32E-01	9, 08E-02	7, 81E-02	7, 33E-01	6, 94E-01	6, 68E-01	6, 62E-01
1, 73E-01	1, 35E-01	9, 48E-02	8, 13E-02	7, 36E-01	7, 06E-01	6, 83E-01	6, 61E-01
1, 62E-01	1, 32E-01	8, 95E-02	7, 70E-02	7, 34E-01	6, 96E-01	6, 65E-01	6, 56E-01
1, 75E-01	1, 39E-01	8, 58E-02	7, 88E-02	7, 27E-01	6, 92E-01	6, 72E-01	6, 65E-01
1, 59E-01	1, 27E-01	8, 58E-02	7, 51E-02	7, 26E-01	7, 00E-01	6, 76E-01	6, 55E-01
1, 62E-01	1, 25E-01	9, 35E-02	7, 68E-02	7, 18E-01	7, 05E-01	6, 68E-01	6, 62E-01
1, 61E-01	1, 19E-01	8, 48E-02	7, 86E-02	7, 38E-01	7, 03E-01	6, 80E-01	6, 54E-01
1, 60E-01	1, 28E-01	8, 75E-02	8, 39E-02	7, 22E-01	7, 02E-01	6, 66E-01	6, 62E-01
1, 60E-01	1, 25E-01	9, 03E-02	8, 13E-02	7, 20E-01	7, 02E-01	6, 74E-01	6, 55E-01

1, 58E-01	1, 26E-01	9, 10E-02	7, 51E-02	7, 34E-01	7, 00E-01	6, 72E-01	6, 60E-01
1, 59E-01	1, 30E-01	8, 88E-02	7, 66E-02	7, 21E-01	7, 01E-01	6, 72E-01	6, 59E-01
1, 50E-01	1, 26E-01	8, 83E-02	7, 24E-02	7, 23E-01	6, 99E-01	6, 67E-01	6, 60E-01
1, 53E-01	1, 25E-01	9, 08E-02	7, 79E-02	7, 14E-01	7, 02E-01	6, 67E-01	6, 55E-01
1, 51E-01	1, 26E-01	8, 79E-02	6, 94E-02	7, 03E-01	7, 01E-01	6, 74E-01	6, 54E-01
1, 55E-01	1, 19E-01	9, 36E-02	7, 21E-02	7, 24E-01	6, 97E-01	6, 68E-01	6, 56E-01
1, 53E-01	1, 27E-01	8, 79E-02	7, 81E-02	7, 19E-01	6, 96E-01	6, 69E-01	6, 51E-01
1, 57E-01	1, 23E-01	8, 54E-02	7, 88E-02	7, 17E-01	7, 02E-01	6, 65E-01	6, 60E-01
1, 43E-01	1, 21E-01	9, 08E-02	6, 77E-02	7, 13E-01	6, 98E-01	6, 75E-01	6, 59E-01
1, 50E-01	1, 18E-01	8, 98E-02	7, 51E-02	7, 14E-01	6, 95E-01	6, 74E-01	6, 52E-01
1, 48E-01	1, 24E-01	8, 39E-02	7, 66E-02	7, 13E-01	7, 04E-01	6, 75E-01	6, 62E-01
1, 45E-01	1, 14E-01	8, 20E-02	8, 03E-02	7, 17E-01	6, 96E-01	6, 77E-01	6, 63E-01
1, 49E-01	1, 24E-01	8, 93E-02	7, 69E-02	7, 13E-01	6, 94E-01	6, 77E-01	6, 62E-01
1, 43E-01	1, 17E-01	8, 16E-02	7, 74E-02	7, 27E-01	6, 99E-01	6, 82E-01	6, 63E-01
1, 46E-01	1, 32E-01	8, 96E-02	8, 31E-02	7, 20E-01	6, 97E-01	6, 66E-01	6, 64E-01
1, 48E-01	1, 17E-01	9, 19E-02	8, 09E-02	7, 14E-01	6, 96E-01	6, 78E-01	6, 61E-01
1, 40E-01	1, 20E-01	8, 11E-02	7, 61E-02	7, 16E-01	6, 89E-01	6, 67E-01	6, 66E-01
1, 34E-01	1, 13E-01	8, 90E-02	7, 86E-02	7, 23E-01	6, 92E-01	6, 80E-01	6, 61E-01
1, 32E-01	1, 19E-01	8, 88E-02	7, 59E-02	7, 08E-01	6, 96E-01	6, 66E-01	6, 53E-01
1, 30E-01	1, 20E-01	9, 21E-02	7, 83E-02	7, 16E-01	6, 94E-01	6, 67E-01	6, 58E-01
1, 36E-01	1, 14E-01	9, 17E-02	7, 55E-02	7, 12E-01	6, 97E-01	6, 69E-01	6, 60E-01
1, 29E-01	1, 15E-01	8, 93E-02	7, 49E-02	7, 16E-01	6, 98E-01	6, 77E-01	6, 65E-01
1, 36E-01	1, 15E-01	9, 56E-02	7, 81E-02	7, 11E-01	6, 97E-01	6, 61E-01	6, 60E-01
1, 40E-01	1, 16E-01	8, 17E-02	7, 10E-02	7, 05E-01	6, 96E-01	6, 75E-01	6, 61E-01
1, 36E-01	1, 19E-01	9, 17E-02	8, 45E-02	7, 23E-01	6, 99E-01	6, 56E-01	6, 49E-01
1, 30E-01	1, 13E-01	9, 19E-02	7, 76E-02	7, 17E-01	6, 95E-01	6, 78E-01	6, 60E-01
1, 35E-01	1, 04E-01	9, 20E-02	7, 87E-02	7, 02E-01	6, 91E-01	6, 76E-01	6, 59E-01
1, 35E-01	1, 22E-01	8, 55E-02	7, 16E-02	7, 17E-01	6, 97E-01	6, 71E-01	6, 58E-01
1, 32E-01	1, 17E-01	8, 78E-02	7, 84E-02	7, 17E-01	6, 94E-01	6, 51E-01	6, 64E-01
1, 29E-01	1, 16E-01	9, 73E-02	7, 66E-02	7, 13E-01	6, 94E-01	6, 72E-01	6, 61E-01
1, 26E-01	1, 21E-01	9, 19E-02	7, 56E-02	7, 09E-01	6, 99E-01	6, 63E-01	6, 60E-01
1, 25E-01	1, 16E-01	8, 07E-02	7, 48E-02	7, 15E-01	6, 92E-01	6, 70E-01	6, 66E-01
1, 31E-01	1, 13E-01	8, 67E-02	7, 67E-02	7, 15E-01	6, 94E-01	6, 55E-01	6, 60E-01
1, 33E-01	1, 15E-01	8, 71E-02	7, 10E-02	7, 16E-01	6, 94E-01	6, 67E-01	6, 59E-01
1, 32E-01	1, 15E-01	8, 82E-02	8, 29E-02	7, 13E-01	6, 93E-01	6, 62E-01	6, 54E-01
1, 29E-01	1, 13E-01	9, 01E-02	7, 63E-02	7, 17E-01	6, 94E-01	6, 75E-01	6, 63E-01

1, 24E-01	1, 10E-01	9, 06E-02	7, 73E-02	7, 20E-01	6, 97E-01	6, 60E-01	6, 62E-01
1, 31E-01	1, 18E-01	8, 95E-02	7, 88E-02	7, 21E-01	6, 93E-01	6, 71E-01	6, 59E-01
1, 21E-01	1, 12E-01	9, 09E-02	7, 82E-02	7, 15E-01	6, 99E-01	6, 82E-01	6, 57E-01
1, 21E-01	1, 12E-01	8, 86E-02	6, 87E-02	7, 17E-01	6, 90E-01	6, 81E-01	6, 59E-01
1, 24E-01	1, 16E-01	8, 48E-02	6, 68E-02	7, 10E-01	6, 93E-01	6, 77E-01	6, 57E-01
1, 22E-01	1, 16E-01	8, 36E-02	7, 63E-02	7, 12E-01	7, 01E-01	6, 69E-01	6, 53E-01
1, 24E-01	1, 17E-01	8, 99E-02	7, 53E-02	7, 13E-01	6, 93E-01	6, 73E-01	6, 65E-01
1, 27E-01	1, 11E-01	8, 94E-02	6, 92E-02	7, 03E-01	6, 81E-01	6, 69E-01	6, 61E-01
1, 23E-01	1, 14E-01	7, 98E-02	7, 69E-02	7, 09E-01	6, 96E-01	6, 67E-01	6, 66E-01
1, 21E-01	1, 12E-01	8, 94E-02	7, 91E-02	7, 12E-01	6, 95E-01	6, 59E-01	6, 51E-01
1, 16E-01	1, 15E-01	8, 64E-02	7, 65E-02	7, 09E-01	6, 94E-01	6, 72E-01	6, 59E-01
1, 18E-01	1, 13E-01	8, 41E-02	7, 48E-02	7, 07E-01	6, 95E-01	6, 67E-01	6, 57E-01
1, 26E-01	1, 14E-01	8, 61E-02	8, 11E-02	7, 05E-01	6, 93E-01	6, 67E-01	6, 62E-01
1, 24E-01	1, 09E-01	8, 90E-02	7, 66E-02	7, 13E-01	6, 88E-01	6, 60E-01	6, 58E-01
1, 18E-01	1, 06E-01	8, 49E-02	7, 85E-02	7, 11E-01	7, 02E-01	6, 65E-01	6, 75E-01
1, 21E-01	1, 12E-01	8, 79E-02	7, 54E-02	7, 10E-01	6, 91E-01	6, 75E-01	6, 61E-01
1, 16E-01	1, 11E-01	8, 13E-02	7, 62E-02	7, 06E-01	6, 95E-01	6, 66E-01	6, 61E-01
1, 24E-01	1, 03E-01	9, 09E-02	7, 54E-02	7, 12E-01	6, 96E-01	6, 69E-01	6, 53E-01
1, 16E-01	1, 08E-01	8, 55E-02	7, 11E-02	7, 08E-01	6, 92E-01	6, 66E-01	6, 58E-01
1, 21E-01	1, 07E-01	7, 86E-02	7, 63E-02	7, 01E-01	6, 91E-01	6, 67E-01	6, 51E-01
1, 18E-01	1, 06E-01	8, 11E-02	8, 03E-02	7, 12E-01	6, 94E-01	6, 76E-01	6, 54E-01
1, 17E-01	1, 10E-01	7, 84E-02	7, 66E-02	7, 01E-01	6, 91E-01	6, 63E-01	6, 57E-01
1, 17E-01	1, 10E-01	8, 32E-02	6, 99E-02	7, 12E-01	6, 92E-01	6, 77E-01	6, 54E-01
1, 16E-01	1, 09E-01	8, 31E-02	7, 52E-02	7, 14E-01	6, 88E-01	6, 67E-01	6, 51E-01
1, 13E-01	1, 10E-01	9, 25E-02	7, 05E-02	7, 03E-01	6, 90E-01	6, 84E-01	6, 46E-01
1, 19E-01	1, 15E-01	8, 59E-02	7, 18E-02	7, 04E-01	6, 91E-01	6, 76E-01	6, 56E-01
1, 23E-01	1, 09E-01	8, 53E-02	7, 91E-02	7, 02E-01	6, 98E-01	6, 65E-01	6, 53E-01
1, 17E-01	1, 09E-01	8, 20E-02	7, 76E-02	7, 12E-01	6, 90E-01	6, 91E-01	6, 56E-01
1, 30E-01	1, 05E-01	8, 38E-02	7, 14E-02	7, 12E-01	6, 96E-01	6, 75E-01	6, 50E-01
1, 21E-01	1, 10E-01	8, 39E-02	7, 26E-02	7, 11E-01	6, 96E-01	6, 71E-01	6, 35E-01
1, 15E-01	1, 08E-01	8, 07E-02	7, 18E-02	7, 07E-01	6, 92E-01	6, 69E-01	6, 52E-01
1, 17E-01	1, 01E-01	8, 47E-02	7, 24E-02	7, 09E-01	6, 88E-01	6, 66E-01	6, 47E-01
1, 12E-01	1, 01E-01	8, 60E-02	7, 66E-02	7, 08E-01	6, 87E-01	6, 75E-01	6, 53E-01
1, 13E-01	1, 03E-01	9, 21E-02	7, 05E-02	7, 07E-01	6, 92E-01	6, 65E-01	6, 51E-01
1, 13E-01	1, 12E-01	8, 58E-02	7, 50E-02	7, 04E-01	6, 82E-01	6, 76E-01	6, 47E-01
1, 15E-01	1, 04E-01	8, 11E-02	7, 57E-02	7, 08E-01	6, 88E-01	6, 66E-01	6, 45E-01

1, 23E-01	1, 12E-01	8, 40E-02	6, 73E-02	7, 01E-01	6, 84E-01	6, 67E-01	6, 54E-01
1, 18E-01	1, 01E-01	8, 48E-02	7, 67E-02	7, 01E-01	6, 93E-01	6, 63E-01	6, 49E-01
1, 15E-01	1, 18E-01	8, 50E-02	7, 50E-02	7, 03E-01	6, 90E-01	6, 74E-01	6, 48E-01
1, 23E-01	1, 02E-01	8, 13E-02	8, 14E-02	7, 04E-01	6, 87E-01	6, 62E-01	6, 63E-01
1, 22E-01	9, 96E-02	8, 13E-02	7, 41E-02	7, 03E-01	6, 86E-01	6, 70E-01	6, 55E-01
1, 08E-01	1, 08E-01	8, 06E-02	7, 46E-02	6, 97E-01	6, 89E-01	6, 59E-01	6, 51E-01
1, 18E-01	1, 03E-01	9, 24E-02	7, 58E-02	7, 00E-01	6, 90E-01	6, 73E-01	6, 46E-01
1, 19E-01	1, 00E-01	7, 92E-02	7, 84E-02	6, 96E-01	6, 91E-01	6, 63E-01	6, 54E-01
1, 14E-01	1, 07E-01	8, 99E-02	7, 09E-02	7, 01E-01	6, 87E-01	6, 85E-01	6, 73E-01
1, 10E-01	1, 00E-01	8, 26E-02	7, 33E-02	7, 00E-01	6, 89E-01	6, 72E-01	6, 51E-01
1, 15E-01	1, 03E-01	8, 38E-02	7, 38E-02	7, 00E-01	6, 81E-01	6, 88E-01	6, 55E-01
1, 07E-01	1, 11E-01	8, 40E-02	8, 01E-02	6, 98E-01	6, 90E-01	6, 72E-01	6, 56E-01
1, 17E-01	1, 13E-01	8, 44E-02	8, 10E-02	6, 95E-01	6, 90E-01	6, 86E-01	6, 68E-01
1, 14E-01	1, 04E-01	9, 55E-02	7, 66E-02	6, 98E-01	6, 82E-01	6, 74E-01	6, 58E-01
1, 08E-01	1, 03E-01	8, 59E-02	7, 91E-02	6, 92E-01	6, 79E-01	6, 77E-01	6, 55E-01
1, 16E-01	1, 17E-01	8, 18E-02	7, 54E-02	7, 02E-01	6, 86E-01	6, 75E-01	6, 53E-01
1, 17E-01	1, 06E-01	8, 64E-02	7, 86E-02	7, 01E-01	6, 89E-01	6, 72E-01	6, 61E-01
1, 11E-01	1, 11E-01	8, 18E-02	8, 10E-02	7, 01E-01	6, 84E-01	6, 79E-01	6, 53E-01
1, 16E-01	1, 02E-01	9, 24E-02	8, 22E-02	6, 89E-01	6, 94E-01	6, 75E-01	6, 51E-01
1, 11E-01	9, 64E-02	8, 50E-02	7, 22E-02	7, 07E-01	6, 80E-01	6, 66E-01	6, 53E-01
1, 09E-01	1, 13E-01	8, 58E-02	8, 27E-02	7, 04E-01	6, 84E-01	6, 73E-01	6, 57E-01
1, 14E-01	1, 01E-01	8, 97E-02	8, 04E-02	7, 05E-01	6, 84E-01	6, 63E-01	6, 57E-01
1, 09E-01	1, 05E-01	8, 51E-02	8, 04E-02	6, 95E-01	6, 77E-01	6, 66E-01	6, 53E-01
1, 10E-01	1, 05E-01	7, 91E-02	7, 68E-02	6, 94E-01	6, 89E-01	6, 68E-01	6, 44E-01
1, 17E-01	1, 02E-01	8, 34E-02	7, 24E-02	6, 98E-01	6, 81E-01	6, 75E-01	6, 54E-01
1, 10E-01	1, 03E-01	7, 80E-02	7, 59E-02	7, 02E-01	6, 81E-01	6, 67E-01	6, 55E-01
1, 11E-01	1, 01E-01	8, 66E-02	6, 81E-02	6, 95E-01	6, 83E-01	6, 67E-01	6, 49E-01
1, 03E-01	1, 09E-01	8, 01E-02	7, 52E-02	6, 95E-01	6, 85E-01	6, 71E-01	6, 56E-01
1, 03E-01	9, 36E-02	7, 61E-02	7, 89E-02	6, 93E-01	6, 86E-01	6, 76E-01	6, 52E-01
1, 13E-01	1, 05E-01	8, 78E-02	7, 61E-02	6, 93E-01	6, 87E-01	6, 66E-01	6, 50E-01
1, 10E-01	9, 53E-02	7, 81E-02	7, 48E-02	6, 91E-01	6, 84E-01	6, 67E-01	6, 46E-01
1, 02E-01	9, 61E-02	8, 00E-02	7, 42E-02	6, 89E-01	6, 80E-01	6, 67E-01	6, 54E-01
1, 09E-01	9, 31E-02	8, 01E-02	7, 72E-02	6, 95E-01	6, 80E-01	6, 67E-01	6, 49E-01
1, 10E-01	1, 04E-01	7, 78E-02	7, 25E-02	6, 97E-01	6, 79E-01	6, 68E-01	6, 54E-01
1, 17E-01	9, 61E-02	9, 12E-02	7, 93E-02	6, 96E-01	6, 74E-01	6, 76E-01	6, 51E-01
1, 09E-01	1, 07E-01	8, 29E-02	7, 65E-02	7, 01E-01	6, 82E-01	6, 68E-01	6, 47E-01

8, 84E-02	1, 04E-01	8, 24E-02	7, 64E-02	6, 96E-01	6, 81E-01	6, 71E-01	6, 50E-01
1, 01E-01	9, 49E-02	8, 84E-02	7, 72E-02	6, 98E-01	6, 81E-01	6, 67E-01	6, 60E-01
1, 12E-01	1, 01E-01	8, 54E-02	7, 89E-02	6, 95E-01	6, 69E-01	6, 70E-01	6, 50E-01
1, 04E-01	1, 00E-01	8, 25E-02	8, 08E-02	6, 94E-01	6, 76E-01	6, 75E-01	6, 52E-01
1, 02E-01	9, 85E-02	9, 13E-02	7, 64E-02	6, 98E-01	6, 79E-01	6, 72E-01	6, 47E-01
1, 06E-01	8, 83E-02	8, 59E-02	7, 81E-02	6, 94E-01	6, 76E-01	6, 71E-01	6, 45E-01
1, 08E-01	1, 02E-01	9, 24E-02	8, 28E-02	7, 03E-01	6, 82E-01	6, 70E-01	6, 47E-01
1, 08E-01	1, 07E-01	8, 82E-02	7, 25E-02	7, 00E-01	6, 88E-01	6, 74E-01	6, 44E-01
1, 16E-01	1, 02E-01	7, 97E-02	7, 97E-02	6, 95E-01	6, 78E-01	6, 73E-01	6, 47E-01
1, 08E-01	1, 03E-01	8, 46E-02	8, 06E-02	7, 06E-01	6, 80E-01	6, 62E-01	6, 53E-01
1, 12E-01	1, 05E-01	8, 05E-02	8, 31E-02	7, 00E-01	6, 78E-01	6, 69E-01	6, 47E-01
1, 05E-01	9, 55E-02	8, 69E-02	6, 83E-02	7, 00E-01	6, 83E-01	6, 67E-01	6, 55E-01
1, 05E-01	9, 74E-02	8, 22E-02	7, 22E-02	6, 94E-01	6, 74E-01	6, 68E-01	6, 44E-01
1, 05E-01	1, 02E-01	8, 49E-02	7, 66E-02	6, 89E-01	6, 57E-01	6, 63E-01	6, 54E-01
1, 06E-01	9, 99E-02	8, 39E-02	7, 64E-02	6, 97E-01	6, 79E-01	6, 70E-01	6, 56E-01
1, 07E-01	1, 00E-01	7, 83E-02	7, 51E-02	6, 93E-01	6, 75E-01	6, 66E-01	6, 50E-01
1, 05E-01	1, 01E-01	8, 87E-02	7, 04E-02	6, 99E-01	6, 81E-01	6, 70E-01	6, 49E-01
1, 13E-01	9, 50E-02	7, 73E-02	7, 07E-02	6, 95E-01	6, 80E-01	6, 64E-01	6, 52E-01
1, 03E-01	1, 04E-01	8, 93E-02	7, 16E-02	6, 96E-01	6, 81E-01	6, 66E-01	6, 50E-01
1, 05E-01	1, 00E-01	9, 09E-02	7, 57E-02	6, 91E-01	6, 88E-01	6, 64E-01	6, 50E-01
1, 05E-01	1, 01E-01	7, 92E-02	7, 79E-02	6, 90E-01	6, 75E-01	6, 64E-01	6, 46E-01
1, 12E-01	1, 01E-01	7, 69E-02	7, 80E-02	6, 93E-01	6, 80E-01	6, 60E-01	6, 50E-01
1, 07E-01	1, 04E-01	8, 67E-02	7, 03E-02	7, 02E-01	6, 88E-01	6, 63E-01	6, 55E-01
1, 04E-01	1, 04E-01	8, 46E-02	7, 94E-02	6, 92E-01	6, 71E-01	6, 61E-01	6, 51E-01
1, 06E-01	1, 03E-01	8, 30E-02	7, 79E-02	6, 89E-01	6, 79E-01	6, 65E-01	6, 53E-01
1, 08E-01	9, 36E-02	8, 76E-02	6, 93E-02	6, 90E-01	6, 75E-01	6, 68E-01	6, 55E-01
9, 90E-02	9, 18E-02	7, 71E-02	6, 82E-02	6, 96E-01	6, 84E-01	6, 72E-01	6, 57E-01
1, 04E-01	1, 01E-01	8, 74E-02	7, 89E-02	6, 86E-01	6, 81E-01	6, 65E-01	6, 55E-01
1, 01E-01	9, 69E-02	8, 04E-02	7, 25E-02	6, 95E-01	6, 77E-01	6, 59E-01	6, 60E-01
1, 03E-01	9, 47E-02	8, 49E-02	7, 73E-02	6, 90E-01	6, 84E-01	6, 62E-01	6, 60E-01
1, 08E-01	1, 05E-01	8, 07E-02	6, 97E-02	6, 89E-01	6, 82E-01	6, 64E-01	6, 55E-01
9, 89E-02	1, 06E-01	8, 38E-02	7, 76E-02	6, 92E-01	6, 77E-01	6, 64E-01	6, 54E-01
1, 10E-01	9, 99E-02	8, 44E-02	7, 51E-02	6, 82E-01	6, 86E-01	6, 60E-01	6, 45E-01
9, 81E-02	1, 04E-01	8, 28E-02	7, 33E-02	6, 92E-01	6, 80E-01	6, 67E-01	6, 56E-01
1, 04E-01	1, 01E-01	7, 59E-02	7, 39E-02	6, 88E-01	6, 79E-01	6, 65E-01	6, 54E-01
9, 62E-02	9, 63E-02	7, 68E-02	6, 43E-02	6, 92E-01	6, 89E-01	6, 59E-01	6, 49E-01

1, 00E-01	9, 91E-02	8, 57E-02	7, 42E-02	6, 91E-01	6, 81E-01	6, 58E-01	6, 55E-01
1, 08E-01	9, 31E-02	8, 42E-02	7, 09E-02	6, 95E-01	6, 80E-01	6, 67E-01	6, 61E-01
1, 03E-01	1, 04E-01	8, 23E-02	7, 33E-02	6, 88E-01	6, 78E-01	6, 67E-01	6, 50E-01
1, 09E-01	1, 06E-01	7, 68E-02	7, 39E-02	6, 88E-01	6, 85E-01	6, 62E-01	6, 58E-01
9, 78E-02	9, 91E-02	7, 28E-02	7, 91E-02	6, 90E-01	6, 73E-01	6, 60E-01	6, 52E-01
1, 04E-01	9, 86E-02	7, 63E-02	7, 59E-02	6, 86E-01	6, 82E-01	6, 66E-01	6, 53E-01
1, 05E-01	9, 47E-02	8, 59E-02	7, 36E-02	6, 90E-01	6, 73E-01	6, 62E-01	6, 52E-01
9, 88E-02	8, 99E-02	7, 83E-02	7, 26E-02	6, 89E-01	6, 81E-01	6, 64E-01	6, 54E-01
1, 06E-01	9, 93E-02	7, 63E-02	7, 33E-02	6, 92E-01	6, 82E-01	6, 61E-01	6, 53E-01
1, 02E-01	9, 56E-02	8, 47E-02	8, 17E-02	6, 89E-01	6, 80E-01	6, 73E-01	6, 57E-01
1, 05E-01	1, 04E-01	8, 56E-02	7, 46E-02	6, 78E-01	6, 84E-01	6, 60E-01	6, 55E-01
9, 98E-02	9, 58E-02	8, 55E-02	7, 01E-02	6, 89E-01	6, 80E-01	6, 67E-01	6, 57E-01
1, 07E-01	9, 32E-02	8, 26E-02	7, 24E-02	6, 84E-01	6, 81E-01	6, 60E-01	6, 54E-01
1, 10E-01	9, 34E-02	8, 03E-02	7, 86E-02	6, 81E-01	6, 86E-01	6, 71E-01	6, 59E-01
1, 03E-01	9, 89E-02	8, 64E-02	8, 18E-02	6, 90E-01	6, 87E-01	6, 61E-01	6, 59E-01
1, 03E-01	9, 55E-02	7, 71E-02	7, 03E-02	6, 94E-01	6, 79E-01	6, 65E-01	6, 48E-01
1, 02E-01	9, 44E-02	7, 75E-02	7, 73E-02	7, 03E-01	6, 86E-01	6, 59E-01	6, 52E-01
1, 04E-01	9, 54E-02	8, 18E-02	7, 74E-02	6, 89E-01	6, 90E-01	6, 60E-01	6, 52E-01
1, 03E-01	1, 01E-01	8, 47E-02	7, 32E-02	7, 00E-01	6, 78E-01	6, 59E-01	6, 54E-01
9, 68E-02	9, 75E-02	7, 88E-02	7, 46E-02	6, 90E-01	6, 86E-01	6, 62E-01	6, 52E-01
1, 07E-01	9, 59E-02	7, 93E-02	7, 36E-02	6, 87E-01	6, 95E-01	6, 61E-01	6, 47E-01
1, 05E-01	9, 70E-02	8, 20E-02	7, 94E-02	6, 94E-01	6, 92E-01	6, 58E-01	6, 48E-01
1, 01E-01	9, 68E-02	8, 64E-02	6, 97E-02	6, 91E-01	6, 80E-01	6, 70E-01	6, 59E-01
9, 81E-02	9, 37E-02	7, 72E-02	7, 51E-02	6, 90E-01	6, 77E-01	6, 64E-01	6, 51E-01
9, 94E-02	9, 89E-02	8, 71E-02	7, 61E-02	6, 88E-01	6, 84E-01	6, 62E-01	6, 51E-01
1, 06E-01	9, 78E-02	8, 55E-02	7, 43E-02	6, 91E-01	6, 79E-01	6, 61E-01	6, 52E-01
1, 01E-01	1, 02E-01	8, 08E-02	7, 81E-02	6, 83E-01	6, 73E-01	6, 61E-01	6, 48E-01
1, 05E-01	9, 45E-02	7, 72E-02	7, 53E-02	6, 77E-01	6, 76E-01	6, 62E-01	6, 47E-01
1, 02E-01	9, 79E-02	7, 66E-02	7, 74E-02	6, 86E-01	6, 80E-01	6, 63E-01	6, 45E-01
1, 02E-01	9, 78E-02	7, 97E-02	7, 48E-02	6, 71E-01	6, 86E-01	6, 60E-01	6, 52E-01
1, 03E-01	9, 55E-02	7, 60E-02	7, 56E-02	6, 88E-01	6, 88E-01	6, 62E-01	6, 54E-01
1, 02E-01	9, 16E-02	8, 18E-02	7, 58E-02	6, 94E-01	6, 81E-01	6, 61E-01	6, 50E-01
1, 09E-01	9, 77E-02	8, 46E-02	7, 44E-02	6, 82E-01	6, 78E-01	6, 74E-01	6, 53E-01
1, 26E-01	9, 26E-02	7, 82E-02	7, 43E-02	6, 99E-01	6, 86E-01	6, 62E-01	6, 54E-01
1, 48E-01	9, 11E-02	6, 06E-02	7, 36E-02	6, 91E-01	6, 89E-01	6, 64E-01	6, 56E-01
1, 69E-01	8, 29E-02	7, 96E-02	7, 09E-02	6, 91E-01	6, 77E-01	6, 63E-01	6, 53E-01

1, 92E-01	9, 03E-02	8, 84E-02	7, 30E-02	6, 85E-01	6, 85E-01	6, 61E-01	6, 54E-01
1, 95E-01	9, 14E-02	7, 98E-02	7, 48E-02	6, 82E-01	6, 79E-01	6, 62E-01	6, 49E-01
1, 91E-01	9, 54E-02	8, 59E-02	8, 27E-02	6, 84E-01	6, 88E-01	6, 59E-01	6, 45E-01
1, 90E-01	9, 33E-02	8, 53E-02	5, 99E-02	6, 84E-01	6, 81E-01	6, 60E-01	6, 55E-01
1, 85E-01	9, 16E-02	8, 14E-02	7, 36E-02	6, 80E-01	6, 72E-01	6, 34E-01	6, 46E-01
1, 89E-01	8, 74E-02	8, 17E-02	6, 97E-02	6, 88E-01	6, 73E-01	6, 61E-01	6, 38E-01
1, 88E-01	8, 88E-02	7, 79E-02	7, 41E-02	6, 81E-01	6, 83E-01	6, 59E-01	6, 51E-01
1, 89E-01	1, 03E-01	8, 71E-02	7, 66E-02	6, 84E-01	6, 79E-01	6, 58E-01	6, 59E-01
1, 86E-01	8, 91E-02	8, 71E-02	7, 29E-02	6, 92E-01	6, 85E-01	6, 44E-01	6, 47E-01
1, 83E-01	9, 69E-02	8, 50E-02	7, 13E-02	6, 83E-01	6, 73E-01	6, 59E-01	6, 73E-01
1, 77E-01	8, 98E-02	7, 83E-02	7, 07E-02	6, 81E-01	6, 81E-01	6, 59E-01	6, 47E-01
1, 78E-01	9, 83E-02	8, 74E-02	7, 18E-02	6, 80E-01	6, 77E-01	6, 62E-01	6, 55E-01
1, 76E-01	9, 02E-02	8, 10E-02	6, 54E-02	6, 83E-01	6, 72E-01	6, 59E-01	6, 54E-01
1, 75E-01	9, 29E-02	7, 96E-02	6, 64E-02	6, 92E-01	6, 73E-01	6, 55E-01	6, 46E-01
1, 72E-01	9, 24E-02	7, 74E-02	6, 98E-02	6, 84E-01	6, 78E-01	6, 58E-01	6, 50E-01
1, 68E-01	9, 88E-02	7, 99E-02	6, 82E-02	6, 75E-01	6, 78E-01	6, 62E-01	6, 43E-01
1, 68E-01	8, 71E-02	8, 01E-02	6, 80E-02	6, 84E-01	6, 75E-01	6, 57E-01	6, 54E-01
1, 68E-01	9, 19E-02	7, 96E-02	7, 31E-02	6, 78E-01	6, 78E-01	6, 57E-01	6, 51E-01
1, 60E-01	8, 25E-02	8, 13E-02	7, 81E-02	6, 81E-01	6, 77E-01	6, 57E-01	6, 54E-01
1, 69E-01	9, 55E-02	8, 10E-02	7, 41E-02	6, 79E-01	6, 83E-01	6, 59E-01	6, 44E-01
1, 58E-01	9, 89E-02	8, 18E-02	8, 00E-02	6, 92E-01	6, 75E-01	6, 63E-01	6, 54E-01
1, 64E-01	9, 31E-02	1, 00E-01	7, 09E-02	6, 71E-01	6, 76E-01	6, 57E-01	6, 53E-01
1, 60E-01	8, 19E-02	5, 49E-02	7, 17E-02	6, 80E-01	6, 72E-01	6, 61E-01	6, 43E-01
1, 67E-01	8, 84E-02	8, 16E-02	7, 41E-02	6, 91E-01	6, 74E-01	6, 61E-01	6, 49E-01
1, 57E-01	8, 47E-02	8, 03E-02	7, 69E-02	6, 85E-01	6, 78E-01	6, 61E-01	6, 47E-01
1, 62E-01	9, 46E-02	7, 73E-02	6, 79E-02	6, 85E-01	6, 72E-01	6, 54E-01	6, 37E-01
1, 57E-01	8, 99E-02	8, 05E-02	7, 31E-02	6, 86E-01	6, 75E-01	6, 59E-01	6, 52E-01
1, 53E-01	9, 25E-02	6, 16E-02	7, 41E-02	6, 81E-01	6, 74E-01	6, 59E-01	6, 50E-01
1, 62E-01	8, 86E-02	8, 06E-02	7, 70E-02	6, 78E-01	6, 78E-01	6, 60E-01	6, 57E-01

1, 51E-01	1, 01E-01	7, 93E-02	7, 91E-02	6, 81E-01	6, 77E-01	6, 62E-01	6, 59E-01
1, 46E-01	8, 68E-02	7, 68E-02	6, 60E-02	6, 82E-01	6, 83E-01	6, 61E-01	6, 49E-01
1, 56E-01	9, 63E-02	8, 14E-02	6, 86E-02	6, 78E-01	6, 75E-01	6, 57E-01	6, 49E-01
1, 45E-01	9, 82E-02	8, 13E-02	7, 15E-02	6, 93E-01	6, 73E-01	6, 62E-01	6, 50E-01
1, 48E-01	8, 97E-02	8, 01E-02	6, 91E-02	6, 93E-01	6, 74E-01	6, 60E-01	6, 48E-01
1, 46E-01	9, 36E-02	7, 55E-02	7, 10E-02	7, 04E-01	6, 73E-01	6, 63E-01	6, 45E-01
1, 44E-01	9, 06E-02	8, 69E-02	7, 58E-02	7, 04E-01	6, 78E-01	6, 70E-01	6, 45E-01
1, 49E-01	9, 66E-02	8, 19E-02	6, 90E-02	7, 13E-01	6, 78E-01	6, 53E-01	6, 47E-01
1, 52E-01	9, 54E-02	8, 12E-02	8, 31E-02	7, 11E-01	6, 77E-01	6, 55E-01	6, 34E-01
1, 43E-01	9, 59E-02	7, 31E-02	6, 73E-02	7, 09E-01	6, 72E-01	6, 57E-01	6, 53E-01

A.2. Output frequency variation, SS case

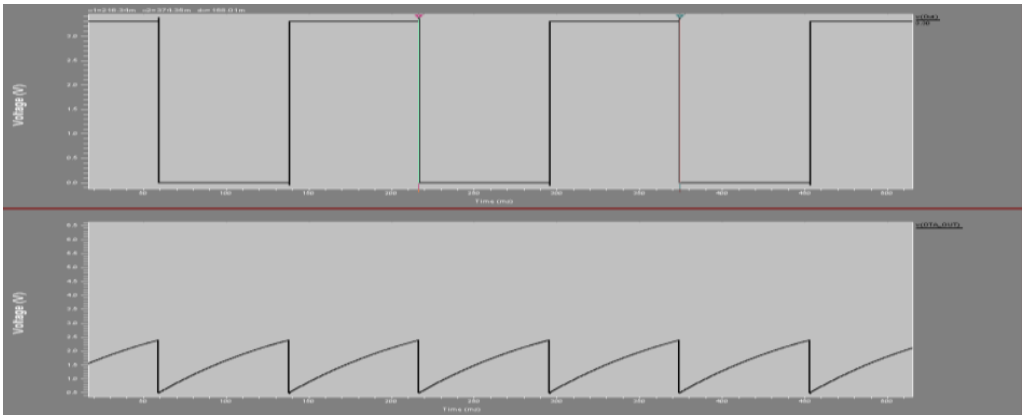

A. 3. Output frequency variation, TT case

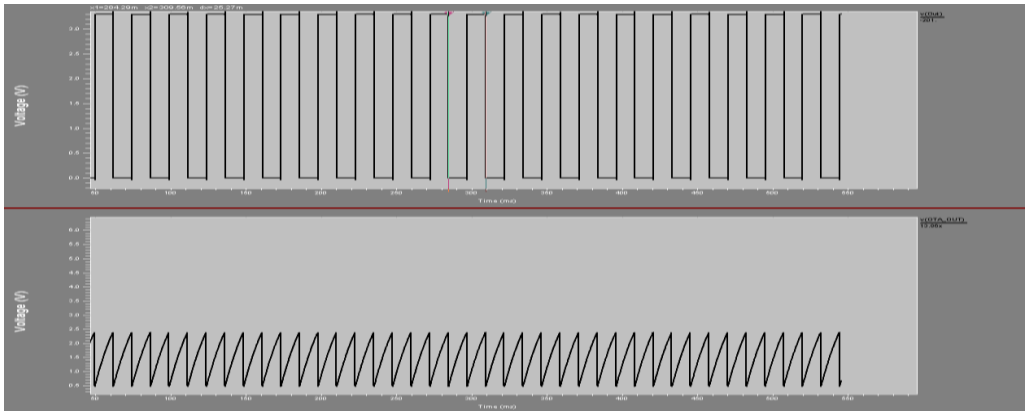

A.4. Output frequency variation, FF case

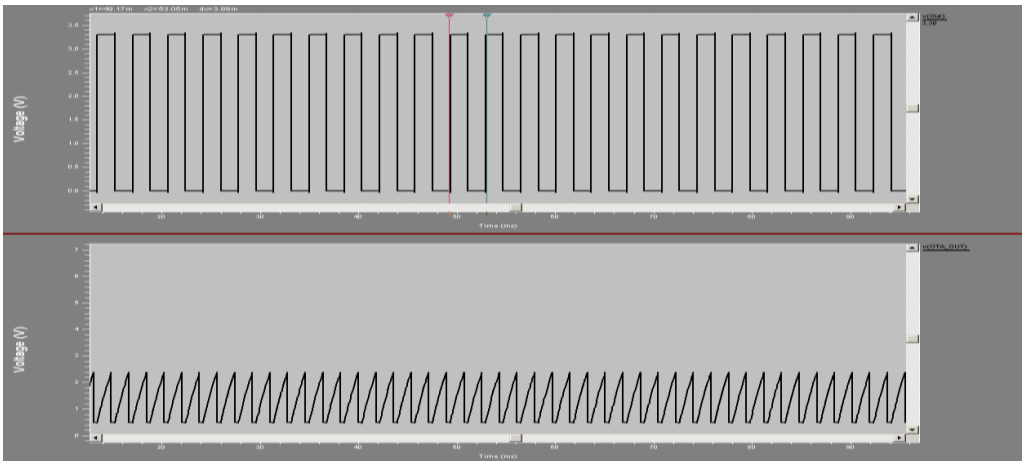

A.5. Output frequency variation, SF case

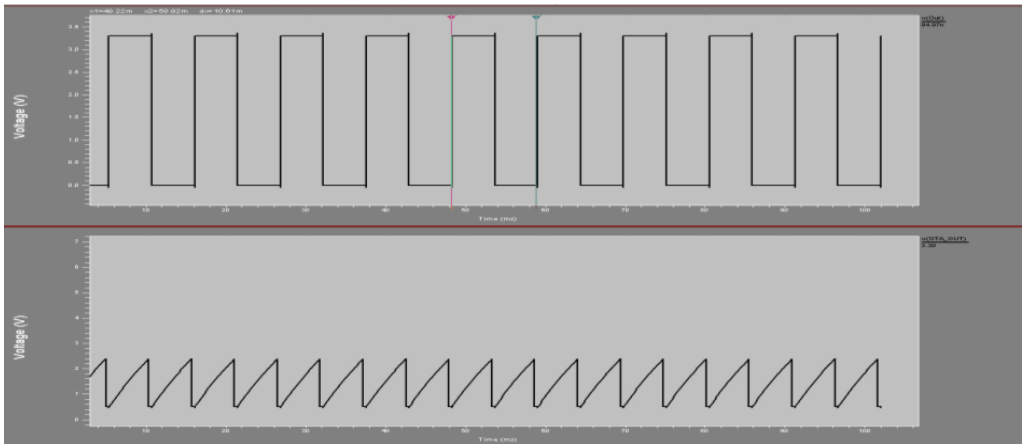

A.6. Output frequency variation, FS case.

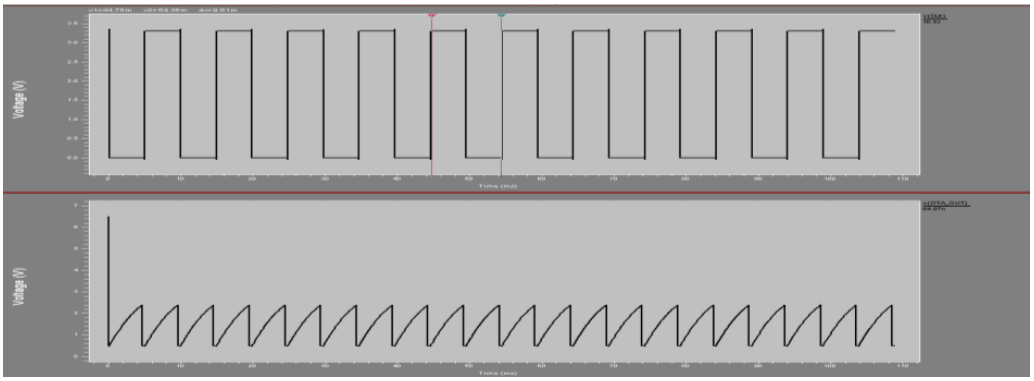

A.7. Output frequency for 1nA input current

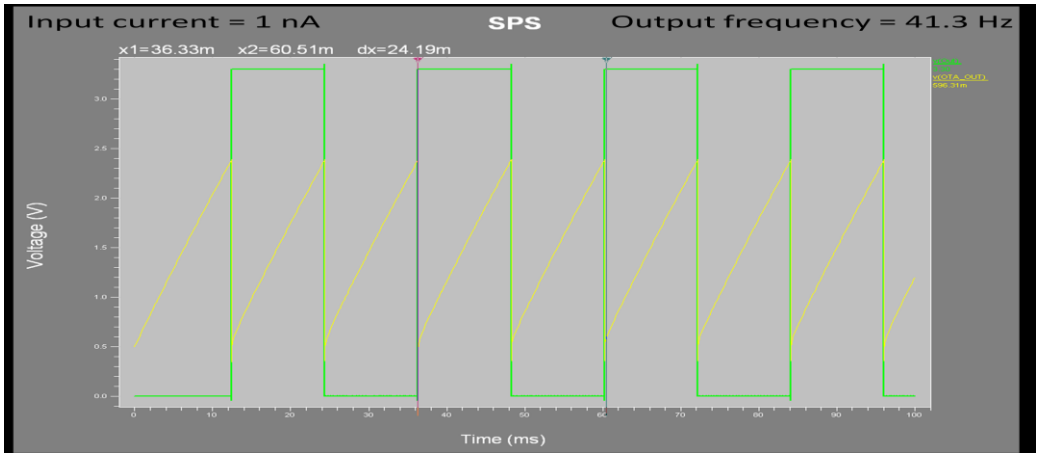

A.8. Output frequency for 10 nA input current

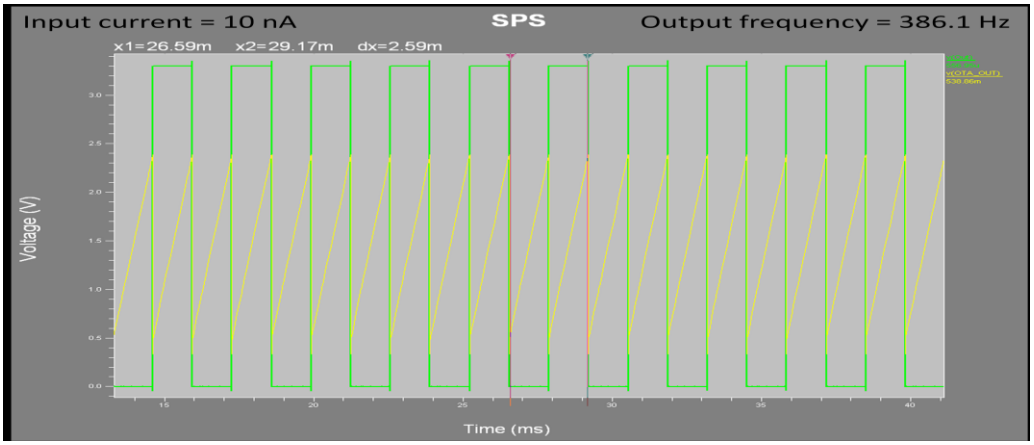

A.9. Output frequency for 100 nA input current

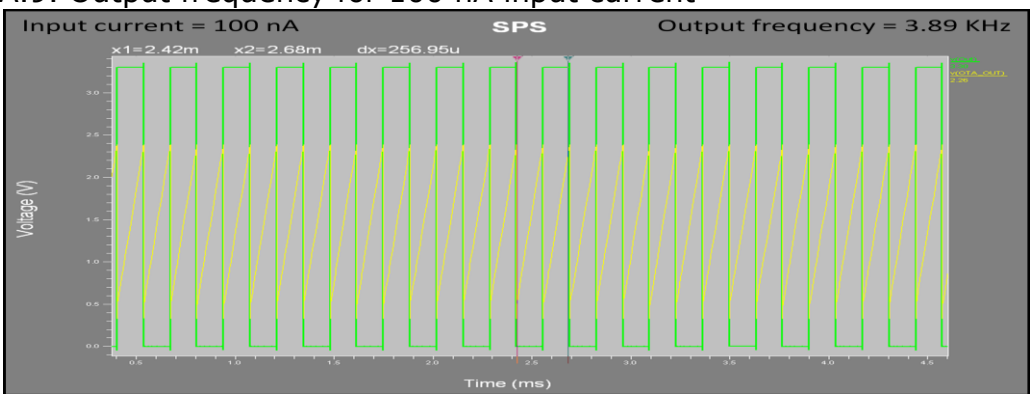

A.10. Output frequency for 1 uA input current

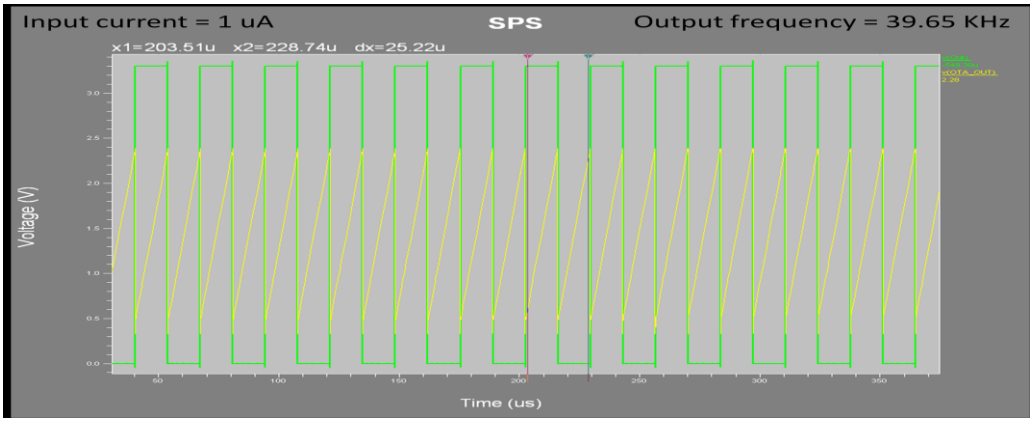

A.11. Output frequency for 10 uA input current

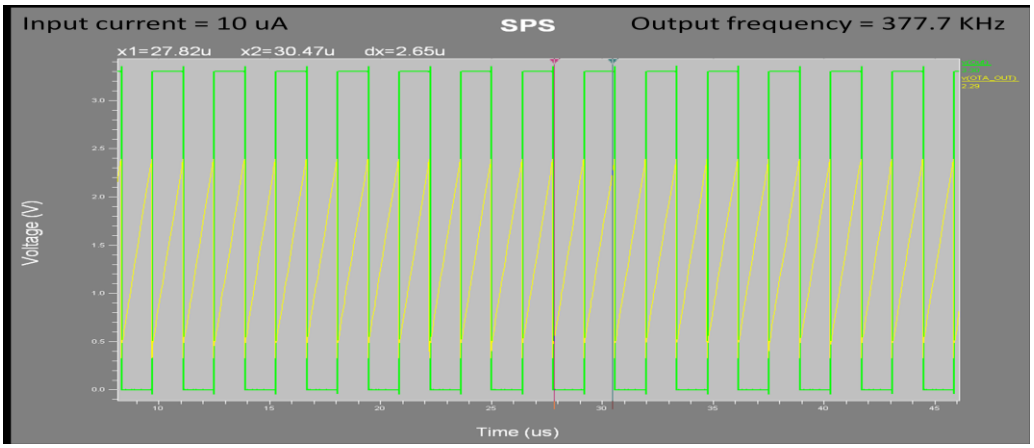

A.12. Output frequency for 100 uA input current

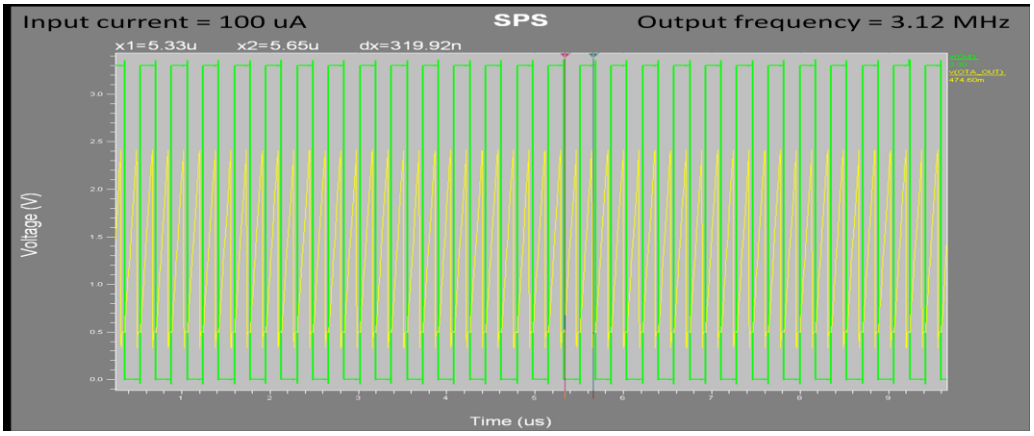

A.13. OTA parameters

MPMOS_1 N_4 InP N_7 Vdd PMOS W=380u L=2.4u AS=360p PS=801.8u AD=360p PD=801.8u
MPMOS_2 N_3 InN N_7 Vdd PMOS W=380u L=2.4u AS=360p PS=801.8u AD=360p PD=801.8u
MPMOS_3 N_7 BIAS1 Vdd Vdd PMOS W=226u L=4u AS=230.4p PS=513.8u AD=230.4p PD=513.8u
MPMOS_6 Out N_5 Vdd Vdd PMOS W=80u L=1.2u AS=81p PS=181.8u AD=81p PD=181.8u
MPMOS_7 N_5 N_5 Vdd Vdd PMOS W=80u L=1.2u AS=81p PS=181.8u AD=81p PD=181.8u
MPMOS_8 N_2 N_4 N_6 Vdd PMOS W=29u L=250n AS=26.1p PS=59.8u AD=26.1p PD=59.8u
MPMOS_9 N_1 N_3 N_6 Vdd PMOS W=29u L=250n AS=26.1p PS=59.8u AD=26.1p PD=59.8u

```
MNMOS_2 N_5 N_2 N_4 Gnd NMOS W=8u L=1u AS=7.2p PS=17.8u AD=7.2p
                                                    PD=17.8u
MNMOS_3 N_4 BIAS3 Gnd Gnd NMOS W=2300u L=14u AS=225p PS=501.8u
                                                    AD=225p PD=501.8u
MNMOS_4 N_3 BIAS3 Gnd Gnd NMOS W=2300u L=14u AS=225p PS=501.8u
                                                    AD=225p PD=501.8u
MNMOS_5 N_2 BIAS2 Gnd Gnd NMOS W=10u L=250n AS=9p PS=21.8u AD=9p
                                                    PD=21.8u
MNMOS_6 N_1 BIAS2 Gnd Gnd NMOS W=10u L=250n AS=9p PS=21.8u AD=9p
                                                    PD=21.8u
MNMOS_7 Out N_1 N_3 Gnd NMOS W=8u L=1u AS=7.2p PS=17.8u AD=7.2p
                                                    PD=17.8u
MPMOS_10 N_6 BIAS1 Vdd Vdd PMOS W=65u L=250n AS=58.5p PS=131.8u
                                                    AD=58.5p PD=131.8u
```

A.14. COMPARATOR parameters

```
MNMOS_3 N_2 BIAS Gnd Gnd NMOS W=7.5u L=250n AS=6.75p PS=16.8u
                                                    AD=6.75p PD=16.8u
MNMOS_4 N_4 N_4 Gnd Gnd NMOS W=2.5u L=250n AS=2.25p PS=6.8u AD=2.25p
                                                    PD=6.8u
MNMOS_5 N_1 N_4 Gnd Gnd NMOS W=2.5u L=250n AS=2.25p PS=6.8u AD=2.25p
                                                    PD=6.8u
MNMOS_6 N_7 N_1 Gnd Gnd NMOS W=2.5u L=250n AS=2.25p PS=6.8u AD=2.25p
                                                    PD=6.8u
MNMOS_7 Out N_7 Gnd Gnd NMOS W=4.5u L=250n AS=4.05p PS=10.8u
                                                    AD=4.05p PD=10.8u
MPMOS_10 N_5 N_3 Vdd Vdd PMOS W=2.5u L=250n AS=2.25p PS=6.8u AD=2.25p
                                                    PD=6.8u
MPMOS_1 N_5 N_5 Vdd Vdd PMOS W=2.5u L=250n AS=2.25p PS=6.8u AD=2.25p
                                                    PD=6.8u
MPMOS_2 N_3 N_3 Vdd Vdd PMOS W=2.5u L=250n AS=2.25p PS=6.8u AD=2.25p
                                                    PD=6.8u
MPMOS_5 N_4 N_5 Vdd Vdd PMOS W=2.5u L=250n AS=2.25p PS=6.8u AD=2.25p
                                                    PD=6.8u
MPMOS_6 N_1 N_3 Vdd Vdd PMOS W=2.5u L=250n AS=2.25p PS=6.8u AD=2.25p
                                                    PD=6.8u
MPMOS_7 N_7 N_1 Vdd Vdd PMOS W=5u L=250n AS=4.5p PS=11.8u AD=4.5p
                                                    PD=11.8u
MPMOS_8 Out N_7 Vdd Vdd PMOS W=10u L=250n AS=9p PS=21.8u AD=9p
                                                    PD=21.8u
MPMOS_9 N_3 N_5 Vdd Vdd PMOS W=2.5u L=250n AS=2.25p PS=6.8u AD=2.25p
                                                    PD=6.8u
MNMOS_1 N_5 InP N_2 Gnd NMOS W=2.5u L=250n AS=2.25p PS=6.8u AD=2.25p
                                                    PD=6.8u
MNMOS_2 N_3 InN N_2 Gnd NMOS W=2.5u L=250n AS=2.25p PS=6.8u AD=2.25p
                                                    PD=6.8u
```

A.15. ONE-SHOT parameters

```
NAND_2/PMOS_1 NAND_2/N_2 N_4 Vdd Vdd PMOS W=2.5u L=250n AS=2.25p
                                                    PS=6.8u AD=2.25p
+PD=6.8u
MNAND_2/PMOS_2 NAND_2/N_2 N_3 Vdd Vdd PMOS W=2.5u L=250n AS=2.25p
                                                    PS=6.8u AD=2.25p
+PD=6.8u
MNAND_2/PMOS_3 NAND_2/N_3 NAND_2/N_2 Vdd Vdd PMOS W=2.5u L=250n
                                                    AS=2.25p PS=6.8u
+AD=2.25p PD=6.8u
MNAND_2/PMOS_4 N_1 NAND_2/N_3 Vdd Vdd PMOS W=2.5u L=250n AS=2.25p
                                                    PS=6.8u AD=2.25p
+PD=6.8u
MNAND_2/NMOS_1 NAND_2/N_1 N_3 Gnd Gnd NMOS W=2.5u L=250n AS=2.25p
                                                    PS=6.8u AD=2.25p
+PD=6.8u
MNAND_2/NMOS_2 NAND_2/N_2 N_4 NAND_2/N_1 Gnd NMOS W=2.5u L=250n
                                                    AS=2.25p PS=6.8u
+AD=2.25p PD=6.8u
MNAND_2/NMOS_3 NAND_2/N_3 NAND_2/N_2 Gnd Gnd NMOS W=2.5u L=250n
                                                    AS=2.25p PS=6.8u
+AD=2.25p PD=6.8u
MNAND_2/NMOS_4 N_1 NAND_2/N_3 Gnd Gnd NMOS W=2.5u L=250n AS=2.25p
                                                    PS=6.8u AD=2.25p
+PD=6.8u
MSCHMITT_TRIGGER_1/PMOS_1 SCHMITT_TRIGGER_1/N_1 N_5 Vdd Vdd PMOS
                                                    W=2.5u L=250n AS=2.25p
+PS=6.8u AD=2.25p PD=6.8u
MSCHMITT_TRIGGER_1/PMOS_2 N_4 N_5 SCHMITT_TRIGGER_1/N_1 Vdd PMOS
                                                    W=2.5u L=250n AS=2.25p
+PS=6.8u AD=2.25p PD=6.8u
MSCHMITT_TRIGGER_1/PMOS_3 Gnd N_4 SCHMITT_TRIGGER_1/N_1 Vdd PMOS
                                                    W=2.5u L=250n AS=2.25p
+PS=6.8u AD=2.25p PD=6.8u
MSCHMITT_TRIGGER_1/NMOS_1 N_4 N_5 SCHMITT_TRIGGER_1/N_2 Gnd NMOS
                                                    W=2.5u L=250n AS=2.25p
+PS=6.8u AD=2.25p PD=6.8u
MSCHMITT_TRIGGER_1/NMOS_2 SCHMITT_TRIGGER_1/N_2 N_5 Gnd Gnd NMOS
                                                    W=2.5u L=250n AS=2.25p
+PS=6.8u AD=2.25p PD=6.8u
MSCHMITT_TRIGGER_1/NMOS_3 Vdd N_4 SCHMITT_TRIGGER_1/N_2 Gnd NMOS
                                                    W=2.5u L=250n AS=2.25p
+PS=6.8u AD=2.25p PD=6.8u
MINV2_1/PMOS_1 Out N_1 Vdd Vdd PMOS W=5u L=250n AS=4.5p PS=11.8u
                                                    AD=4.5p PD=11.8u
MINV2_1/NMOS_1 Out N_1 Gnd Gnd NMOS W=2.5u L=250n AS=2.25p PS=6.8u
                                                    AD=2.25p PD=6.8u
MSW_1/INV_1/PMOS_1 SW_1/N_1 N_7 Vdd Vdd PMOS W=5u L=250n AS=4.5p
                                                    PS=11.8u AD=4.5p
+PD=11.8u
```

```
MSW_1/INV_1/NMOS_1 SW_1/N_1 N_7 Gnd Gnd NMOS W=2.5u L=250n AS=2.25p
                                                    PS=6.8u AD=2.25p
+PD=6.8u
MSW_1/PMOS_1 N_2 SW_1/N_1 N_6 Vdd PMOS W=2.5u L=250n AS=2.25p
                                                    PS=6.8u AD=2.25p
                                                    PD=6.8u
MSW_1/NMOS_1 N_2 N_7 N_6 Gnd NMOS W=2.5u L=250n AS=2.25p PS=6.8u
                                                    AD=2.25p PD=6.8u
MINV2_2/PMOS_1 N_7 SEL Vdd Vdd PMOS W=5u L=250n AS=4.5p PS=11.8u
                                                    AD=4.5p PD=11.8u
MINV2_2/NMOS_1 N_7 SEL Gnd Gnd NMOS W=2.5u L=250n AS=2.25p PS=6.8u
                                                    AD=2.25p PD=6.8u
MSW_2/INV_1/PMOS_1 SW_2/N_1 SEL Vdd Vdd PMOS W=5u L=250n AS=4.5p
                                                    PS=11.8u AD=4.5p
+PD=11.8u
MSW_2/INV_1/NMOS_1 SW_2/N_1 SEL Gnd Gnd NMOS W=2.5u L=250n AS=2.25p
                                                    PS=6.8u AD=2.25p
+PD=6.8u
MSW_2/PMOS_1 N_2 SW_2/N_1 In Vdd PMOS W=2.5u L=250n AS=2.25p PS=6.8u
                                                    AD=2.25p PD=6.8u
MSW_2/NMOS_1 N_2 SEL In Gnd NMOS W=2.5u L=250n AS=2.25p PS=6.8u
                                                    AD=2.25p PD=6.8u
MINV2_3/PMOS_1 N_6 In Vdd Vdd PMOS W=5u L=250n AS=4.5p PS=11.8u
                                                    AD=4.5p PD=11.8u
MINV2_3/NMOS_1 N_6 In Gnd Gnd NMOS W=2.5u L=250n AS=2.25p PS=6.8u
                                                    AD=2.25p PD=6.8u
MNAND_1/PMOS_1 NAND_1/N_2 N_1 Vdd Vdd PMOS W=2.5u L=250n AS=2.25p
                                                    PS=6.8u AD=2.25p
+PD=6.8u
MNAND_1/PMOS_2 NAND_1/N_2 N_2 Vdd Vdd PMOS W=2.5u L=250n AS=2.25p
                                                    PS=6.8u AD=2.25p
+PD=6.8u
MNAND_1/PMOS_3 NAND_1/N_3 NAND_1/N_2 Vdd Vdd PMOS W=2.5u L=250n
                                                    AS=2.25p PS=6.8u
+AD=2.25p PD=6.8u
MNAND_1/PMOS_4 N_3 NAND_1/N_3 Vdd Vdd PMOS W=2.5u L=250n AS=2.25p
                                                    PS=6.8u AD=2.25p
+PD=6.8u
MNAND_1/NMOS_1 NAND_1/N_1 N_2 Gnd Gnd NMOS W=2.5u L=250n AS=2.25p
                                                    PS=6.8u AD=2.25p
+PD=6.8u
MNAND_1/NMOS_2 NAND_1/N_2 N_1 NAND_1/N_1 Gnd NMOS W=2.5u L=250n
                                                    AS=2.25p PS=6.8u
+AD=2.25p PD=6.8u
MNAND_1/NMOS_3 NAND_1/N_3 NAND_1/N_2 Gnd Gnd NMOS W=2.5u L=250n
                                                    AS=2.25p PS=6.8u
+AD=2.25p PD=6.8u
MNAND_1/NMOS_4 N_3 NAND_1/N_3 Gnd Gnd NMOS W=2.5u L=250n AS=2.25p
                                                    PS=6.8u AD=2.25p
+PD=6.8u
```

```
MNMOS_1 N_5 N_1 Gnd Gnd NMOS W=15u L=250n AS=13.5p PS=31.8u AD=13.5p
                                                        PD=31.8u
CCapacitor_1 N_5 Gnd  1p
ICurrentSource_1 Vdd N_5  DC 50u
```

A.16. TFF parameters

```
MTG_1/INV_1/PMOS_1 TG_1/N_1 In Vdd Vdd PMOS W=5u L=250n AS=4.5p
                                                        PS=11.8u AD=4.5p
+PD=11.8u
MTG_1/INV_1/NMOS_1 TG_1/N_1 In Gnd Gnd NMOS W=2.5u L=250n AS=2.25p
                                                        PS=6.8u AD=2.25p
+PD=6.8u
MTG_1/PMOS_1 N_2 TG_1/N_1 N_1 Vdd PMOS W=2.5u L=250n AS=2.25p PS=6.8u
                                                        AD=2.25p PD=6.8u
MTG_1/NMOS_1 N_2 In N_1 Gnd NMOS W=2.5u L=250n AS=2.25p PS=6.8u
                                                        AD=2.25p PD=6.8u
MINV3_1/PMOS_1 N_3 N_2 Vdd Vdd PMOS W=5u L=250n AS=4.5p PS=11.8u
                                                        AD=4.5p PD=11.8u
MINV3_1/NMOS_1 N_3 N_2 Gnd Gnd NMOS W=2.5u L=250n AS=2.25p PS=6.8u
                                                        AD=2.25p PD=6.8u
MTG_2/INV_1/PMOS_1 TG_2/N_1 N_4 Vdd Vdd PMOS W=5u L=250n AS=4.5p
                                                        PS=11.8u AD=4.5p
+PD=11.8u
MTG_2/INV_1/NMOS_1 TG_2/N_1 N_4 Gnd Gnd NMOS W=2.5u L=250n AS=2.25p
                                                        PS=6.8u AD=2.25p
+PD=6.8u
MTG_2/PMOS_1 N_5 TG_2/N_1 N_3 Vdd PMOS W=2.5u L=250n AS=2.25p PS=6.8u
                                                        AD=2.25p PD=6.8u
MTG_2/NMOS_1 N_5 N_4 N_3 Gnd NMOS W=2.5u L=250n AS=2.25p PS=6.8u
                                                        AD=2.25p PD=6.8u
MINV3_2/PMOS_1 N_8 N_5 Vdd Vdd PMOS W=5u L=250n AS=4.5p PS=11.8u
                                                        AD=4.5p PD=11.8u
MINV3_2/NMOS_1 N_8 N_5 Gnd Gnd NMOS W=2.5u L=250n AS=2.25p PS=6.8u
                                                        AD=2.25p PD=6.8u
MTG_3/INV_1/PMOS_1 TG_3/N_1 N_4 Vdd Vdd PMOS W=5u L=250n AS=4.5p
                                                        PS=11.8u AD=4.5p
+PD=11.8u
MTG_3/INV_1/NMOS_1 TG_3/N_1 N_4 Gnd Gnd NMOS W=2.5u L=250n AS=2.25p
                                                        PS=6.8u AD=2.25p
+PD=6.8u
MTG_3/PMOS_1 N_2 TG_3/N_1 N_6 Vdd PMOS W=2.5u L=250n AS=2.25p PS=6.8u
                                                        AD=2.25p PD=6.8u
MTG_3/NMOS_1 N_2 N_4 N_6 Gnd NMOS W=2.5u L=250n AS=2.25p PS=6.8u
                                                        AD=2.25p PD=6.8u
MINV3_3/PMOS_1 N_7 N_8 Vdd Vdd PMOS W=5u L=250n AS=4.5p PS=11.8u
                                                        AD=4.5p PD=11.8u
MINV3_3/NMOS_1 N_7 N_8 Gnd Gnd NMOS W=2.5u L=250n AS=2.25p PS=6.8u
                                                        AD=2.25p PD=6.8u
```

```
MTG_4/INV_1/PMOS_1 TG_4/N_1 In Vdd Vdd PMOS W=5u L=250n AS=4.5p
                                                    PS=11.8u AD=4.5p
+PD=11.8u
MTG_4/INV_1/NMOS_1 TG_4/N_1 In Gnd Gnd NMOS W=2.5u L=250n AS=2.25p
                                                    PS=6.8u AD=2.25p
+PD=6.8u
MTG_4/PMOS_1 N_5 TG_4/N_1 N_7 Vdd PMOS W=2.5u L=250n AS=2.25p PS=6.8u
                                                    AD=2.25p PD=6.8u
MTG_4/NMOS_1 N_5 In N_7 Gnd NMOS W=2.5u L=250n AS=2.25p PS=6.8u
                                                    AD=2.25p PD=6.8u
MINV3_4/PMOS_1 N_6 N_3 Vdd Vdd PMOS W=5u L=250n AS=4.5p PS=11.8u
                                                    AD=4.5p PD=11.8u
MINV3_4/NMOS_1 N_6 N_3 Gnd Gnd NMOS W=2.5u L=250n AS=2.25p PS=6.8u
                                                    AD=2.25p PD=6.8u
MINV3_5/PMOS_1 N_1 N_8 Vdd Vdd PMOS W=5u L=250n AS=4.5p PS=11.8u
                                                    AD=4.5p PD=11.8u
MINV3_5/NMOS_1 N_1 N_8 Gnd Gnd NMOS W=2.5u L=250n AS=2.25p PS=6.8u
                                                    AD=2.25p PD=6.8u
MINV3_6/PMOS_1 Out N_7 Vdd Vdd PMOS W=5u L=250n AS=4.5p PS=11.8u
                                                    AD=4.5p PD=11.8u
MINV3_6/NMOS_1 Out N_7 Gnd Gnd NMOS W=2.5u L=250n AS=2.25p PS=6.8u
                                                    AD=2.25p PD=6.8u
MINV3_7/PMOS_1 N_4 In Vdd Vdd PMOS W=5u L=250n AS=4.5p PS=11.8u
                                                    AD=4.5p PD=11.8u
MINV3_7/NMOS_1 N_4 In Gnd Gnd NMOS W=2.5u L=250n AS=2.25p PS=6.8u
                                                    AD=2.25p PD=6.8u
```

A.17. SW KEY parameters

```
ICurrentSource_2 Vdd In  DC 50u
MPMOS_1 N_1 N_2 Vdd Vdd PMOS W=5u L=250n AS=4.5p PS=11.8u AD=4.5p
                                                    PD=11.8u
MPMOS_2 N_2 N_2 Vdd Vdd PMOS W=5u L=250n AS=4.5p PS=11.8u AD=4.5p
                                                    PD=11.8u
MNMOS_1 In In Gnd Gnd NMOS W=2.5u L=250n AS=2.25p PS=6.8u AD=2.25p
                                                    PD=6.8u
MNMOS_2 N_1 Out Gnd Gnd NMOS W=2.5u L=250n AS=2.25p PS=6.8u AD=2.25p
                                                    PD=6.8u
MNMOS_3 Out CLK In Gnd NMOS W=2.5u L=250n AS=2.25p PS=6.8u AD=2.25p
                                                    PD=6.8u
MNMOS_5 N_3 N_3 Gnd Gnd NMOS W=2.5u L=250n AS=2.25p PS=6.8u AD=2.25p
                                                    PD=6.8u
MNMOS_7 N_4 CLK N_3 Gnd NMOS W=2.5u L=250n AS=2.25p PS=6.8u AD=2.25p
                                                    PD=6.8u
MNMOS_8 N_2 N_4 Gnd Gnd NMOS W=2.5u L=250n AS=2.25p PS=6.8u AD=2.25p
                                                    PD=6.8u
ICurrentSource_1 Vdd N_3  DC 50u
```